Angewandte Chemie
Eine Zeitschrift der Gesellschaft Deutscher Chemiker

Supporting Information

B–B vs. B–H Bond Activation in a (μ-Hydrido)diborane(4) Anion upon Cycloaddition with CO_2, Isocyanates, or Carbodiimides

*Timo Trageser, Dariusz Bebej, Michael Bolte, Hans-Wolfram Lerner, and Matthias Wagner**

anie_202103427_sm_miscellaneous_information.pdf
anie_202103427_sm_cif.zip

Table of contents

1. Experimental details and characterization data

General considerations. All reactions and manipulations were carried out in an argon-filled glovebox or by applying standard Schlenk techniques under an argon atmosphere. The solvents *n*-pentane and *n*-hexane were dried over Na, tetrahydrofuran (THF) was dried over Na/benzophenone, [D$_8$]THF was dried over Na-K alloy. Prior to use, the solvents were distilled from the respective drying agent, degassed by applying three freeze-pump-thaw cycles, and stored over activated molecular sieves (3 Å). Similarly, all liquid reactants as well as the two additives, dimethoxyethane (DME) and *N,N,N′,N″,N″*-pentamethyldiethylenetriamine (PMDTA), were degassed by applying three freeze-pump-thaw cycles and stored over activated molecular sieves (3 Å). CO_2 from a stainless-steel gas cylinder was passed through a CO_2-cooled cold trap before being introduced into the reaction vessel. The compounds **1**H$_2$ and M[**1**H] (M^+ = Li^+, K^+) were synthesized according to literature procedures.[S1,S2] *Note:* (i) The compounds M[**1**H] crystallize from THF as solvates [Li(thf)$_3$][**1**H], [Na(thf)$_2$][**1**H], and [K(thf)$_2$][**1**H]; according to ^{1}H NMR spectroscopy, the amounts of coordinated solvent molecules remain unchanged even after drying under a dynamic vacuum (oil pump; approximately 10^{-3} torr, room temperature, 10 to 20 min). The alkali metal salts M[**2**H], M[**3**], M[**4**H], M[**5**], M[**6**], Li[**7**], M[**8**], and Li[**9**] also crystallize as THF solvates, but lose some of their coordinated thf ligands during this drying process. Thus, the number of remaining thf ligands typically varies between samples and with respect to the THF content of corresponding single-crystalline material (cf. the X-ray crystal structure analyses, if available). It is therefore advisable to determine the individual THF content of each sample by ^{1}H NMR spectroscopy before using it as a reactant. (ii) Whenever a molecule (DME, PMDTA, THF) serves as a ligand, its acronym is written in lower case letters (dme, pmdta, thf).

NMR spectra were recorded using Bruker Avance 300 and Avance III 500 HD spectrometers; NMR samples were investigated in flame-sealed NMR tubes at room temperature (298 K). Chemical shifts are referenced to (residual) solvent signals (^{1}H; ^{1}H{^{11}B}/^{13}C{^{1}H}; [D$_8$]THF: δ = 3.58/67.2 ppm[S3]), external LiCl in D_2O (^{7}Li), $BF_3{\cdot}OEt_2$ (^{11}B; ^{11}B{^{1}H}), or Me_4Si (^{29}Si{^{1}H}, ^{29}Si INEPT). Abbreviations: s = singlet, d = doublet, dd = doublet of doublets, m = multiplet, q = quartet, sept = septet, br = broad, n.r. = not resolved.

The IR spectrum was measured on a JASCO FT/IR spectrometer (4200 series) by attenuated total reflection (ATR).

Synthesis of [Li(thf)$_2$][2H]. In a round-bottom flask equipped with a magnetic stirring bar, [Li(thf)$_3$][**1**H] (72 mg, 92.9 µmol) was dissolved in THF (5.0 mL). The flask was closed with a three-way PTFE spindle valve and attached to a Schlenk line. The solution was frozen with liquid nitrogen, the system evacuated, and CO_2 (quality grade 4.5; 1 atm) was filled in. The content of the flask was allowed to warm to room temperature and the excess pressure released through a Hg bubbler. After 15 min of stirring at room temperature, all volatiles were removed *in vacuo* and a colorless solid was obtained. In a glovebox, the solid was re-dissolved in THF (1.5 mL) and the solution transferred to an 8 mL vial, which was left open and placed into a screw-capped 100 mL vial containing *n*-hexane (20 mL). The outer vial was closed to allow for gas-phase diffusion of the *n*-hexane into the THF solution. After 4 d, colorless crystals had formed. The mother liquor was removed from the crystals via syringe. The crystals were washed with *n*-hexane (3 x 0.2 mL) and dried *in vacuo*. Yield of [Li(thf)$_2$][**2**H]: 52 mg (69.7 µmol, 75%).

Colorless single crystals of [Li(pmdta)][**2**H], which were more suitable for X-ray diffraction, were grown through gas-phase diffusion of *n*-hexane into a concentrated THF solution of Li[**2**H] containing PMDTA (0.1 mL), followed by slow evaporation of the solvents under ambient pressure and temperature while maintaining inert conditions.

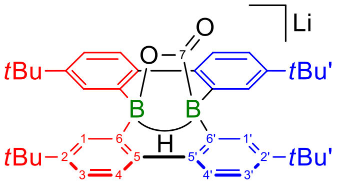

Figure S1. NMR numbering scheme for Li[**2**H].

*NMR shifts of compound Li[**2**H]*

^{1}H NMR (500.2 MHz, [D$_8$]THF): δ = 8.14 (d, ^4J(H,H) = 2.4 Hz, 2H; H-1), 8.04 (d, ^4J(H,H) = 2.4 Hz, 2H; H-1'), 7.74 (d, ^3J(H,H) = 8.5 Hz, 2H; H-4), 7.71 (d, ^3J(H,H) = 8.5 Hz, 2H; H-4'), 7.28 (dd, ^3J(H,H) = 8.5 Hz, ^4J(H,H) = 2.4 Hz, 2H; H-3), 7.22 (dd, ^3J(H,H) = 8.5 Hz, ^4J(H,H) = 2.4 Hz, 2H; H-3'), 4.93 (br, 1H†; BH), 1.40 (s, 18H; CH_3 or CH_3'), 1.39 ppm (s, 18H; CH_3 or CH_3'). † The relative integral value of 1H was further confirmed by an ^{1}H{^{11}B} NMR experiment.

^{11}B NMR (160.5 MHz, [D$_8$]THF): δ = –2.2 (br), –6.4 ppm (br).

^{13}C{^{1}H} NMR (125.8 MHz, [D$_8$]THF): δ = 199.2* (br, C-7), 147.5 (C-2 or C-2'), 147.5 (C-2 or C-2'), 144.4* (br, C-6), 142.6* (br, C-6'), 142.2 (C-5), 141.9 (C-5'), 129.9 (C-4), 129.5 (C-1), 129.2 (C-4'), 129.2 (C-1'), 124.2 (C-3), 123.4 (C-3'), 34.8 (*C*CH_3 or *C*CH_3'), 34.7 (*C*CH_3 or *C*CH_3'), 31.8 ppm (CH_3, CH_3').

* These resonances were detected through cross-peaks in the ^{1}H-^{13}C-HMBC experiment.

Reaction of [Na(thf)$_2$][1H] with CO$_2$. In a round-bottom flask equipped with a magnetic stirring bar, [Na(thf)$_2$][**1**H] (60 mg, 83.5 µmol) was dissolved in THF (5.0 mL). The flask was closed with a three-way PTFE spindle valve and attached to a Schlenk line. The solution was frozen with liquid nitrogen, the system evacuated, and CO$_2$ (quality grade 4.5; 1 atm) was filled in. The content of the flask was allowed to warm to room temperature and the excess pressure released through a Hg bubbler. After 30 min of stirring at room temperature, all volatiles were removed *in vacuo* and an ocher-colored solid was obtained. In a glovebox, the solid was re-dissolved in THF (1.5 mL) and the solution transferred to an 8 mL vial, which was left open and placed into a screw-capped 100 mL vial containing *n*-hexane (20 mL). The outer vial was closed to allow for gas-phase diffusion of the *n*-hexane into the THF solution. After 3 d, the volume of the THF solution was slowly reduced by evaporation under ambient pressure and temperature while maintaining inert conditions. After 3 d, colorless crystals had formed. The mother liquor was removed from the crystals via syringe. The crystals were washed with *n*-pentane (4 x 0.2 mL) and dried *in vacuo*. NMR spectroscopic investigations revealed that the crystalline material (yield: 42 mg) consisted of an inseparable mixture of Na[**2**H] and Na[**6**] (6.7:1 according to ^{1}H NMR).

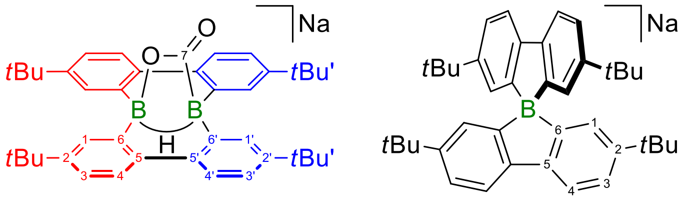

Figure S2. NMR numbering scheme for Na[**2**H] (left) and Na[**6**] (right).

*NMR shifts of compound Na[**2**H]*

^{1}H NMR (500.2 MHz, [D$_8$]THF): δ = 8.18 (d, ^4J(H,H) = 2.4 Hz, 2H; H-1), 8.07 (d, ^4J(H,H) = 2.4 Hz, 2H; H-1′), 7.76 (d, ^3J(H,H) = 8.5 Hz, 2H; H-4), 7.70 (d, ^3J(H,H) = 8.5 Hz, 2H; H-4′), 7.28 (dd, ^3J(H,H) = 8.5 Hz, ^4J(H,H) = 2.4 Hz, 2H; H-3), 7.21 (dd, ^3J(H,H) = 8.5 Hz, ^4J(H,H) = 2.4 Hz, 2H; H-3′), 4.80 (br, 1H†; BH), 1.40 (s, 18H; CH$_3$ or CH$_3$′), 1.39 ppm (s, 18H; CH$_3$ or CH$_3$′). † The relative integral value of 1H was further confirmed by an ^{1}H{^{11}B} NMR experiment.

^{11}B NMR (160.5 MHz, [D$_8$]THF): δ = –1.6 (br), –5.1 ppm (br).

^{13}C{^{1}H} NMR (125.8 MHz, [D$_8$]THF): δ = 195.9* (br, C-7), 147.5 (C-2 or C-2′), 147.4 (C-2 or C-2′), 144.6* (br, C-6), 142.7* (br, C-6′), 142.4 (C-5), 141.6 (C-5′), 129.9 (C-4), 129.5 (C-1), 129.3 (C-4′), 129.3 (C-1′), 124.1 (C-3), 123.4 (C-3′), 34.8 (*C*CH$_3$ and *C*CH$_3$′), 31.8 (CH$_3$ or CH$_3$′), 31.8 ppm (CH$_3$ or CH$_3$′).

* These resonances were detected through cross-peaks in the ^{1}H-^{13}C-HMBC experiment.

*NMR shifts of compound Na[**6**]*

^{1}H NMR (500.2 MHz, [D$_8$]THF): δ = 7.41 (d, ^3J(H,H) = 7.8 Hz, 4H; H-4), 6.89 (dd, ^3J(H,H) = 7.8 Hz, ^4J(H,H) = 2.1 Hz, 4H; H-3), 1.13 ppm (s, 36H; CH$_3$).

^{11}B NMR (160.5 MHz, [D$_8$]THF): δ = –6.3 ppm (s).

^{13}C{^{1}H} NMR (125.8 MHz, [D$_8$]THF): δ = 168.4* (br, C-6), 149.0 (C-5), 145.3 (C-2), 128.1 (C-1), 119.6 (C-3), 116.8 (C-4), 34.8 (*C*CH$_3$), 32.3 ppm (CH$_3$).

* This resonance was detected through cross-peaks in the ^{1}H-^{13}C-HMBC experiment.

Synthesis of [K(thf)$_{2.5}$][2H]. In an NMR tube, [K(thf)$_2$][**1**H] (15 mg, 20.4 µmol) was dissolved in THF (0.6 mL). The tube was closed with a three-way PTFE spindle valve and attached to a Schlenk line. The solution was frozen with liquid nitrogen, the system evacuated, and CO_2 (quality grade 4.5; 1 atm) was filled in. The content of the tube was allowed to warm to room temperature and the excess pressure released through a Hg bubbler. After 15 min at room temperature, all volatiles were removed *in vacuo* and a pale-yellow solid was obtained. In a glovebox, the solid was re-dissolved in THF (0.5 mL) and the solution transferred to a 1.5 mL vial, which was left open and placed into a screw-capped 12 mL vial containing *n*-hexane (2 mL). The outer vial was closed to allow for gas-phase diffusion of the *n*-hexane into the THF solution. After 2 d, colorless crystals had formed. The mother liquor was removed from the crystals via syringe and the crystals were dried *in vacuo*. Yield of [K(thf)$_{2.5}$][**2**H]: 14 mg (16.4 µmol, 81%).

The number of thf ligands in [K(thf)$_{2.5}$][**2**H] was determined by ^{1}H NMR spectroscopy; X-ray analysis of the crystals before vacuum exposure revealed a larger number of thf ligands in the dimeric solid-state structure of {[K(thf)$_{3.5}$][**2**H]}$_2$. However, these crystals were too weakly diffracting for a precise determination of the structural parameters. Colorless single crystals of {[K(pmdta)][**2**H]}$_2$·THF, which were more suitable for X-ray diffraction, were grown through gas-phase diffusion of *n*-hexane into a concentrated THF solution of K[**2**H] containing PMDTA (0.1 mL).

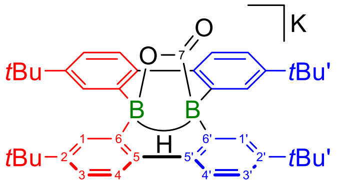

Figure S3. NMR numbering scheme for K[**2**H].

*NMR shifts of compound K[**2**H]*

^{1}H NMR (500.2 MHz, [D$_8$]THF): δ = 8.15 (d, ^{4}J(H,H) = 2.4 Hz, 2H; H-1), 8.04 (d, ^{4}J(H,H) = 2.4 Hz, 2H; H-1'), 7.75 (d, ^{3}J(H,H) = 8.5 Hz, 2H; H-4), 7.70 (d, ^{3}J(H,H) = 8.5 Hz, 2H; H-4'), 7.26 (dd, ^{3}J(H,H) = 8.5 Hz, ^{4}J(H,H) = 2.4 Hz, 2H; H-3), 7.20 (dd, ^{3}J(H,H) = 8.5 Hz, ^{4}J(H,H) = 2.4 Hz, 2H; H-3'), 4.76 (br, 1H†; BH), 1.40 (s, 18H; CH_3 or CH_3'), 1.38 ppm (s, 18H; CH_3 or CH_3'). † The relative integral value of 1H was further confirmed by an ^{1}H{^{11}B} NMR experiment.

^{11}B NMR (160.5 MHz, [D$_8$]THF): δ = –1.6 (br), –5.1 ppm (br).

^{13}C{^{1}H} NMR (125.8 MHz, [D$_8$]THF): δ = 195.5* (br, C-7), 147.3 (C-2'), 147.3 (C-2), 144.8* (br, C-6), 143.0* (br, C-6'), 142.4 (C-5), 141.6 (C-5'), 129.8 (C-4), 129.4 (C-1), 129.2 (C-1' or C-4'), 129.2 (C-1' or C-4'), 124.0 (C-3), 123.3 (C-3'), 34.8 (*C*CH_3 or *C*CH_3'), 34.7 (*C*CH_3 or *C*CH_3'), 31.8 (CH_3 or CH_3'), 31.8 ppm (CH_3 or CH_3').

* These resonances were detected through cross-peaks in the ^{1}H-^{13}C-HMBC experiment.

Synthesis of [Li(thf)][3]. In a glovebox, a screw-capped 8 mL vial was charged with a solution of [Li(thf)$_3$][**1**H] (100.0 mg, 129.1 µmol) in THF (1.2 mL). Neat *N,N'*-diisopropylcarbodiimide (20.0 µl, 16.3 mg, 129.1 µmol) was added at room temperature with stirring. The resulting yellow solution was stirred for 3 h. The open vial was placed into a 100 mL vial containing *n*-pentane (20 mL). The outer vial was closed to allow for gas-phase diffusion of the *n*-pentane into the THF solution. After 4 d, a microcrystalline solid had precipitated. The mother liquor was removed via syringe and the solid was dried *in vacuo*. Yield of [Li(thf)][**3**]: 89 mg (117.6 µmol, 91%).

The number of thf ligands in [Li(thf)][**3**] was determined by ^{1}H NMR spectroscopy; X-ray analysis of the crystals before vacuum exposure revealed a larger number of thf ligands in the solid-state structure of [Li(thf)$_5$][**3**]. However, these crystals were too weakly diffracting for a precise determination of the structural parameters. Yellow single crystals of [Li(12-c-4)$_2$][**3**], which were more suitable for X-ray diffraction, were grown by layering a concentrated THF solution of Li[**3**] with a solution of 12-crown-4 (12-c-4) in *n*-hexane at room temperature.

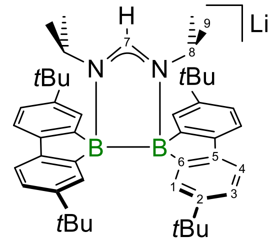

Figure S4. NMR numbering scheme for Li[**3**].

*NMR shifts of compound Li[**3**]*

^{1}H NMR (500.2 MHz, [D$_8$]THF): δ = 7.94 (s, 1H; H-7), 7.70 (d, ^4J(H,H) = 2.0 Hz, 4H; H-1), 7.07 (d, ^3J(H,H) = 7.7 Hz, 4H; H-4), 6.66 (dd, ^3J(H,H) = 7.7 Hz, ^4J(H,H) = 2.0 Hz, 4H; H-3), 3.13 (sept, ^3J(H,H) = 6.7 Hz, 2H; H-8), 1.25 (s, 36H; CH$_3$), 0.96 ppm (d, ^3J(H,H) = 6.7 Hz, 12H; H-9).

^{7}Li NMR (194.4 MHz, [D$_8$]THF): δ = –0.9 ppm (s).

^{11}B NMR (160.5 MHz, [D$_8$]THF): δ = 1.0 ppm (br, $h_{1/2} \approx$ 240 Hz).

^{13}C{^{1}H} NMR (125.8 MHz, [D$_8$]THF): δ = 167.4* (br, C-6), 157.2 (C-7), 145.2 (C-5), 143.7 (C-2), 128.4 (C-1), 118.2 (C-3), 116.6 (C-4), 51.1 (C-8), 34.8 (*C*CH$_3$), 32.6 (CH$_3$), 24.7 ppm (C-9).

* This resonance was detected through cross-peaks in the ^{1}H-^{13}C-HMBC experiment.

Synthesis of [Na(thf)][3]. In a glovebox, a screw-capped 8 mL vial was charged with a solution of [Na(thf)$_2$][**1**H] (40.0 mg, 55.7 µmol) in THF (2.0 mL). Neat *N,N'*-diisopropylcarbodiimide (9.3 µl, 7.6 mg, 60.1 µmol) was added at room temperature with stirring. The resulting yellow solution was stirred for 3 h. The open vial was placed into a 100 mL vial containing *n*-hexane (20 mL). The outer vial was closed to allow for gas-phase diffusion of the *n*-hexane into the THF solution. After 3 d, the volume of the THF solution was slowly reduced by evaporation under ambient pressure and temperature while maintaining inert conditions, whereupon yellow crystals of [Na(thf)$_2$][**3**]·*n*-hexane suitable for single-crystal X-ray diffraction formed. The mother liquor was removed from the crystals via syringe and the crystals were dried *in vacuo*. Yield of [Na(thf)][**3**]: 37 mg (47.9 µmol, 86%; the presence of one coordinated thf molecule was inferred by ^{1}H NMR spectroscopy).

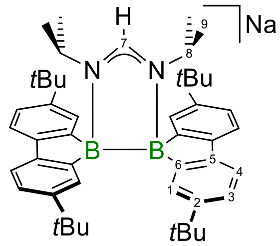

Figure S5. NMR numbering scheme for Na[**3**].

*NMR shifts of compound Na[**3**]*

^{1}H NMR (500.2 MHz, [D$_8$]THF): δ = 8.09 (s, 1H; H-7), 7.90 (d, ^4J(H,H) = 2.0 Hz, 4H; H-1), 7.33 (d, ^3J(H,H) = 7.9 Hz, 4H; H-4), 6.95 (dd, ^3J(H,H) = 7.9 Hz, ^4J(H,H) = 2.0 Hz, 4H; H-3), 2.86 (sept, ^3J(H,H) = 6.7 Hz, 2H; H-8), 1.31 (s, 36H; CH$_3$), 0.98 ppm (d, ^3J(H,H) = 6.7 Hz, 12H; H-9).

^{11}B NMR (160.5 MHz, [D$_8$]THF): δ = 0.6 ppm (br, $h_{1/2} \approx$ 260 Hz).

^{13}C{^{1}H} NMR (125.8 MHz, [D$_8$]THF): δ = 164.9* (br, C-6), 158.2 (C-7), 146.3 (C-2), 143.9 (C-5), 129.4 (C-1), 121.2 (C-3), 118.7 (C-4), 49.9 (C-8), 35.1 (*C*CH$_3$), 32.3 (CH$_3$), 24.7 ppm (C-9).

* This resonance was detected through cross-peaks in the ^{1}H-^{13}C-HMBC experiment.

Synthesis of [K(thf)][3]. In a glovebox, a screw-capped 8 mL vial was charged with a solution of [K(thf)$_2$][**1**H] (200 mg, 272.2 µmol) in THF (2.2 mL). Neat *N,N'*-diisopropylcarbodiimide (50.0 µl, 40.7 mg, 322.6 µmol) was added at room temperature with stirring. The resulting yellow solution was stirred for 3 h. The open vial was placed into a 100 mL vial containing *n*-hexane (20 mL). The outer vial was closed to allow for gas-phase diffusion of the *n*-hexane into the THF solution. After 5 d, the solvents were slowly evaporated to dryness under ambient pressure and temperature while maintaining inert conditions, whereupon yellow crystals of [K(thf)$_2$][**3**] suitable for single-crystal X-ray diffraction formed. The crystals were dried *in vacuo*. Yield of [K(thf)][**3**]: 207 mg (262 µmol, 96%; the presence of one coordinated thf molecule was inferred by ^{1}H NMR spectroscopy).

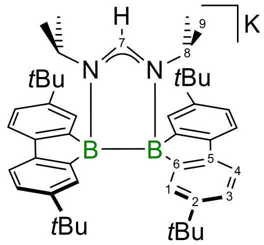

Figure S6. NMR numbering scheme for K[**3**].

*NMR shifts of compound K[**3**]*

^{1}H NMR (500.2 MHz, [D$_8$]THF): *δ* = 8.07 (s, 1H; H-7), 7.77 (d, ^{4}J(H,H) = 2.0 Hz, 4H; H-1), 7.24 (d, ^{3}J(H,H) = 7.8 Hz, 4H; H-4), 6.86 (dd, ^{3}J(H,H) = 7.8 Hz, ^{4}J(H,H) = 2.0 Hz, 4H; H-3), 3.26 (sept, ^{3}J(H,H) = 6.7 Hz, 2H; H-8), 1.27 (s, 36H; CH$_3$), 0.98 ppm (d, ^{3}J(H,H) = 6.7 Hz, 12H; H-9).

^{11}B NMR (160.5 MHz, [D$_8$]THF): *δ* = 0.7 ppm (br, $h_{1/2} \approx 290$ Hz).

^{13}C{^{1}H} NMR (125.8 MHz, [D$_8$]THF): *δ* = 166.6* (br, C-6), 158.8 (C-7), 146.1 (C-2), 143.1 (C-5), 128.9 (C-1), 119.7 (C-3), 117.5 (C-4), 51.9 (C-8), 35.0 (*C*CH$_3$), 32.2 (CH$_3$), 24.5 ppm (C-9).

* This resonance was detected through cross-peaks in the ^{1}H-^{13}C-HMBC experiment.

Reaction of [K(thf)$_2$][1D] with *N,N'*-diisopropylcarbodiimide. In an NMR tube, [K(thf)$_2$][**1**D] (10 mg, 13.6 µmol) was dissolved in THF (0.55 mL) and neat *N,N'*-diisopropylcarbodiimide (2.7 µl, 2.2 mg, 17.7 µmol) was added at room temperature. A drop of [D$_8$]THF was added as internal reference. A ^{2}H NMR spectrum recorded after 2 h showed only one broadened singlet signal at 8.09 ppm besides the two singlets expected for [D$_8$]THF, which proves the transfer of the B···B-bridging ^{2}H atom to the C atom of the carbodiimide (C-7 in the product).

The experiment was parallelly performed in 0.55 mL [D$_8$]THF employing the same molar amounts of the reactants. ^{1}H, ^{11}B, and ^{13}C{^{1}H} NMR spectra were recorded on this sample. As expected, only a signal of very low intensity (relative integral ratio 0.1H) is visible at 8.07 ppm (H-7), which originates from residual protons in the sample of incompletely deuterated starting material [K(thf)$_2$][**1**D]. All other signals are unchanged compared to the fully hydrogenated congener K[**3**] (see above) and have, therefore, been assigned accordingly.

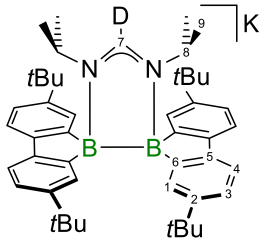

Figure S7. NMR numbering scheme for K[**3**$^{\text{D}}$].

*NMR shifts of compound K[**3**^{D}]*

^{1}H NMR (500.2 MHz, [D$_8$]THF): δ = 8.07 (s, 0.1H; H-7), 7.77 (d, ^4J(H,H) = 2.0 Hz, 4H; H-1), 7.24 (d, ^3J(H,H) = 7.8 Hz, 4H; H-4), 6.86 (dd, ^3J(H,H) = 7.8 Hz, ^4J(H,H) = 2.0 Hz, 4H; H-3), 3.26 (sept, ^3J(H,H) = 6.7 Hz, 2H; H-8), 1.27 (s, 36H; CH$_3$), 0.98 ppm (d, ^3J(H,H) = 6.7 Hz, 12H; H-9).

^{2}H NMR (76.8 MHz, THF): δ = 8.09 ppm (br s).

^{11}B NMR (160.5 MHz, [D$_8$]THF): δ = 0.7 ppm (br, $h_{1/2} \approx$ 290 Hz).

^{13}C{^{1}H} NMR (125.8 MHz, [D$_8$]THF): δ = 166.6 (br, C-6), 158.8 (n.r., C-7), 146.1 (C-2), 143.1 (C-5), 128.9 (C-1), 119.7 (C-3), 117.5 (C-4), 51.9 (C-8), 35.0 (*C*CH$_3$), 32.2 (CH$_3$), 24.5 ppm (C-9).

Synthesis of [Li(thf)$_n$][7]. In an NMR tube, [Li(thf)$_3$][**1**H] (10 mg, 12.9 µmol) was dissolved in [D$_8$]THF (0.55 mL) and neat *N,N'*-bis(*p*-tolyl)carbodiimide (5 mg, 22.5 µmol) was added at room temperature. An ^{1}H NMR spectrum recorded after 30 min showed the quantitative consumption of [Li(thf)$_3$][**1**H] and the formation of one major product, Li[**7**]. In a glovebox, the light orange reaction solution was transferred to a 1.5 mL vial. The open vial was placed into a 12 mL vial containing *n*-hexane (2 mL). The outer vial was closed to allow for gas-phase diffusion of the *n*-hexane into the THF solution. After 3 d, yellow crystals had formed. The mother liquor was removed from the crystals via syringe. The crystals were washed with *n*-hexane (3 x 0.05 mL) and dried *in vacuo* (yield of [Li(thf)$_n$][**7**]: 7 mg; since the number *n* of coordinated [D$_8$]thf ligands in the dried product cannot be determined by ^{1}H NMR spectroscopy, no molar yield can be reported).

Yellow single crystals of [Li(dme)$_3$][**7**] suitable for X-ray diffraction were grown through gas-phase diffusion of *n*-hexane into a concentrated THF/DME (1:1) solution of Li[**7**].

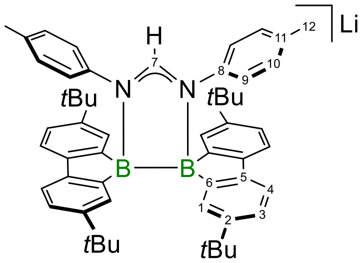

Figure S8. NMR numbering scheme for Li[**7**].

*NMR shifts of compound Li[**7**]*

^{1}H NMR (500.2 MHz, [D$_8$]THF): δ = 8.62 (s, 1H; H-7), 7.54 (d, ^4J(H,H) = 2.0 Hz, 4H; H-1), 7.09 (d, ^3J(H,H) = 7.8 Hz, 4H; H-4), 6.71–6.63 (m, 12H; H-3, H-9, H-10), 2.07 (s, 6H; H-12), 1.16 ppm (s, 36H; CH$_3$).

^{7}Li NMR (116.6 MHz, [D$_8$]THF): δ = –2.6 ppm (s).

^{11}B NMR (160.5 MHz, [D$_8$]THF): δ = 3.0 ppm (br, $h_{1/2} \approx$ 370 Hz).

^{13}C{^{1}H} NMR (125.8 MHz, [D$_8$]THF): δ = 165.0* (br, C-6), 157.0 (C-7), 145.1 (C-8), 145.0 (C-5), 144.2 (C-2), 130.8 (C-11), 128.8 (C-10), 127.6 (C-1), 121.3 (C-9), 118.9 (C-3), 116.9 (C-4), 34.8 (*C*CH$_3$), 32.5 (CH$_3$), 20.6 ppm (C-12).

* This resonance was detected through cross-peaks in the ^{1}H-^{13}C-HMBC experiment.

Heating of a mixture of [Li(thf)$_3$][1H] and *N,N′*-bis(trimethylsilyl)carbodiimide. A [D$_8$]THF solution of [Li(thf)$_3$][**1**H] and *N,N′*-bis(trimethylsilyl)carbodiimide (molar ratio = 1:1.7) in a flame-sealed NMR tube was heated stepwise up to a temperature of 90 °C. ^{1}H NMR spectroscopy revealed no conversion of both starting materials under these conditions.

Reaction of [Na(thf)$_2$][1H] with *N,N'*-bis(trimethylsilyl)carbodiimide. An NMR tube was charged with a solution of [Na(thf)$_2$][**1**H] (10 mg, 13.9 µmol) in [D$_8$]THF (0.55 mL). Neat *N,N'*-bis(trimethylsilyl)carbodiimide (4.4 µl, 3.6 mg, 19.5 µmol) was added at room temperature. An ^{1}H NMR spectrum recorded after 30 min revealed that no reaction had taken place. The flame-sealed NMR tube was heated to 120 °C for 1.5 h, whereupon a selective transformation occurred (approx. 75% conversion according to ^{1}H NMR). Heating was continued overnight (16 h, 120 °C), which led to the quantitative consumption of [Na(thf)$_2$][**1**H]. An ^{1}H NMR spectroscopic investigation revealed that Na[**8**] had formed with 91% selectivity.

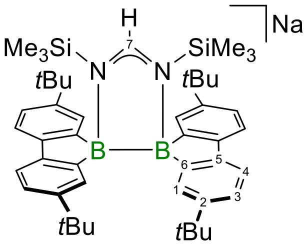

Figure S9. NMR numbering scheme for Na[**8**].

*NMR shifts of compound Na[**8**]*

^{1}H NMR (500.2 MHz, [D$_8$]THF): δ = 8.20 (s, 1H; H-7), 7.76 (d, ^4J(H,H) = 2.0 Hz, 4H; H-1), 7.31 (d, ^3J(H,H) = 7.9 Hz, 4H; H-4), 6.94 (dd, ^3J(H,H) = 7.9 Hz, ^4J(H,H) = 2.0 Hz, 4H; H-3), 1.30 (s, 36H; CCH$_3$), –0.26 ppm (s, 18H; SiCH$_3$).

^{11}B NMR (160.5 MHz, [D$_8$]THF): δ = 1.2 ppm (br, $h_{1/2} \approx$ 290 Hz).

^{13}C{^{1}H} NMR (125.8 MHz, [D$_8$]THF): δ = 166.6 (C-7), 165.9* (br, C-6), 146.4 (C-2), 143.3 (C-5), 129.2 (C-1), 120.9 (C-3), 118.6 (C-4), 35.1 (*C*CH$_3$), 32.3 (C*C*H$_3$), 0.5 ppm (SiCH$_3$). * This resonance was detected through cross-peaks in the ^{1}H-^{13}C-HMBC experiment.

^{29}Si INEPT NMR (99.4 MHz, [D$_8$]THF): δ = 8.1 ppm (s).

Synthesis of K[8]. In a PTFE-tap flask, [K(thf)$_2$][**1**H] (100 mg, 136.1 µmol) was dissolved in THF (4.0 mL). Neat *N,N′*-bis(trimethylsilyl)carbodiimide (40.0 µl, 32.9 mg, 176.3 µmol) was added at room temperature with stirring. The flask was closed and the resulting yellow solution was heated to 90 °C for 10 h. All volatiles were removed *in vacuo*. Yield of K[**8**]: 103 mg (133 µmol, 97%; the absence of coordinated thf was inferred by ^{1}H NMR spectroscopy).

Yellow single crystals of [K(dme)][**8**] suitable for single-crystal X-ray diffraction were grown in the following way: First, *n*-hexane was slowly added to a concentrated DME solution of K[**8**] through gas-phase diffusion. After 4 d, the volume of the solution was slowly reduced by evaporation under ambient pressure and temperature while maintaining inert conditions.

Note: A previous NMR experiment in [D$_8$]THF did not show any reaction between [K(thf)$_2$][**1**H] and *N,N′*-bis(trimethylsilyl)carbodiimide at room temperature within 20 h. At 55 °C, the reaction required 2 d to reach 98% conversion. However, this procedure resulted in a lower selectivity of the reaction compared to the above protocol.

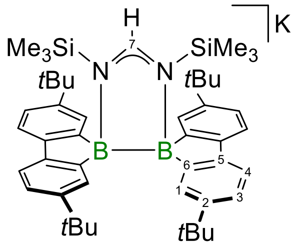

Figure S10. NMR numbering scheme for K[**8**].

*NMR shifts of compound K[**8**]*

^{1}H NMR (500.2 MHz, [D$_8$]THF): δ = 8.22 (s, 1H; H-7), 7.66 (d, ^4J(H,H) = 2.1 Hz, 4H; H-1), 7.23 (d, ^3J(H,H) = 7.8 Hz, 4H; H-4), 6.86 (dd, ^3J(H,H) = 7.8 Hz, ^4J(H,H) = 2.1 Hz, 4H; H-3), 1.26 (s, 36H; CCH$_3$), –0.19 ppm (s, 18H; SiCH$_3$).

^{11}B NMR (160.5 MHz, [D$_8$]THF): δ = 1.4 ppm (br, $h_{1/2} \approx$ 350 Hz).

^{13}C{^{1}H} NMR (125.8 MHz, [D$_8$]THF): δ = 167.0* (br, C-6), 165.9 (C-7), 146.3 (C-2), 143.1 (C-5), 129.0 (C-1), 119.7 (C-3), 117.5 (C-4), 35.0 (*C*CH$_3$), 32.2 (C*C*H$_3$), 0.5 ppm (SiCH$_3$). * This resonance was detected through cross-peaks in the ^{1}H-^{13}C-HMBC experiment.

^{29}Si{^{1}H} NMR (99.4 MHz, [D$_8$]THF): δ = 7.7 ppm (s).

Reaction of [Li(thf)$_3$][1H] with isopropyl isocyanate. In an NMR tube, [Li(thf)$_3$][**1**H] (20 mg, 25.8 µmol) was dissolved in [D$_8$]THF (0.55 mL) and neat isopropyl isocyanate (4.1 µl, 3.6 mg, 41.8 µmol) was added at room temperature. An ^{1}H NMR spectrum recorded after 30 min showed a mixture of Li[**4**H] and Li[**5**] as the major components besides residual [Li(thf)$_3$][**1**H] (one of the minor products could be identified as Li[**6**] by NMR spectroscopy). After 1 d, the conversion of [Li(thf)$_3$][**1**H] was complete and the reaction solution contained Li[**4**H] and Li[**5**] (ratio = 1:1.3) as the major components.

Colorless single crystals of [Li(pmdta)][**4**H] suitable for X-ray diffraction were grown in the following way: First, *n*-hexane was slowly added to one half of the reaction mixture containing PMDTA (0.1 mL) through gas-phase diffusion. After 3 d, the volume of the solution was slowly reduced by evaporation under ambient pressure and temperature while maintaining inert conditions.

Colorless single crystals of [Li(thf)$_3$][**5**] suitable for X-ray diffraction were grown in the following way: First, *n*-hexane was slowly added to the other half of the reaction mixture through gas-phase diffusion. After 2 d, the volume of the solution was slowly reduced by evaporation under ambient pressure and temperature while maintaining inert conditions.

Note: When using the theoretically required one equivalent of isopropyl isocyanate, some of the starting material [Li(thf)$_3$][**1**H] is still left when the isocyanate is already quantitatively consumed.

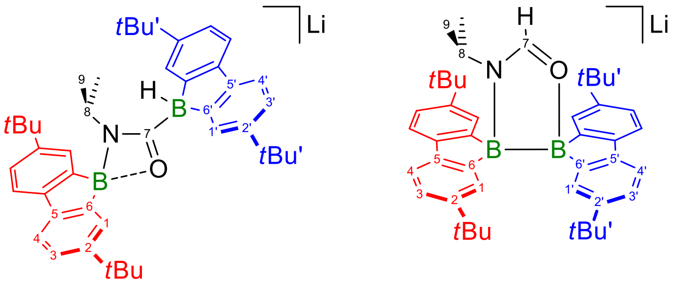

Figure S11. NMR numbering scheme for Li[**4**H] (left) and Li[**5**] (right).

*NMR shifts of compound Li[**4**H]*

^{1}H NMR (500.2 MHz, [D$_8$]THF): δ = 7.82 (d, ^4J(H,H) = 2.0 Hz, 2H; H-1 or H-1'), 7.49 (d, ^3J(H,H) = 7.8 Hz, 2H; H-4 or H-4'), 7.42 (d, ^4J(H,H) = 2.0 Hz, 2H; H-1 or H-1'), 7.30 (d, ^3J(H,H) = 7.8 Hz, 2H; H-4 or H-4'), 7.20 (dd, ^3J(H,H) = 7.8 Hz, ^4J(H,H) = 2.0 Hz, 2H; H-3 or H-3'), 7.10 (dd, ^3J(H,H) = 7.8 Hz, ^4J(H,H) = 2.0 Hz, 2H; H-3 or H-3'), 2.86 (sept, ^3J(H,H) = 6.5 Hz, 1H; H-8), 2.78 (q, ^1J(H,B) = 85 Hz, 1H†; BH), 1.41 (s, 18H; CH_3 or CH_3'), 1.31 (s, 18H; CH_3 or CH_3'), 0.22 ppm (d, ^3J(H,H) = 6.5 Hz, 6H; H-9). † The relative integral value of 1H was further confirmed by an ^{1}H{^{11}B} NMR experiment.

^{11}B NMR (160.5 MHz, [D$_8$]THF): δ = 13.1 (br), –17.0 ppm (d, ^1J(B,H) = 85 Hz).

^{13}C{^{1}H} NMR (125.8 MHz, [D$_8$]THF): δ = 212.0* (br, C-7), 155.9* (br, C-6 or C-6'), 149.5* (br, C-6 or C-6'), 148.1** (C-5 or C-5'), 148.0**(C-5 or C-5'), 147.9 (C-2 or C-2'), 147.8 (C-2 or C-2'), 128.8 (C-1 or C-1'), 127.8 (C-1 or C-1'), 124.4 (C-3 or C-3'), 123.2 (C-3 or C-3'), 118.8 (C-4 or C-4'), 118.2 (C-4 or C-4'), 45.5 (C-8), 35.1 (*C*CH_3 or *C*CH_3'), 34.9 (*C*CH_3 or *C*CH_3'), 32.2 (CH_3 or CH_3'), 32.0 (CH_3 or CH_3'), 22.6 ppm (C-9).

* These resonances were detected through cross-peaks in the ^{1}H-^{13}C-HMBC NMR experiment.

** The general assignment of these signals to carbon atoms at the 5-positions is evident from the 2D-NMR experiments. However, due to extensively overlapping resonances/cross-peaks, the assignment to either Li[**4**H] or Li[**5**] is arbitrary.

*NMR shifts of compound Li[**5**]*

^{1}H NMR (500.2 MHz, [D$_8$]THF): *δ* = 8.38 (s, 1H; H-7), 7.76 (d, ^4J(H,H) = 2.0 Hz, 2H; H-1 or H-1'), 7.58 (d, ^4J(H,H) = 2.0 Hz, 2H; H-1 or H-1'), 7.51 (d, ^3J(H,H) = 7.9 Hz, 2H; H-4 or H-4'), 7.37 (d, ^3J(H,H) = 7.9 Hz, 2H; H-4 or H-4'), 7.18 (dd, ^3J(H,H) = 7.9 Hz, ^4J(H,H) = 2.0 Hz, 2H; H-3 or H-3'), 7.13 (dd, ^3J(H,H) = 7.9 Hz, ^4J(H,H) = 2.0 Hz, 2H; H-3 or H-3'), 3.78 (sept, ^3J(H,H) = 6.5 Hz, 1H; H-8), 1.43 (s, 18H; CH_3 or CH_3'), 1.35 (s, 18H CH_3 or CH_3'), 0.34 ppm (d, ^3J(H,H) = 6.5 Hz, 6H; H-9).

^{11}B NMR (160.5 MHz, [D$_8$]THF): *δ* = 13.1 (br), –0.3 ppm (br).

Note: As for a mixture of K[**4**H] and K[**5**], we assume that one ^{11}B NMR signal of Li[**5**] overlaps with the signal of Li[**4**H] at 13.1 ppm. A second ^{11}B NMR signal cannot be unequivocally detected. However, comparison with the signals of K[**5**] suggests an assignment to the signal observed at –0.3 ppm is plausible.

^{13}C{^{1}H} NMR (125.8 MHz, [D$_8$]THF): *δ* = 167.1 (C-7), 160.0* (br, C-6 or C-6'), 149.5* (br, , C-6 or C-6'), 148.8 (C-2 or C-2'), 147.8** (C-5 or C-5'), 147.7** (C-5 or C-5'), 146.8 (C-2 or C-2'), 128.0 (C-1 or C-1'), 127.9 (C-1 or C-1'), 125.2 (C-3 or C-3'), 121.5 (C-3 or C-3'), 118.6 (C-4 or C-4'), 118.5 (C-4 or C-4'), 50.5 (C-8), 35.0 (*C*CH_3 or *C*CH_3'), 35.0 (*C*CH_3 or *C*CH_3'), 32.3 (CH_3 or CH_3'), 31.9 (CH_3 or CH_3'), 20.8 ppm (C-9).

* Theses resonances were detected through cross-peaks in the ^{1}H-^{13}C-HMBC experiment.

** The general assignment of these signals to carbon atoms at the 5-positions is evident from the 2D NMR experiments. However, due to extensively overlapping resonances/cross-peaks, the assignment to either Li[**4**H] or Li[**5**] is arbitrary.

Synthesis of [Na(pmdta)][4H]. In a glovebox, a screw-capped 4 mL vial was charged with a solution of [Na(thf)$_2$][**1**H] (15 mg, 20.9 µmol) in THF (1.0 mL). Excess neat isopropyl isocyanate (6.2 µl, 5.3 mg, 62.6 µmol) was added at room temperature with stirring. The resulting pale-yellow solution was stirred for 16 h and subsequently transferred to a 1.5 mL vial. Neat PMDTA (0.1 mL) was added to the solution and the open vial was placed into a 12 mL vial containing *n*-hexane (2 mL). The outer vial was closed to allow for gas-phase diffusion of the *n*-hexane into the THF solution. After 2 d, the volume of the solution was slowly reduced by evaporation under ambient pressure and temperature while maintaining inert conditions, whereupon colorless crystals of [Na(pmdta)][**4**H] suitable for single-crystal X-ray diffraction formed. The mother liquor was removed from the crystals via syringe. The crystals were washed with *n*-hexane (3 x 0.1 mL) and dried *in vacuo*. Yield of [Na(pmdta)][**4**H]: 14 mg (20.9 µmol, 80%; the presence of one coordinated pmdta molecule was inferred by ^{1}H NMR spectroscopy and confirmed by an X-ray crystal structure analysis of [Na(pmdta)][**4**H]).

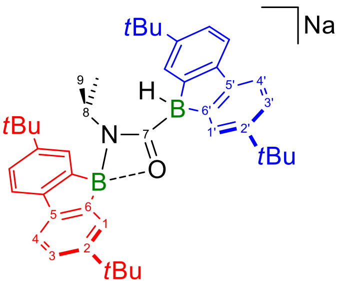

Figure S12. NMR numbering scheme for Na[**4**H].

*NMR shifts of compound Na[**4**H]*

^{1}H NMR (500.2 MHz, [D$_8$]THF): δ = 7.77 (d, ^{4}J(H,H) = 2.0 Hz, 2H; H-1'), 7.53–7.51 (m, 4H; H-1, H-4'), 7.34 (d, ^{3}J(H,H) = 7.9 Hz, 2H; H-4), 7.17–7.13 (m, 4H; H-3, H-3'), 3.28–3.23 (m, 1H; H-8), 2.66 (q, ^{1}J(H,B) = 82 Hz, 1H†; BH), 1.41 (s, 18H; CH$_3$'), 1.33 (s, 18H; CH$_3$), 0.50 ppm (d, ^{3}J(H,H) = 6.5 Hz, 6H; H-9). † The relative integral value of 1H was further confirmed by an ^{1}H{^{11}B} NMR experiment.

^{11}B NMR (160.5 MHz, [D$_8$]THF): δ = 13.6 (br, $h_{1/2} \approx$ 385 Hz), –17.2 ppm (d, ^{1}J(B,H) = 82 Hz).

^{13}C{^{1}H} NMR (125.8 MHz, [D$_8$]THF): δ = 211.6* (br, C-7), 159.4* (br, C-6'), 148.5 (C-2), 148.3* (br, C-6), 148.0 (C-5'), 147.8 (C-5), 147.1 (C-2'), 128.1 (C-1'), 127.9 (C-1), 125.2 (C-3), 121.8 (C-3'), 118.6 (C-4'), 118.5 (C-4), 46.0 (C-8), 35.0 (*C*CH$_3$'), 35.0 (*C*CH$_3$), 32.3 (CH$_3$'), 31.9 (CH$_3$), 22.7 ppm (C-9).

* These resonances were detected through cross-peaks in the ^{1}H-^{13}C-HMBC experiment.

Reaction of [K(thf)$_2$][1H] with isopropyl isocyanate. In an NMR tube, [K(thf)$_2$][**1**H] (20 mg, 27.2 µmol) was dissolved in [D$_8$]THF (0.70 mL) and neat isopropyl isocyanate (3.5 µl, 3.0 mg, 35.7 µmol) was added at room temperature. An ^{1}H NMR spectrum recorded after 30 min showed the quantitative consumption of [K(thf)$_2$][**1**H] and the formation of K[**4**H] and K[**5**] (ratio = 1.5:1).

Colorless single crystals of [K(dme)$_3$][K][**4**H]$_2$ suitable for X-ray diffraction were grown in the following way: First, the same volume of DME was added to the reaction mixture. Second, *n*-hexane was slowly added through gas-phase diffusion. After 3 d, the volume of the solution was slowly reduced by evaporation under ambient pressure and temperature while maintaining inert conditions. The obtained crystals of [K(dme)$_3$][K][**4**H]$_2$ were washed with *n*-pentane (3 x 0.1 mL) and dried *in vacuo*.

Note: Heating a mixture of K[**4**H] and K[**5**] in [D$_8$]THF to 55 °C did not cause thermolysis or conversion of one species to the other.

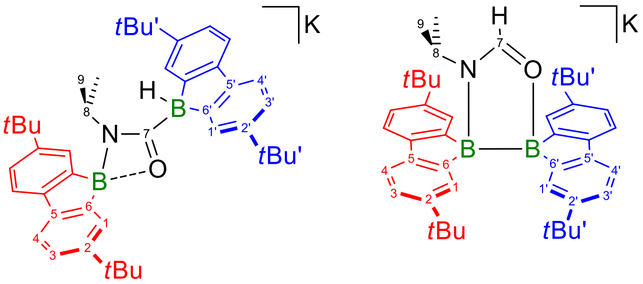

Figure S13. NMR numbering scheme for K[**4**H] (left) and K[**5**] (right). *Note:* Compound K[**4**H] has been isolated; the NMR data of K[**5**] have been taken from spectra recorded on a K[**4**H]/K[**5**] mixture (1.5:1).

*NMR shifts of compound K[**4**H]*

^{1}H NMR (500.2 MHz, [D$_8$]THF): δ = 7.82 (d, ^4J(H,H) = 2.0 Hz, 2H; H-1’), 7.54 (d, ^3J(H,H) = 7.9 Hz, 2H; H-4’), 7.46 (d, ^4J(H,H) = 2.1 Hz, 2H; H-1), 7.31 (d, ^3J(H,H) = 7.8 Hz, 2H; H-4), 7.17 (dd, ^3J(H,H) = 7.9 Hz, ^4J(H,H) = 2.0 Hz, 2H; H-3’), 7.13 (dd, ^3J(H,H) = 7.8 Hz, ^4J(H,H) = 2.1 Hz, 2H; H-3), 4.27 (sept, ^3J(H,H) = 6.5 Hz, 1H; H-8), 3.06 (q, ^1J(H,B) = 84 Hz, 1H†; BH), 1.41 (s, 18H; CH$_3$’), 1.31 (s, 18H; CH$_3$), 0.94 ppm (d, ^3J(H,H) = 6.5 Hz, 6H; H-9). † The relative integral value of 1H was further confirmed by an ^{1}H{^{11}B} NMR experiment.

^{11}B NMR (160.5 MHz, [D$_8$]THF): δ = 13.7 (br), –18.5 ppm (d, ^1J(B,H) = 84 Hz).

^{13}C{^{1}H} NMR (125.8 MHz, [D$_8$]THF): δ = 212.1* (br, C-7), 161.4* (br, C-6’), 148.9* (br, C-6), 148.4 (C-2), 147.8 (C-5’), 147.7 (C-5), 147.5 (C-2’), 128.5 (C-1’), 127.8 (C-1), 125.0 (C-3), 121.8 (C-3’), 118.4 (C-4, C-4’), 46.5 (C-8), 35.1 (*C*CH$_3$’), 34.9 (*C*CH$_3$), 32.2 (CH$_3$’), 31.9 (CH$_3$), 23.7 ppm (C-9).

* These resonances were detected through cross-peaks in the ^{1}H-^{13}C-HMBC experiment.

Note: The assignment of the spin systems X (red) vs. X’ (blue) was achieved through a cross-peak between the doublet resonance at δ(^{1}H) = 7.82 ppm and the doublet resonance at δ(^{11}B) = –18.5 ppm in the ^{1}H-^{11}B-HMBC experiment.

*NMR shifts of compound K[**5**]*

^{1}H NMR (500.2 MHz, [D$_8$]THF): *δ* = 8.41 (s, 1H; H-7), 7.74 (d, ^4J(H,H) = 2.0 Hz, 2H; H-1 or H-1’), 7.73 (d, ^4J(H,H) = 2.0 Hz, 2H; H-1 or H-1’), 7.30 (d, ^3J(H,H) = 7.7 Hz, 2H; H-4 or H-4’), 7.22 (d, ^3J(H,H) = 7.8 Hz, 2H; H-4 or H-4’), 6.93–6.91 (m, 4H; H-3, H-3’), 3.45 (sept, ^3J(H,H) = 6.7 Hz, 1H; H-8), 1.28 (s, 18H; CH_3 or CH_3’), 1.28 (s, 18H; CH_3 or CH_3’), 1.05 ppm (d, ^3J(H,H) = 6.7 Hz, 6H; H-9).

^{11}B NMR (160.5 MHz, [D$_8$]THF): *δ* = 13.1 (br), –1.5 ppm (br).

Note: The signal at –1.5 ppm was unequivocally detected; since we do not observe a fourth ^{11}B NMR signal in the K[**4**H]/K[**5**] mixture, we assume that the second ^{11}B signal of K[**5**] overlaps with the signal at 13.7 ppm of K[**4**H]. The resulting superimposed signal is visible at 13.1 ppm.

^{13}C{^{1}H} NMR (125.8 MHz, [D$_8$]THF): *δ* = 167.6 (C-7), 164.5* (br, C-6 or C-6’), 163.4* (br, C-6 or C-6’), 146.8 (C-2 or C-2’), 146.6 (C-2 or C-2’), 144.0 (C-5 or C-5’), 143.8 (C-5 or C-5’), 129.2 (C-1 or C-1’), 128.2 (C-1 or C-1’), 121.3 (C-3 or C-3’), 120.5 (C-3 or C-3’), 117.9 (C-4 or C-4’), 117.8 (C-4 or C-4’), 51.4 (C-8), 35.0 (*C*CH_3, *C*CH_3’), 32.3 (CH_3 or CH_3’), 32.2 (CH_3 or CH_3’), 24.1 ppm (C-9).

* This resonance was detected through cross-peaks in the ^{1}H-^{13}C-HMBC experiment.

Synthesis of [Na(thf)$_2$][1H]. In an argon-filled glovebox, THF (6.0 mL) was added at room temperature to a 12 mL vial charged with a solid mixture of **1**H$_2$ (211 mg, 0.382 mmol) and (Me$_3$Si)$_2$NNa (79 mg, 0.43 mmol). The resulting ocher-colored solution was stirred at room temperature for 2 d. The open vial was placed into a screw-capped 100 mL vial containing *n*-hexane (15 mL). The vessel was closed to allow for gas-phase diffusion of the *n*-hexane into the THF solution. After 5d, yellow crystals of [Na(thf)$_3$][**1**H] suitable for single-crystal X-Ray diffraction had formed. The mother liquor was removed from the crystals via syringe, the crystals washed with *n*-hexane (3 x 0.8 mL) and dried *in vacuo*. Yield of [Na(thf)$_2$][**1**H]: 184 mg (0.256 mmol, 67%; the presence of two coordinated thf molecules was inferred by ^{1}H NMR spectroscopy).

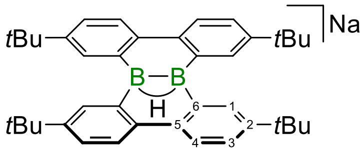

Figure S14. NMR numbering scheme for Na[**1**H].

*NMR shifts of compound Na[**1**H]*

^{1}H NMR (300.0 MHz, [D$_8$]THF): δ = 8.92 (d, ^4J(H,H) = 2.4 Hz, 4H; H-1), 8.51 (d, ^3J(H,H) = 8.6 Hz, 4H; H-4), 7.40 (dd, ^3J(H,H) = 8.6 Hz, ^4J(H,H) = 2.4 Hz, 4H; H-3), 1.51 (s, 36H; CH$_3$), –1.00 ppm (br, 1H†; BH).

† The relative integral value of 1H was further confirmed by an ^{1}H{^{11}B} NMR experiment.

^{11}B NMR (96.3 MHz, [D$_8$]THF): δ = 20.6 ppm (br).

^{13}C{^{1}H} NMR (125.8 MHz, [D$_8$]THF): δ = 145.9 (C-2), 144.6* (br, C-6), 138.6 (C-5), 128.0 (C-1), 125.7 (C-4), 121.7 (C-3), 35.1 (*C*CH$_3$), 32.3 ppm (CH$_3$).

* This resonance was detected through cross-peaks in the ^{1}H-^{13}C-HMBC experiment.

2. Plot of the IR spectrum of K[2H]

The highlighted area ($\tilde{\upsilon}$ = 1600-1800 cm^{-1}) is characteristic for C=O stretches of carboxylic esters.[S4]

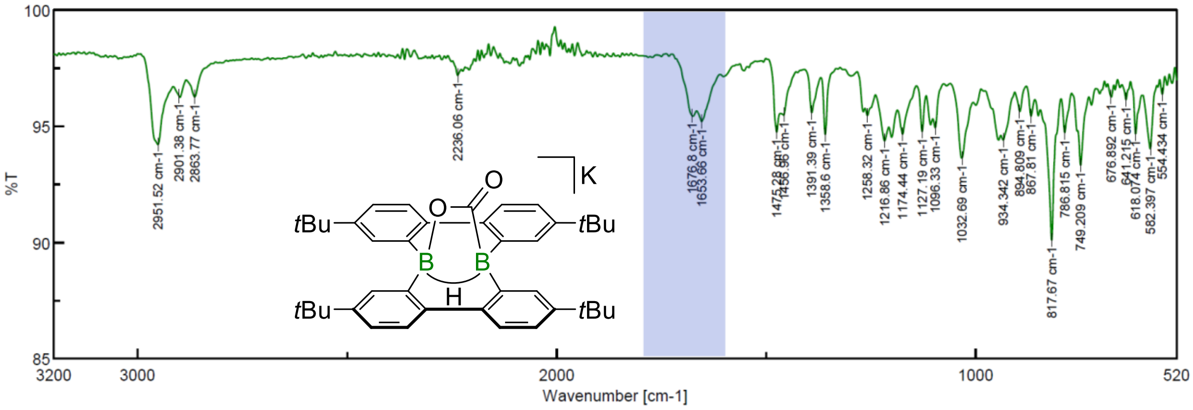

Figure S15. IR spectrum of K[**2**H] recorded with an ATR probe.

3. Plots of NMR spectra

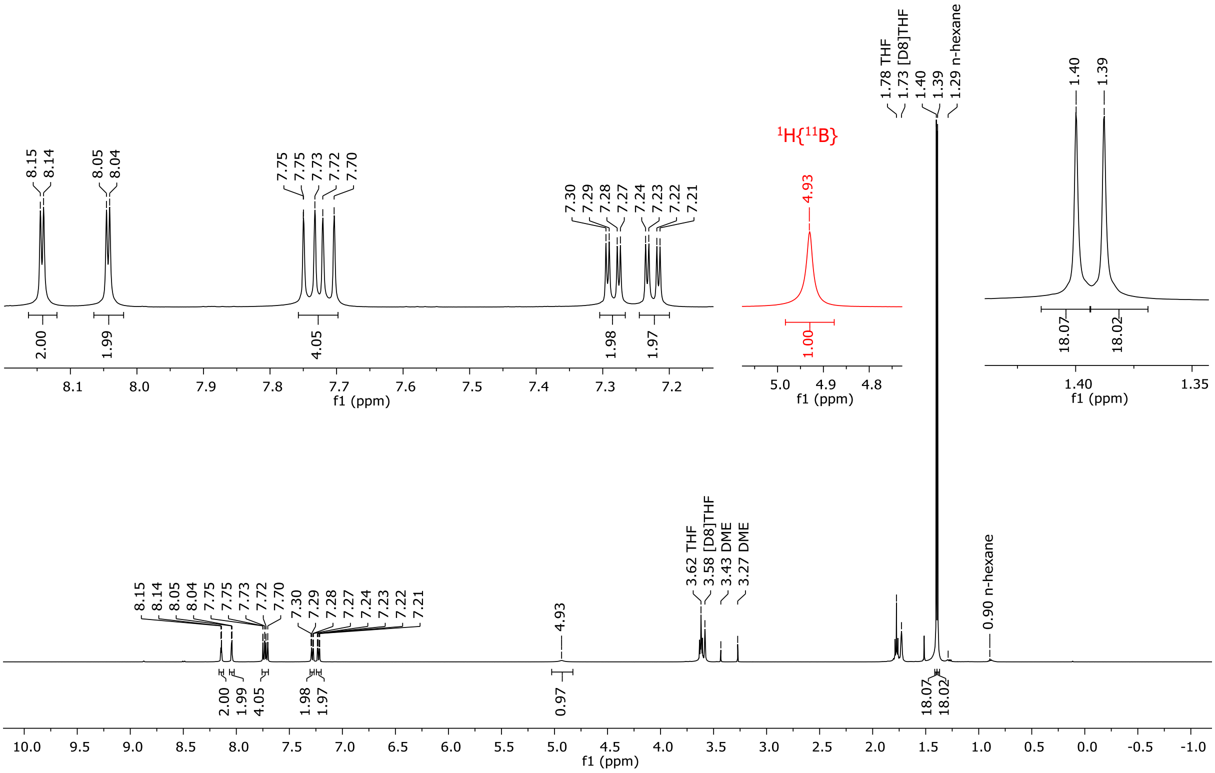

Figure S16. ^{1}H NMR spectrum of Li[**2**H] (500.2 MHz, [D$_8$]THF).

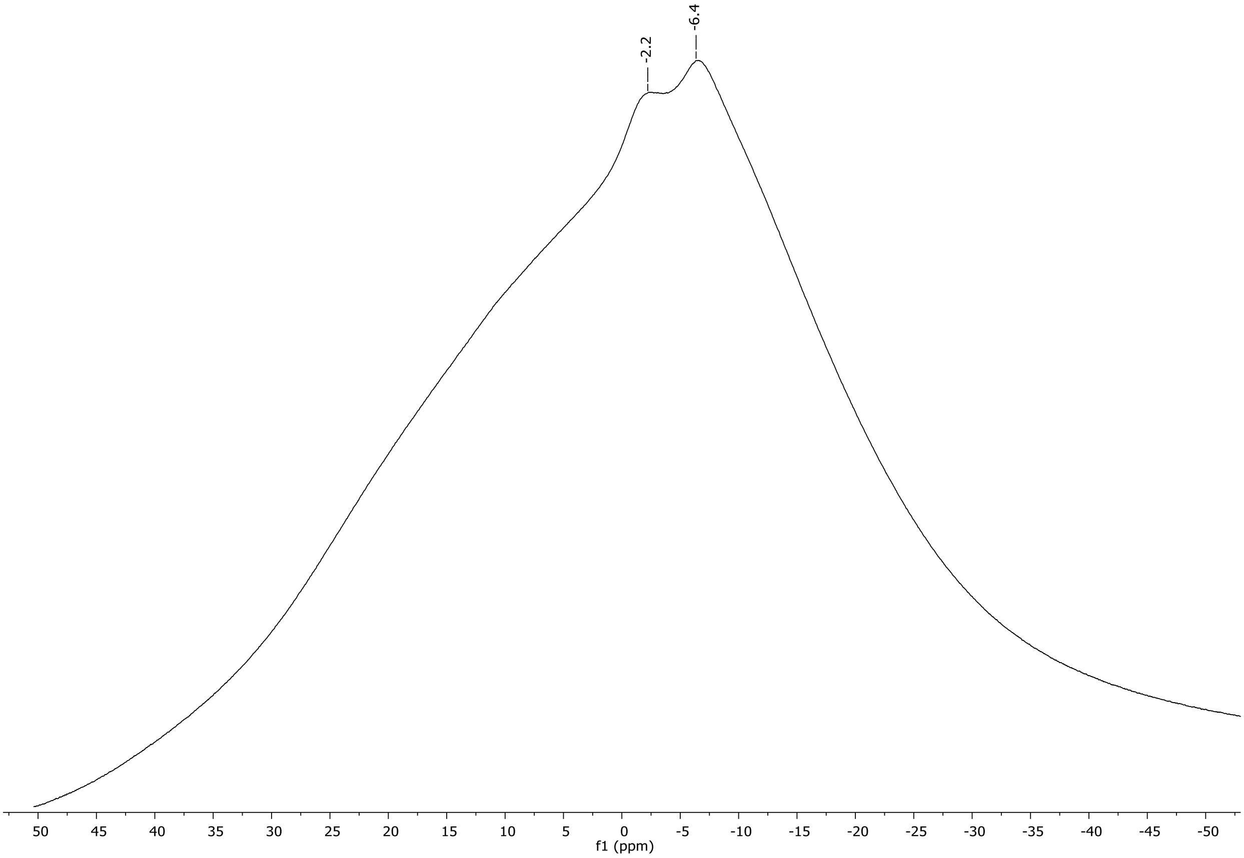

Figure S17. ^{11}B NMR spectrum of Li[**2**H] (160.5 MHz, [D$_8$]THF).

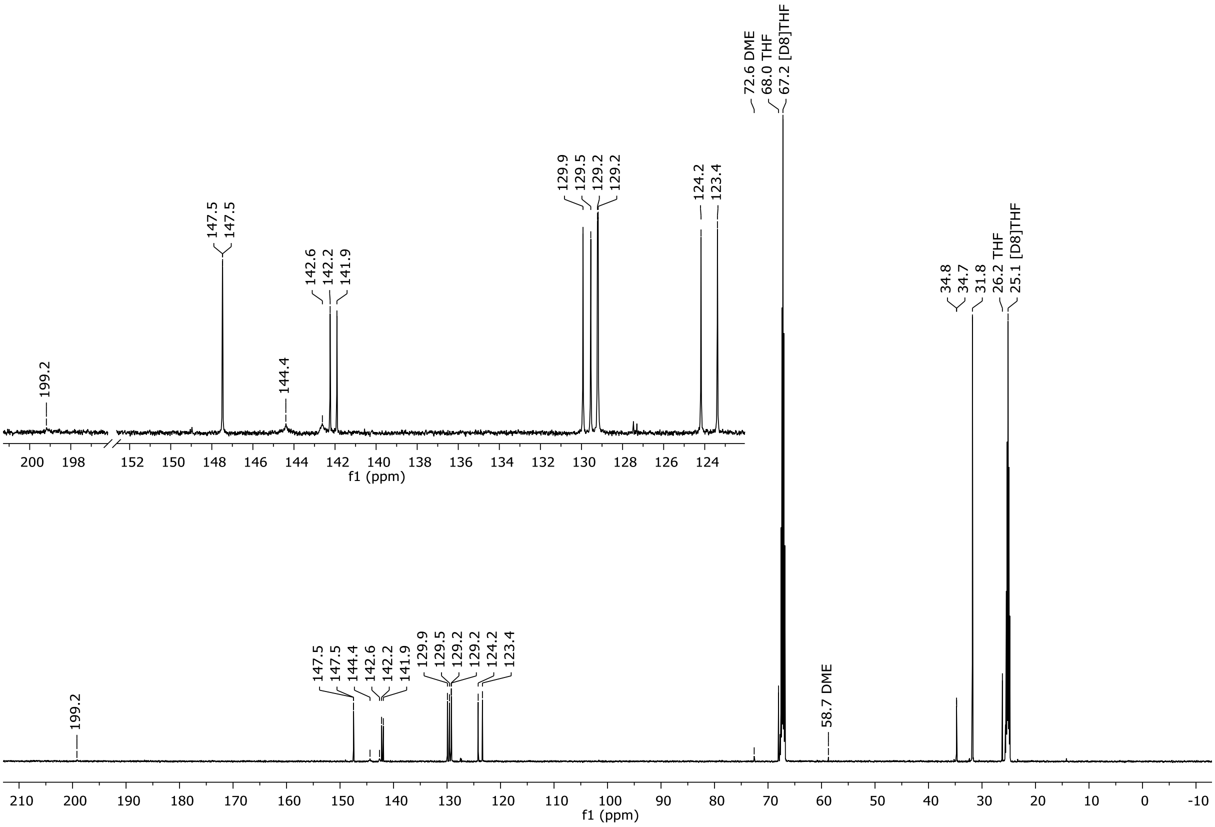

Figure S18. $^{13}C\{^{1}H\}$ NMR spectrum of Li[**2**H] (125.8 MHz, [D$_8$]THF).

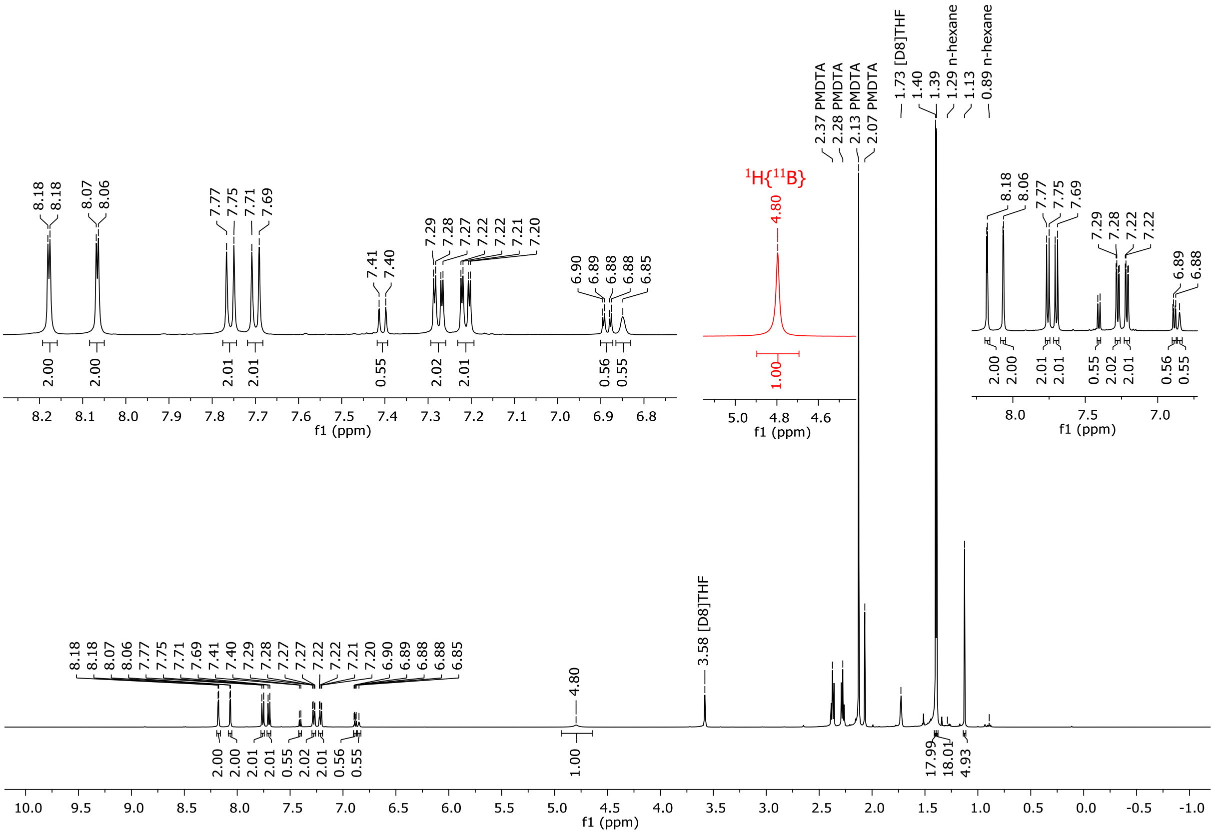

Figure S19. ^{1}H NMR spectrum of a mixture of Na[**2**H] and Na[**6**] (500.2 MHz, [D$_8$]THF).

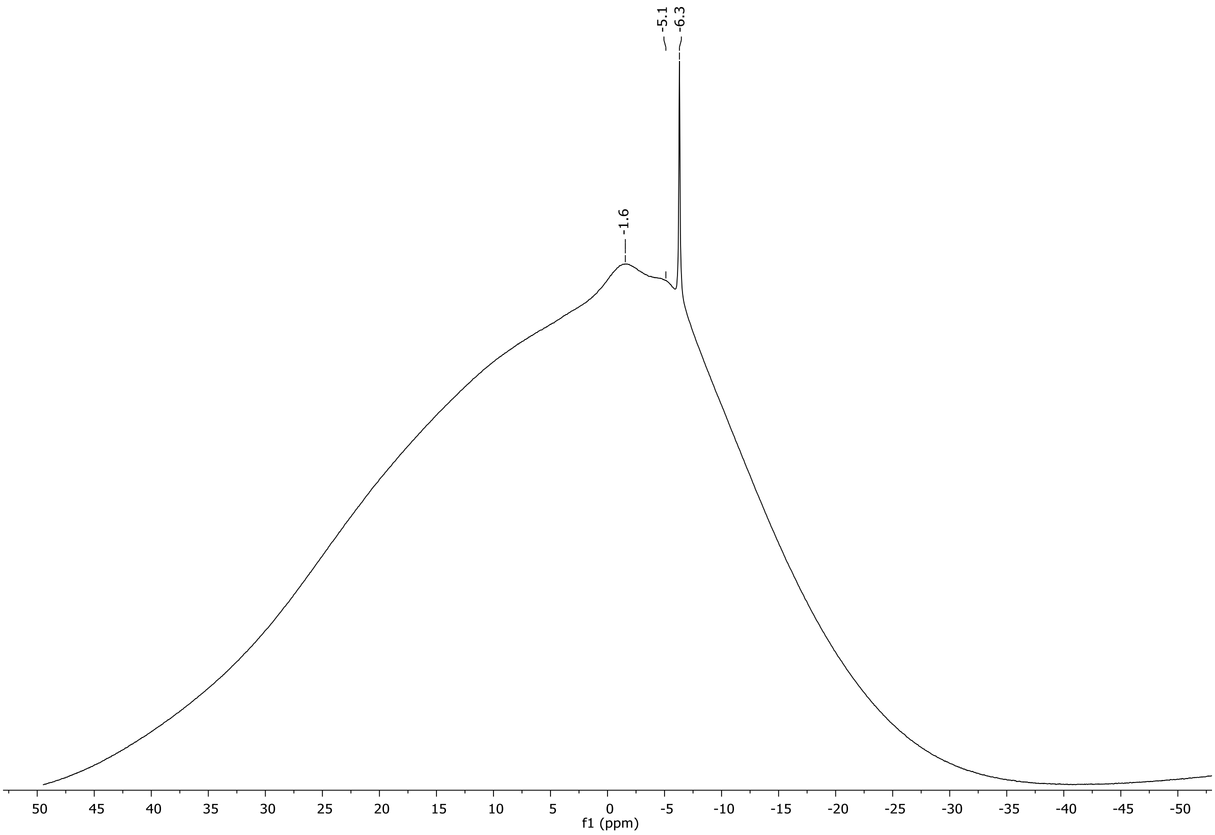

Figure S20. ^{11}B NMR spectrum of a mixture of Na[**2**H] and Na[**6**] (160.5 MHz, [D$_8$]THF).

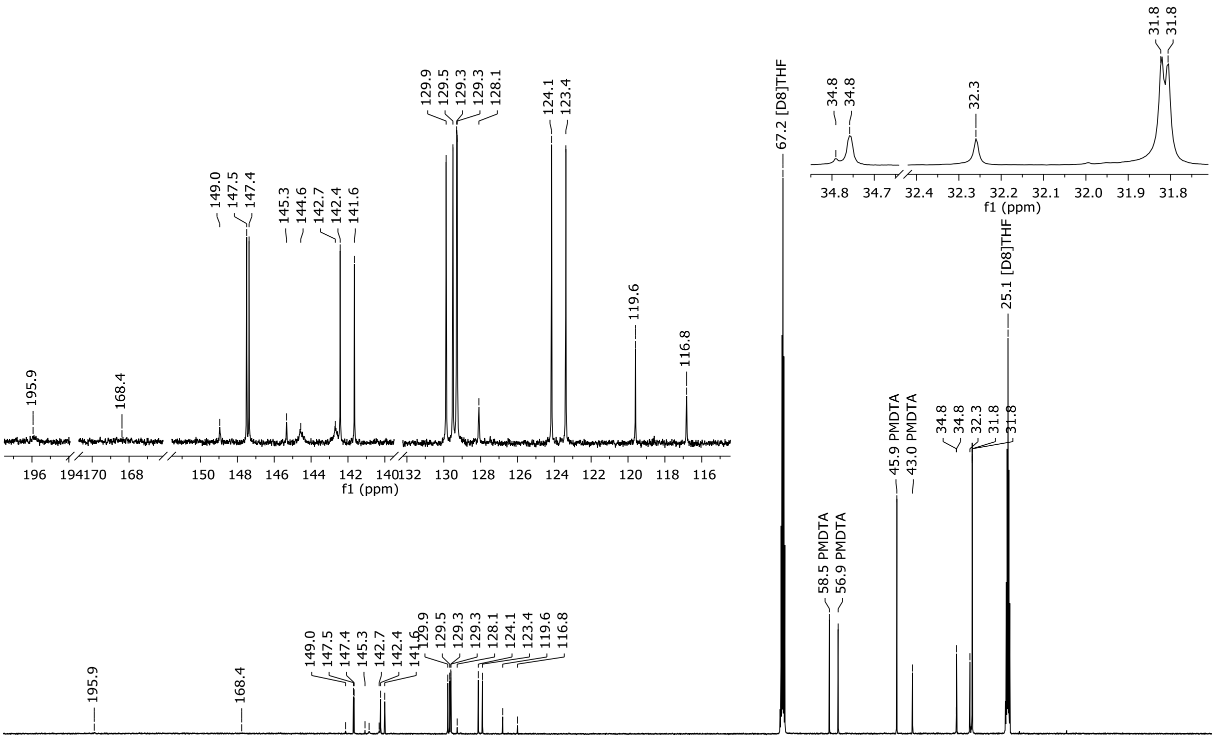

Figure S21. $^{13}C\{^{1}H\}$ NMR spectrum of a mixture of Na[**2**H] and Na[**6**] (125.8 MHz, [D$_8$]THF).

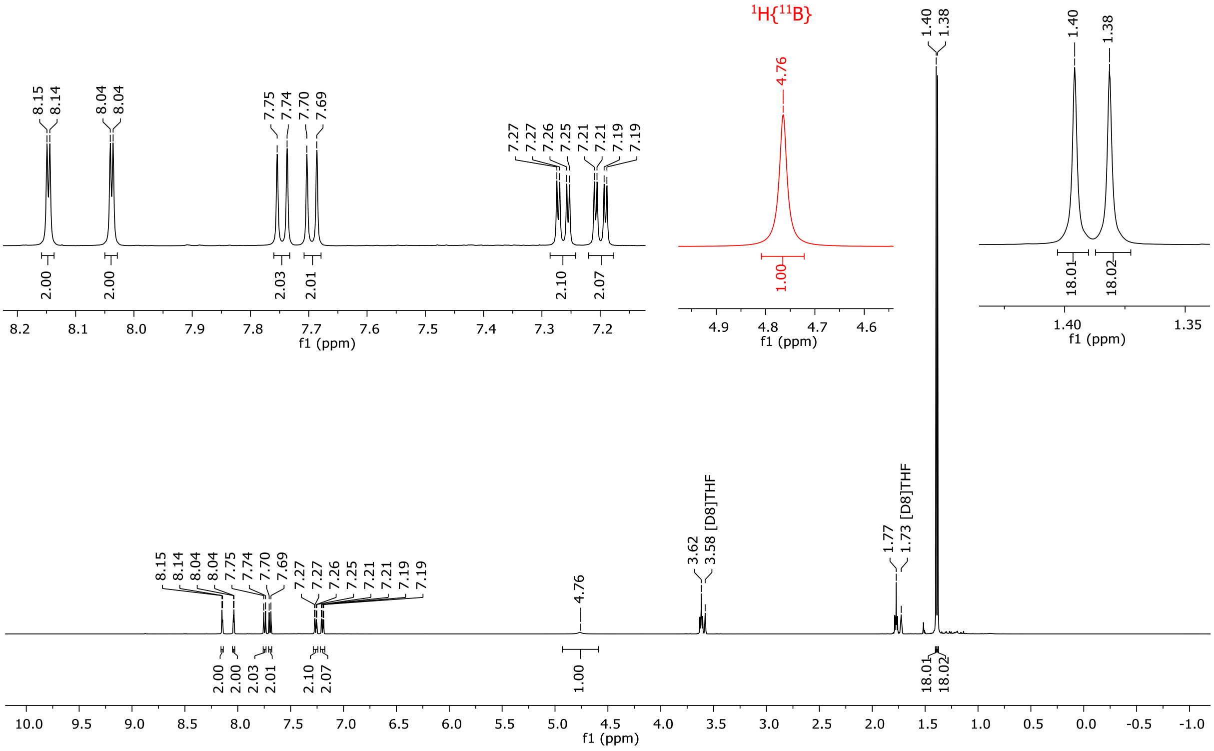

Figure S22. ^{1}H NMR spectrum of K[**2**H] (500.2 MHz, [D$_8$]THF).

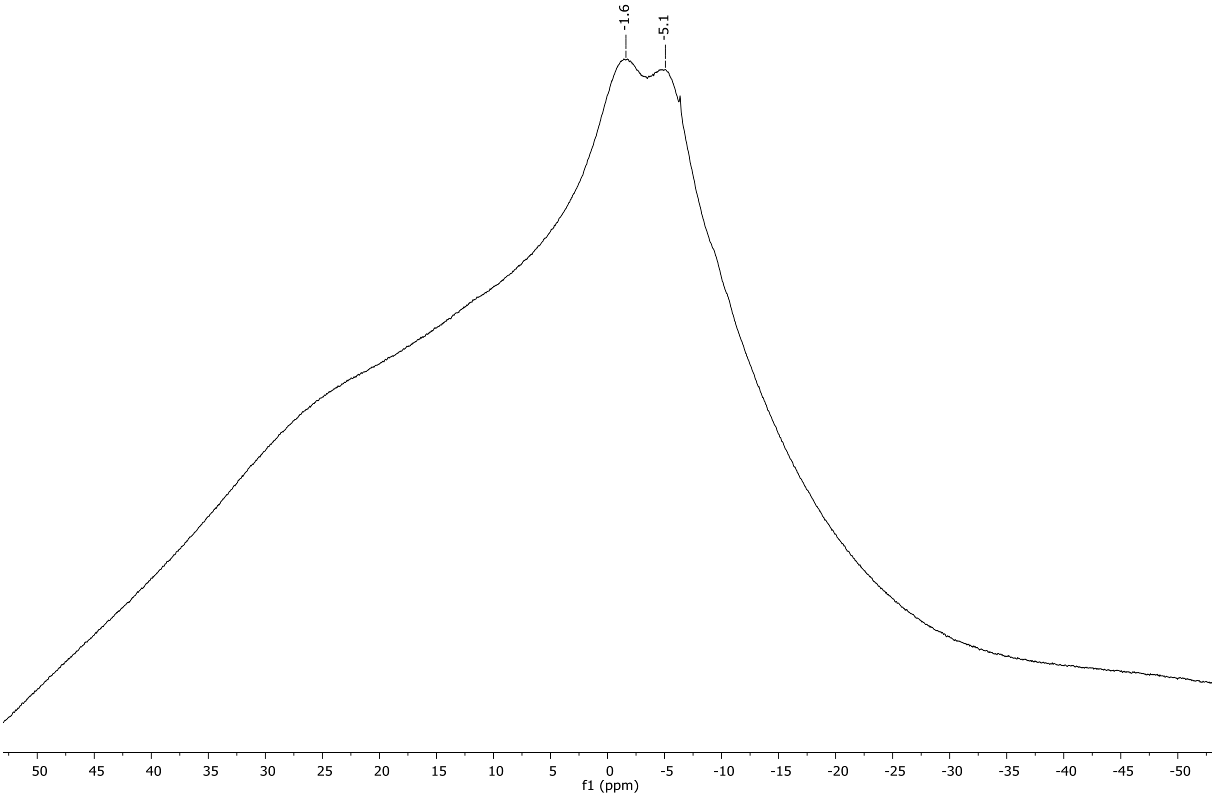

Figure S23. ^{11}B NMR spectrum of K[**2**H] (160.5 MHz, [D$_8$]THF).

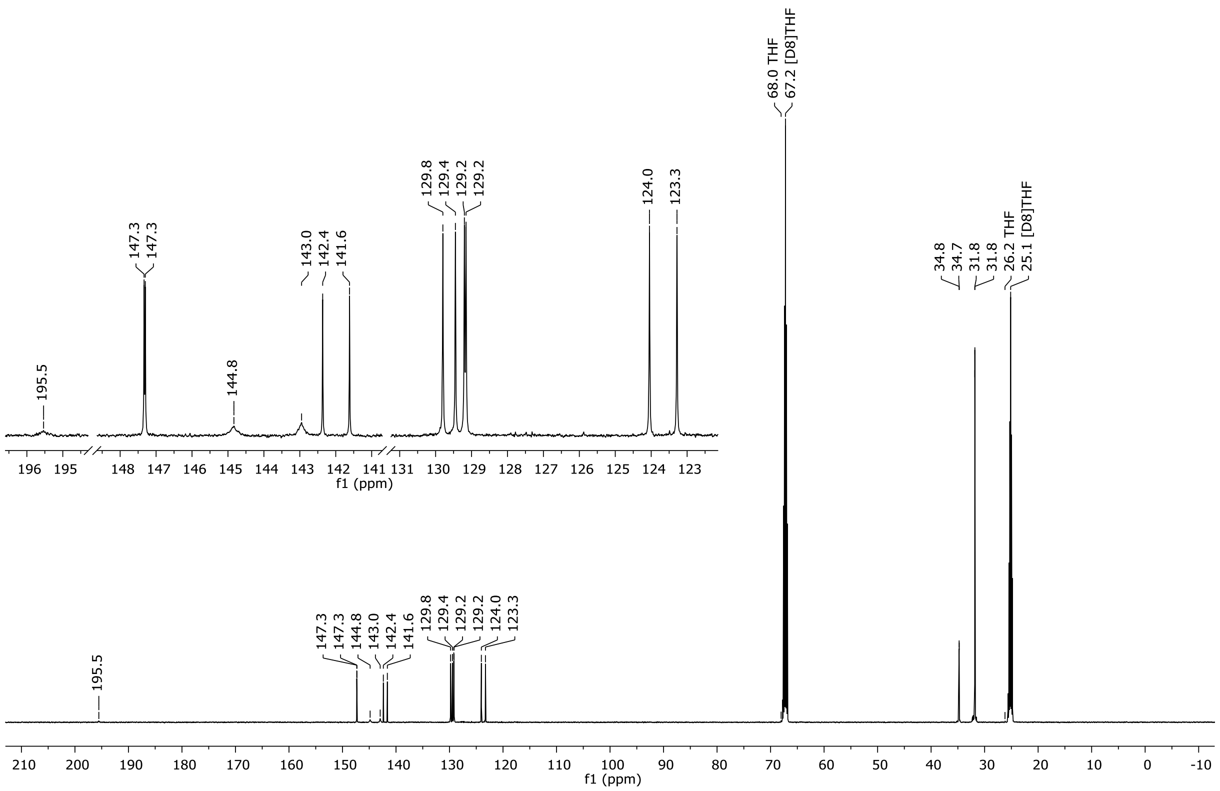

Figure S24. $^{13}C\{^{1}H\}$ NMR spectrum of K[**2**H] (125.8 MHz, [D$_8$]THF).

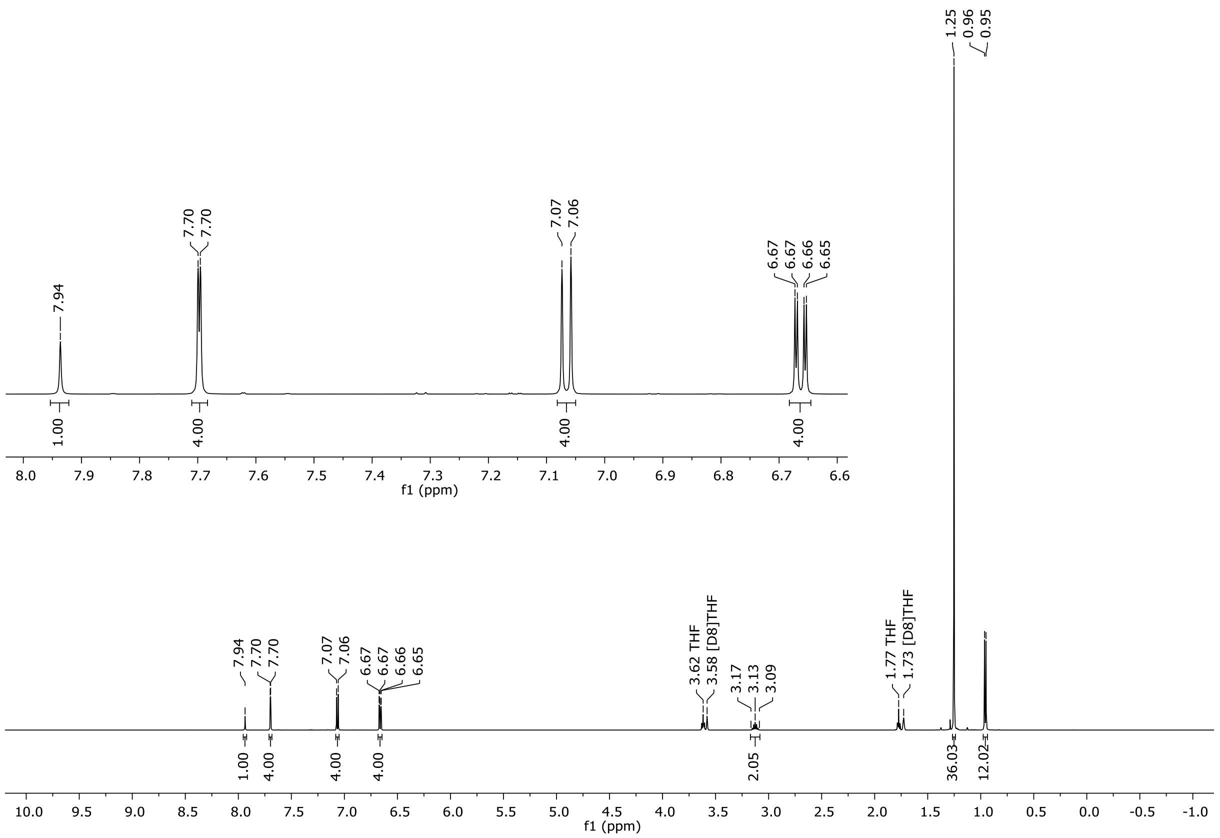

Figure S25. ^{1}H NMR spectrum of Li[**3**] (500.2 MHz, [D$_8$]THF).

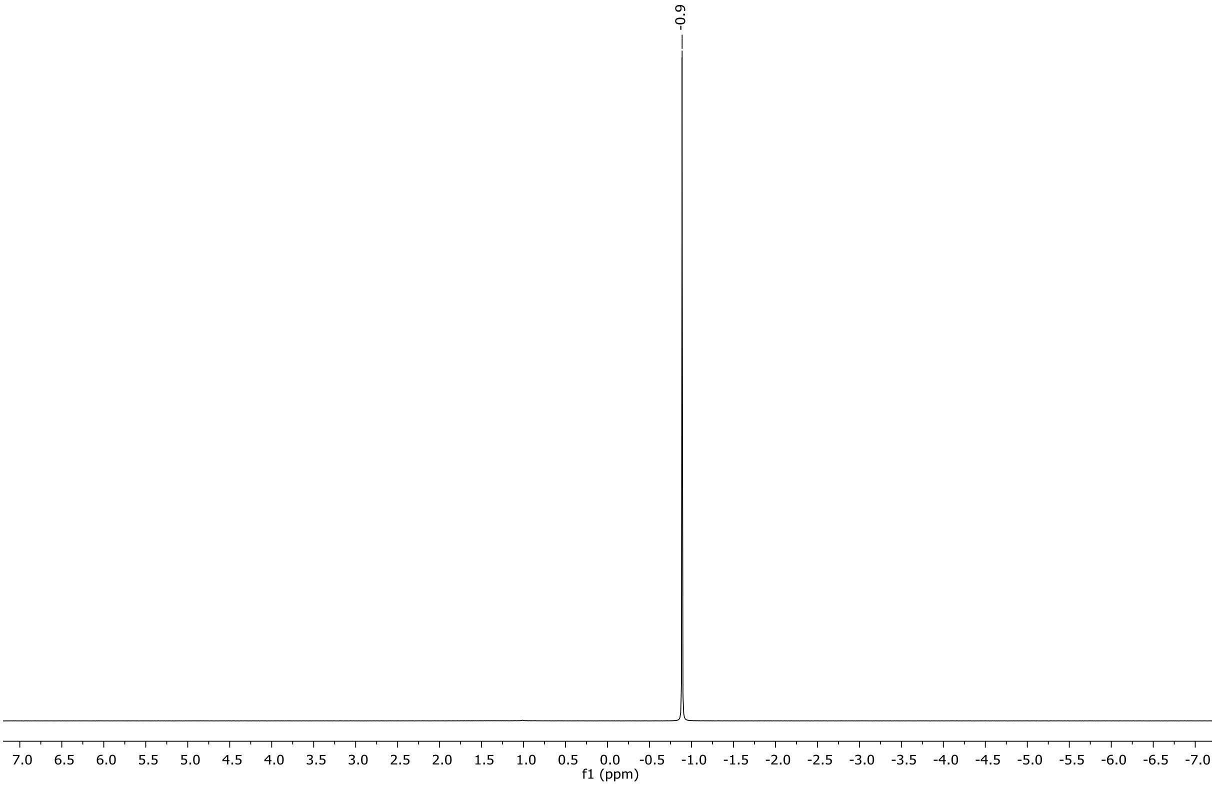

Figure S26. ^{7}Li NMR spectrum of Li[**3**] (194.4 MHz, [D$_8$]THF).

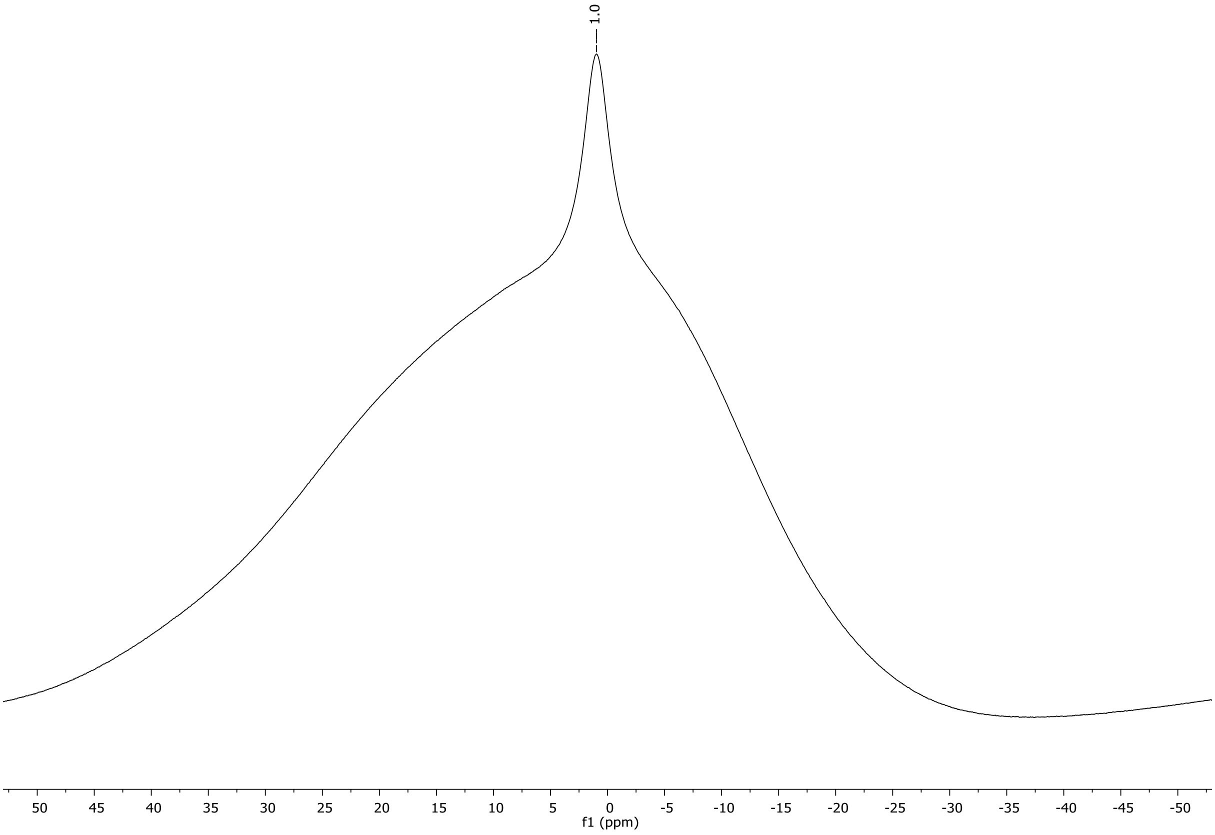

Figure S27. ^{11}B NMR spectrum of Li[**3**] (160.5 MHz, [D$_8$]THF).

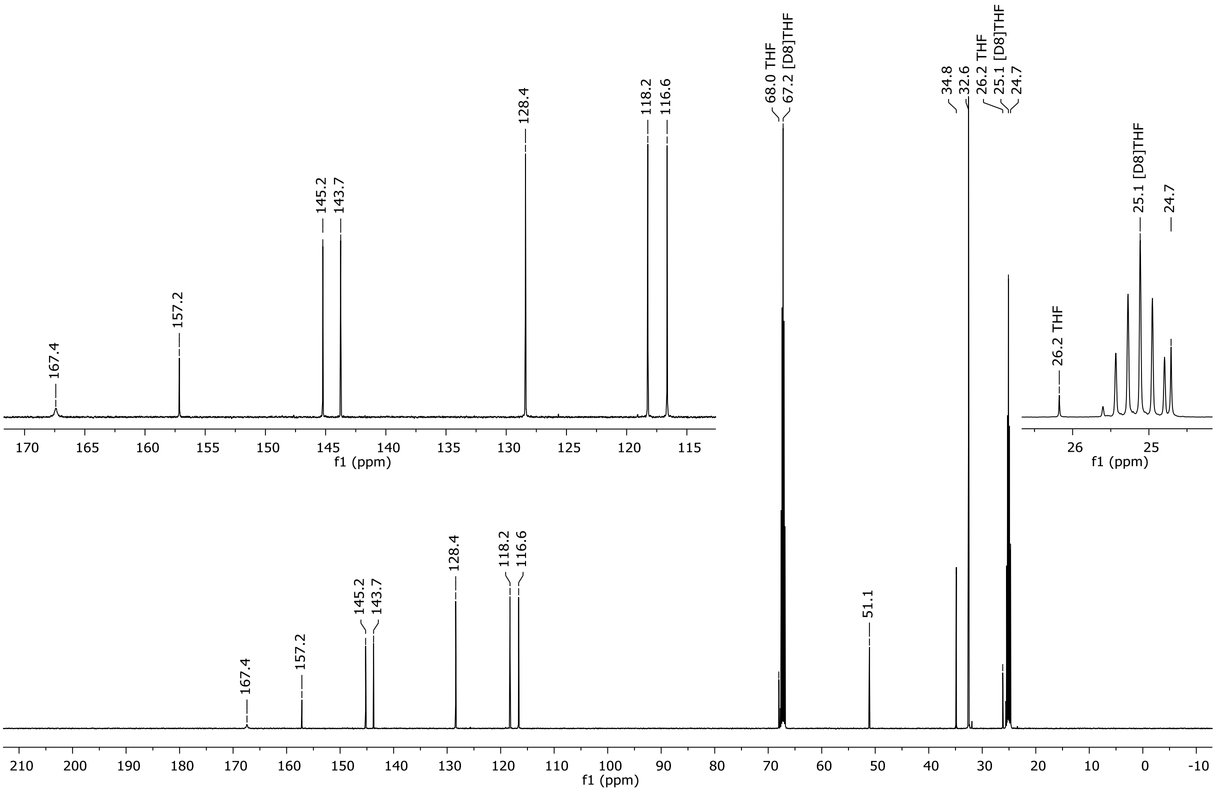

Figure S28. $^{13}C\{^1H\}$ NMR spectrum of Li[**3**] (125.8 MHz, [D$_8$]THF).

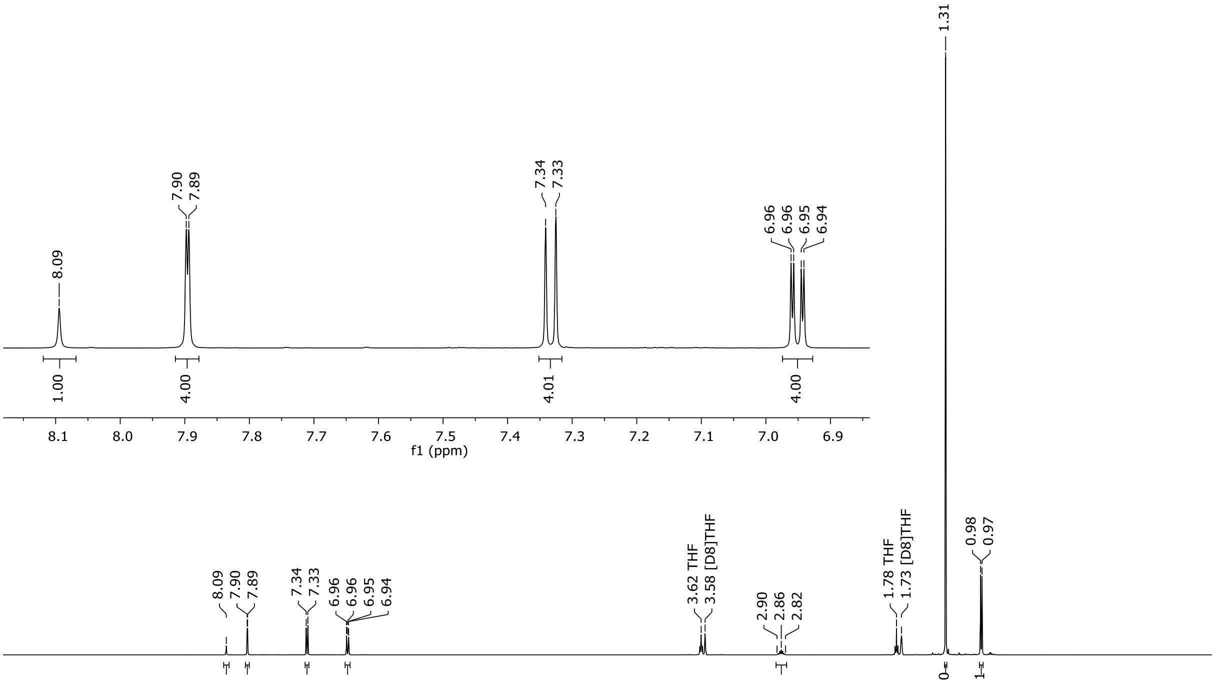

Figure S29. ^1H NMR spectrum of Na[**3**] (500.2 MHz, [D$_8$]THF).

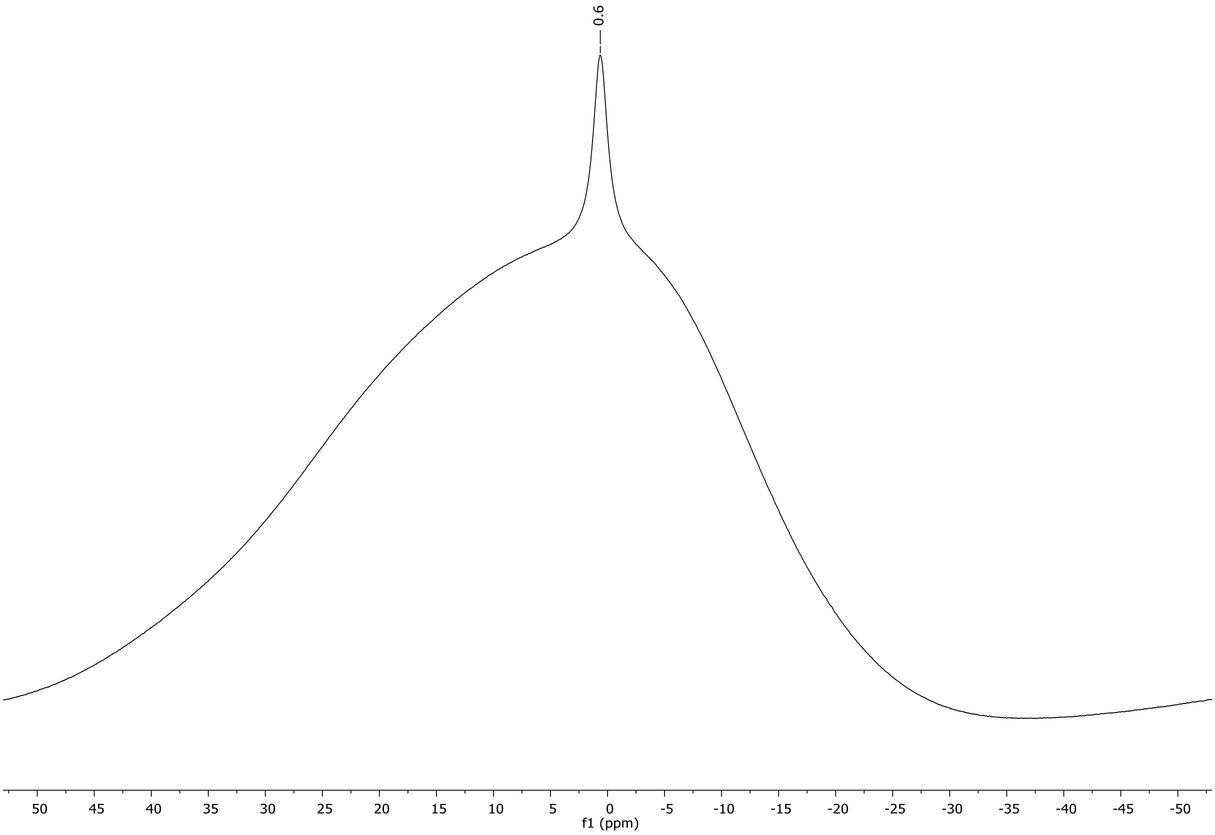

Figure S30. ^{11}B NMR spectrum of Na[**3**] (160.5 MHz, [D$_8$]THF).

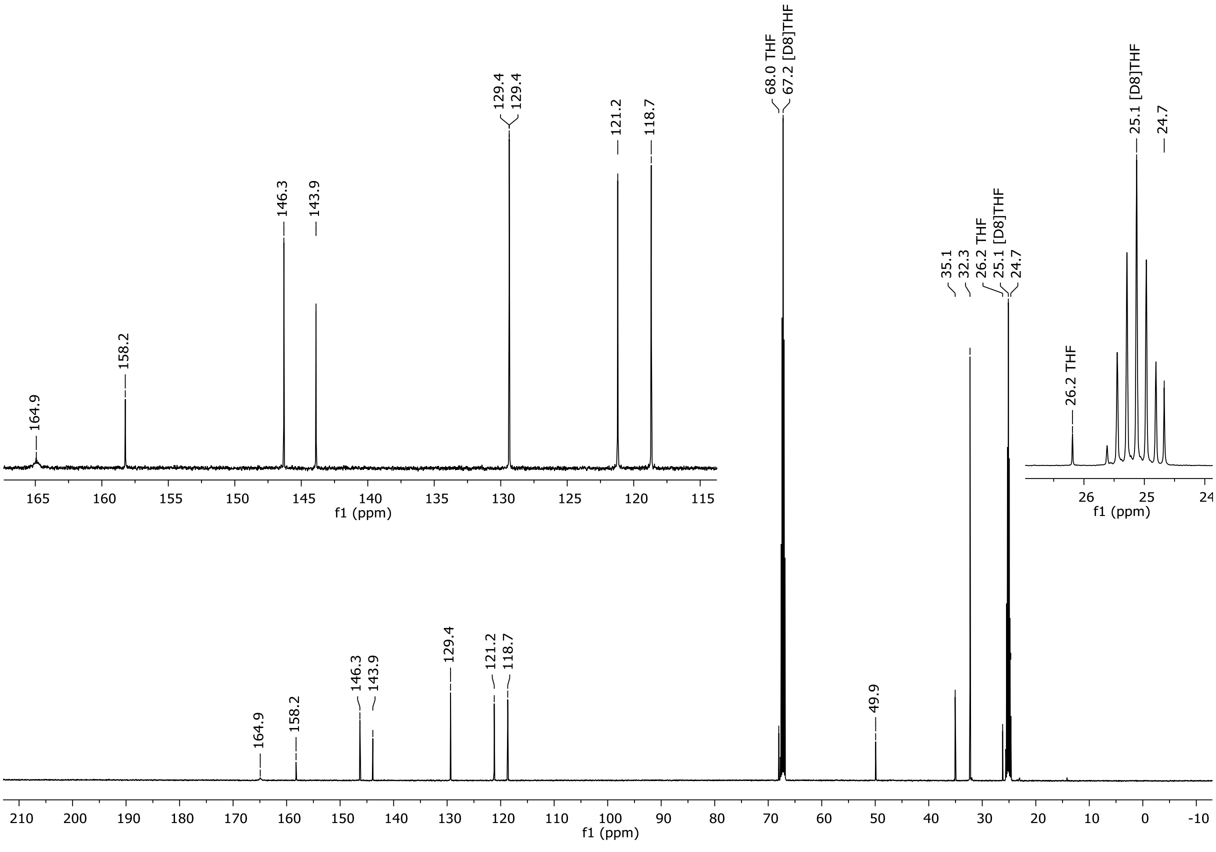

Figure S31. ^{13}C{^{1}H} NMR spectrum of Na[**3**] (125.8 MHz, [D$_8$]THF).

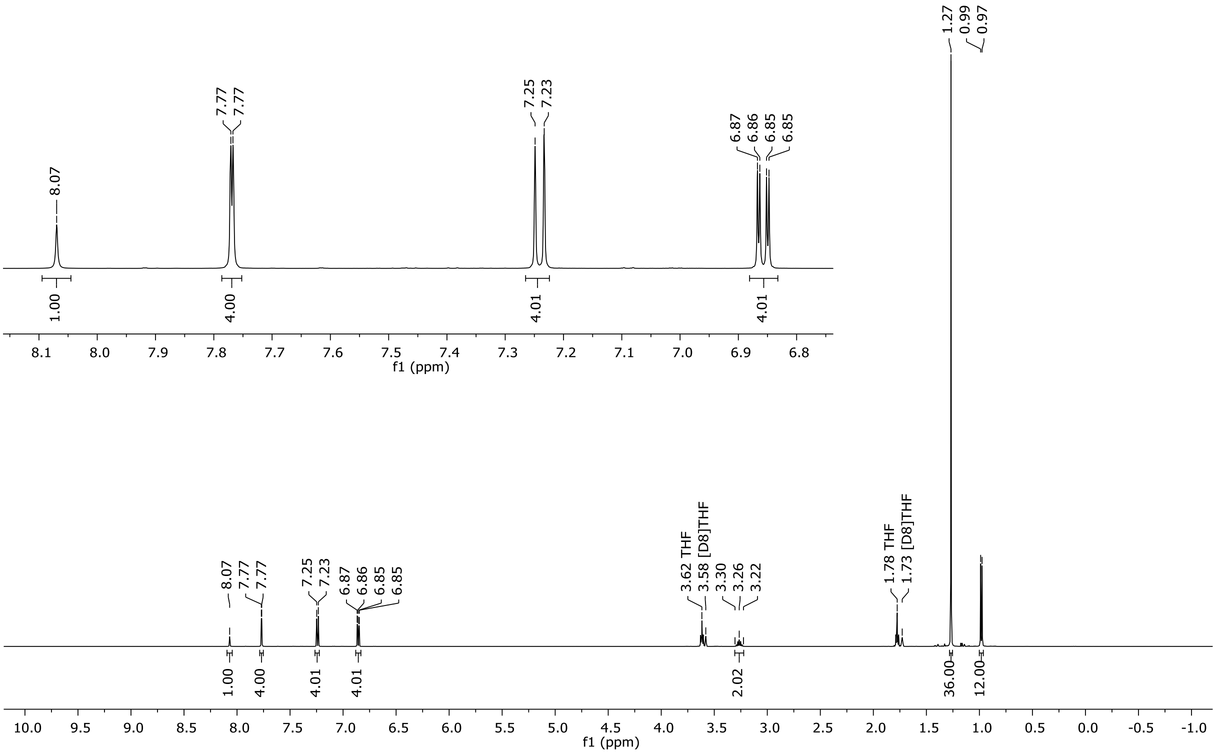

Figure S32. ^{1}H NMR spectrum of K[**3**] (500.2 MHz, [D$_8$]THF).

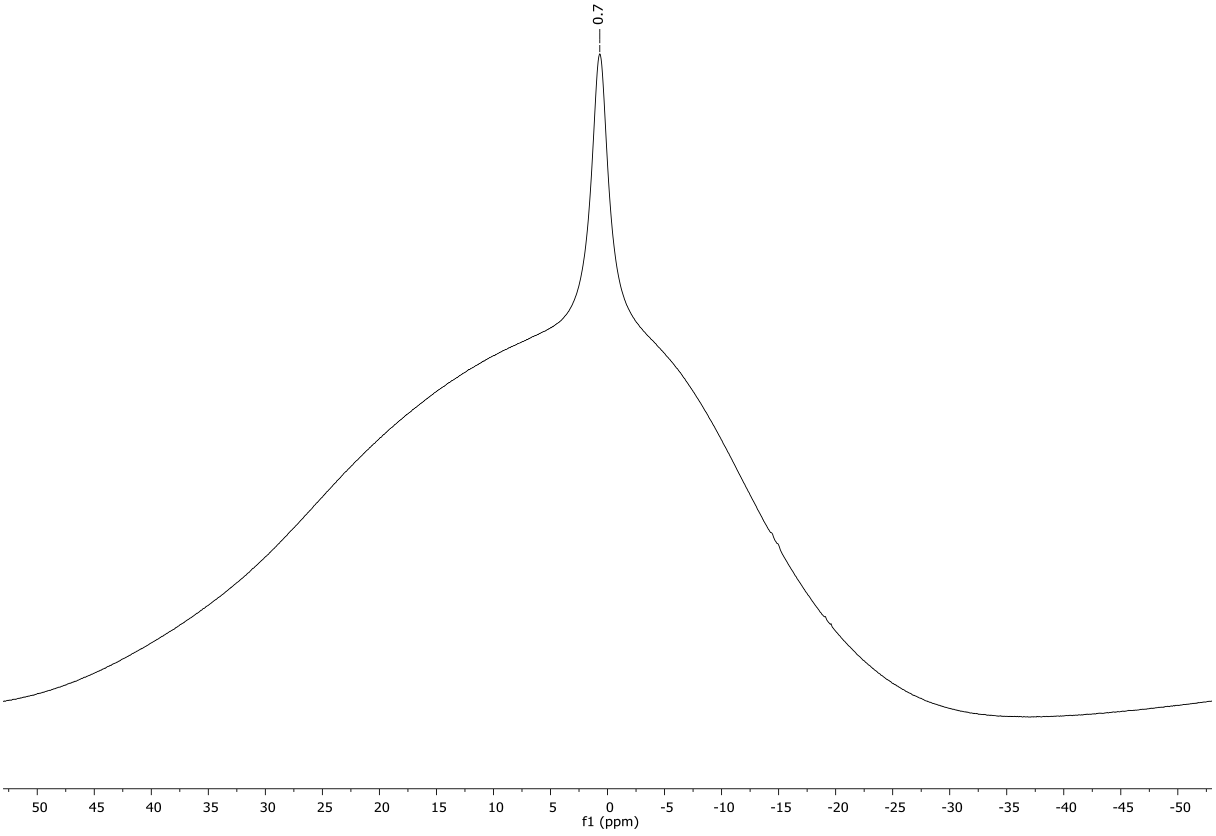

Figure S33. ^{11}B NMR spectrum of K[**3**] (160.5 MHz, [D$_8$]THF).

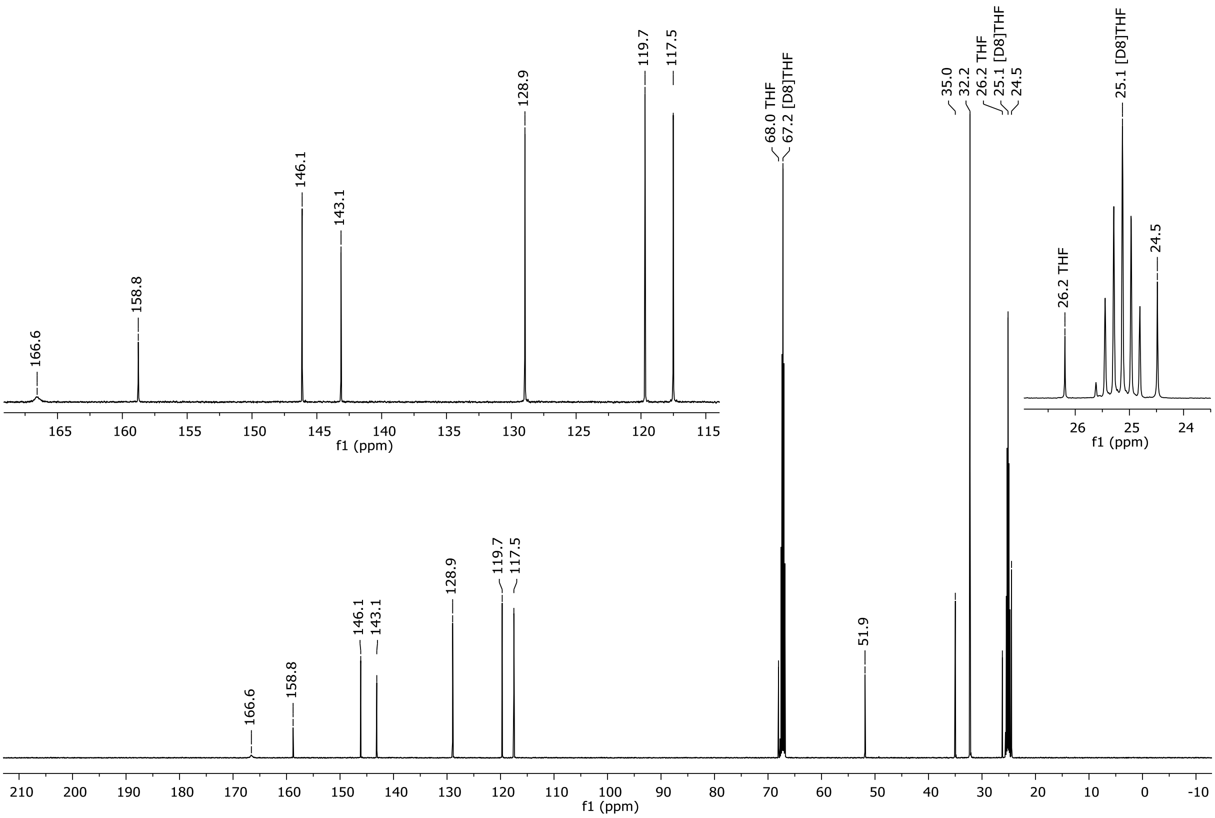

Figure S34. $^{13}C\{^{1}H\}$ NMR spectrum of K[**3**] (125.8 MHz, $[D_8]THF$).

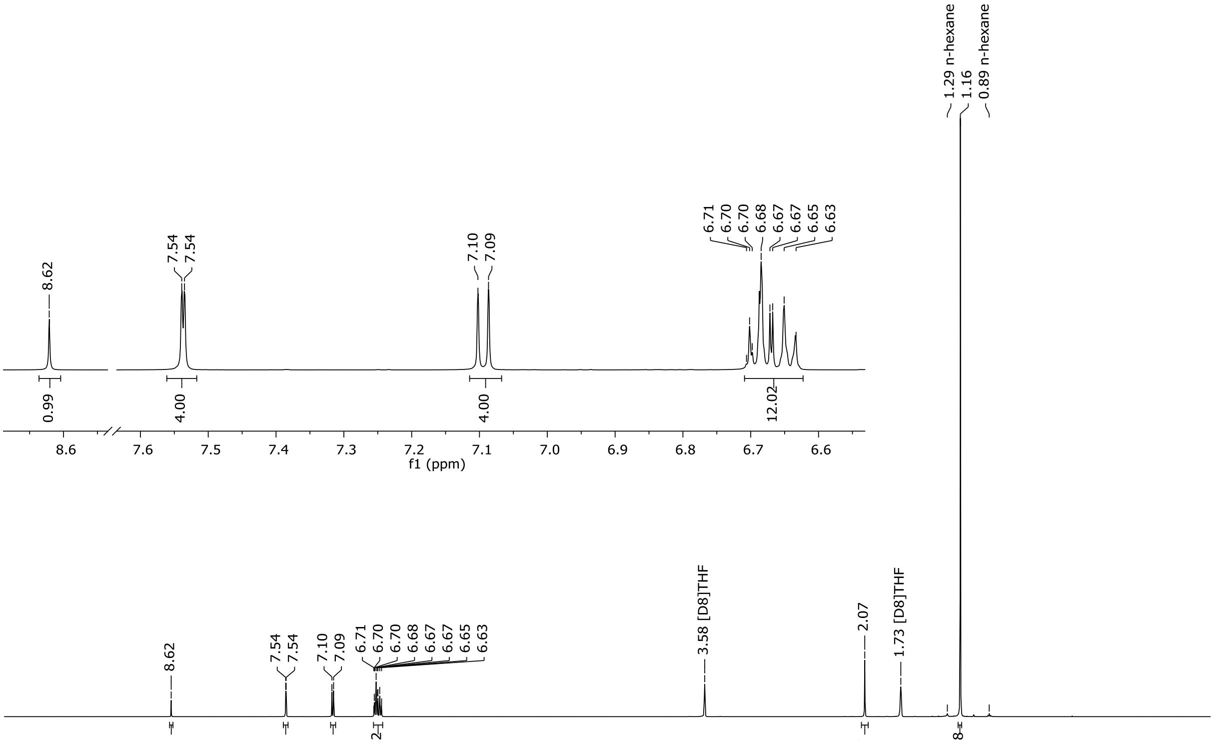

Figure S35. ^{1}H NMR spectrum of Li[**7**] (500.2 MHz, $[D_8]THF$).

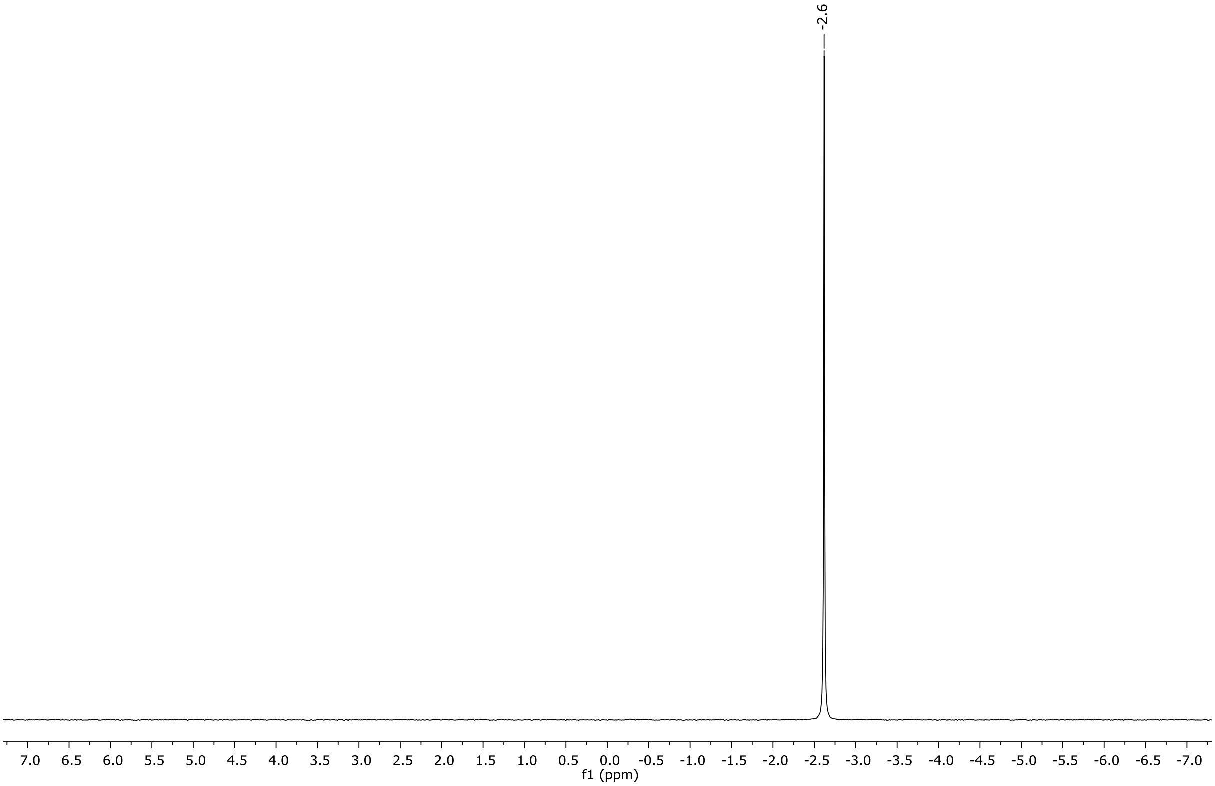

Figure S36. ^{7}Li NMR spectrum of Li[**7**] (116.6 MHz, [D$_8$]THF).

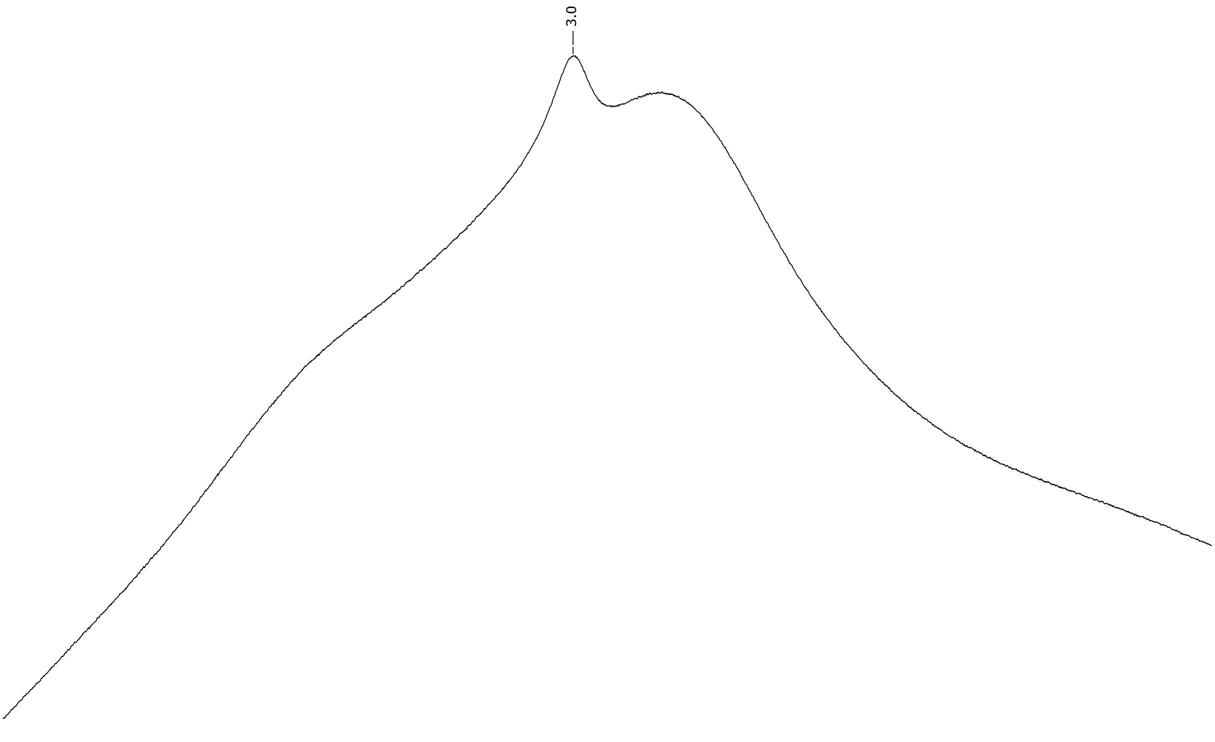

Figure S37. ^{11}B NMR spectrum of Li[**7**] (160.5 MHz, [D$_8$]THF).

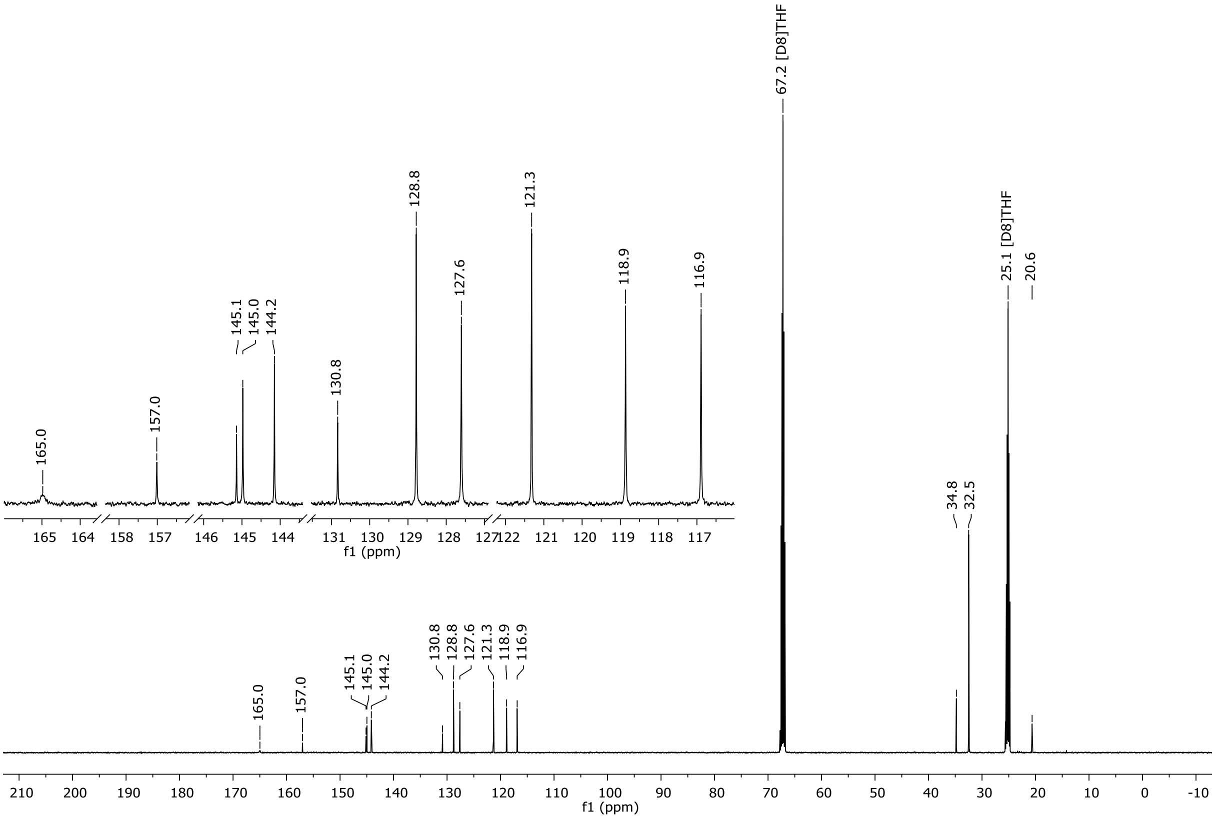

Figure S38. $^{13}C\{^{1}H\}$ NMR spectrum of Li[**7**] (125.8 MHz, [D$_8$]THF).

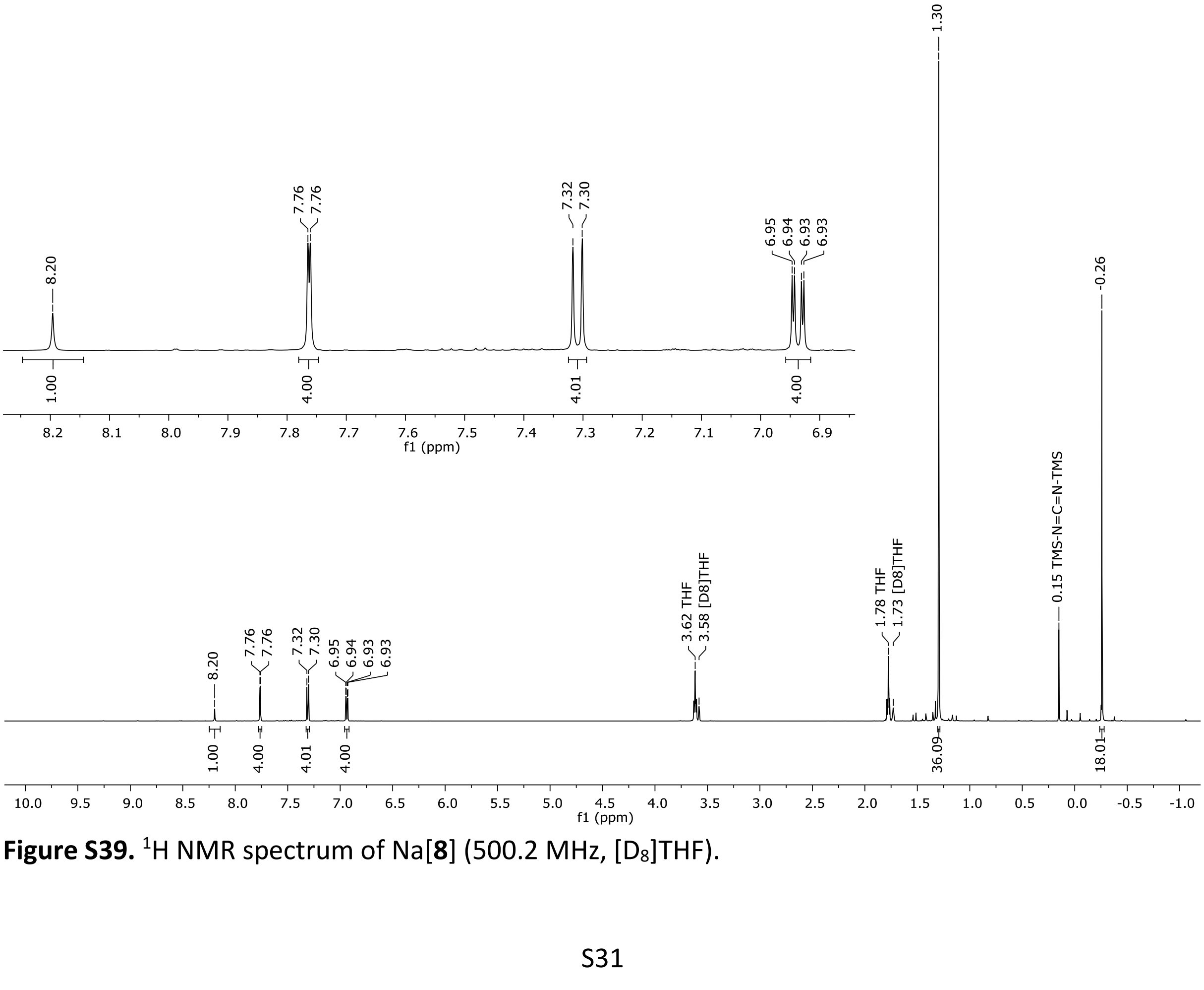

Figure S39. ^{1}H NMR spectrum of Na[**8**] (500.2 MHz, [D$_8$]THF).

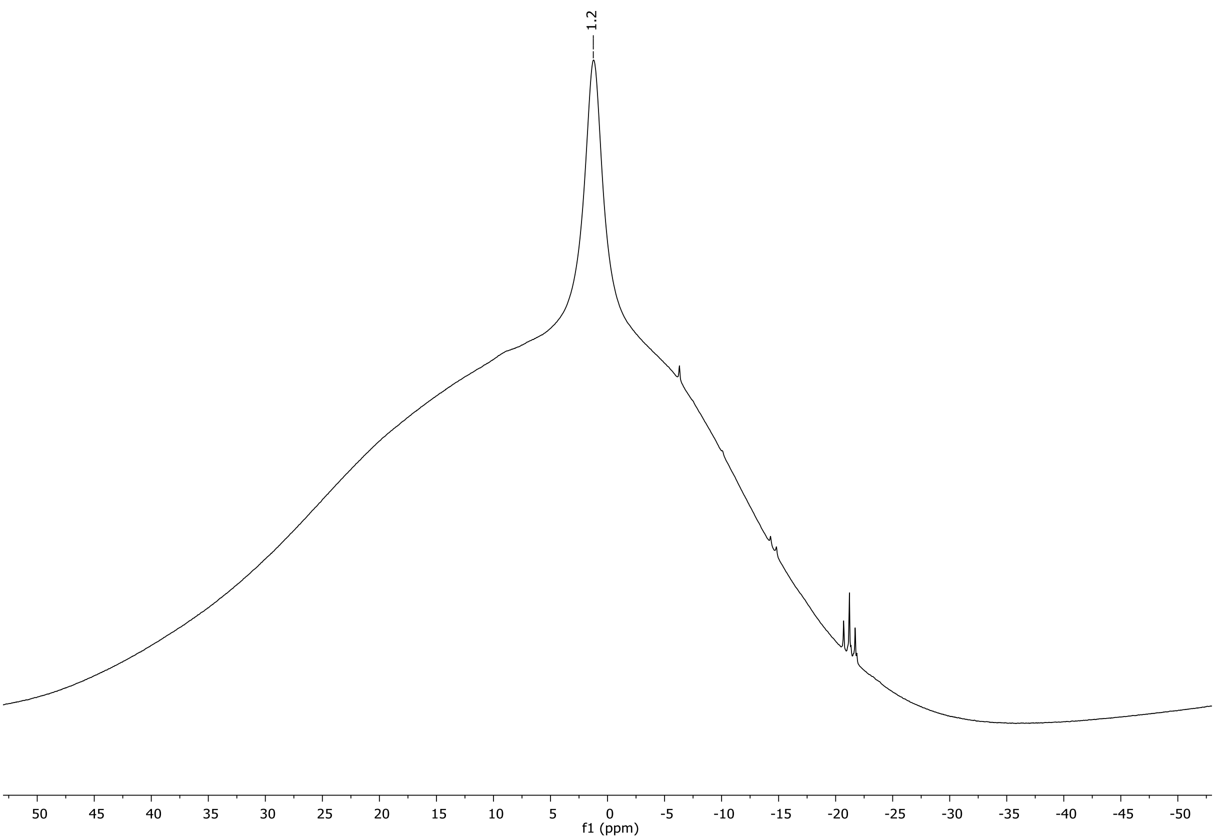

Figure S40. ^{11}B NMR spectrum of Na[**8**] (160.5 MHz, [D$_8$]THF).

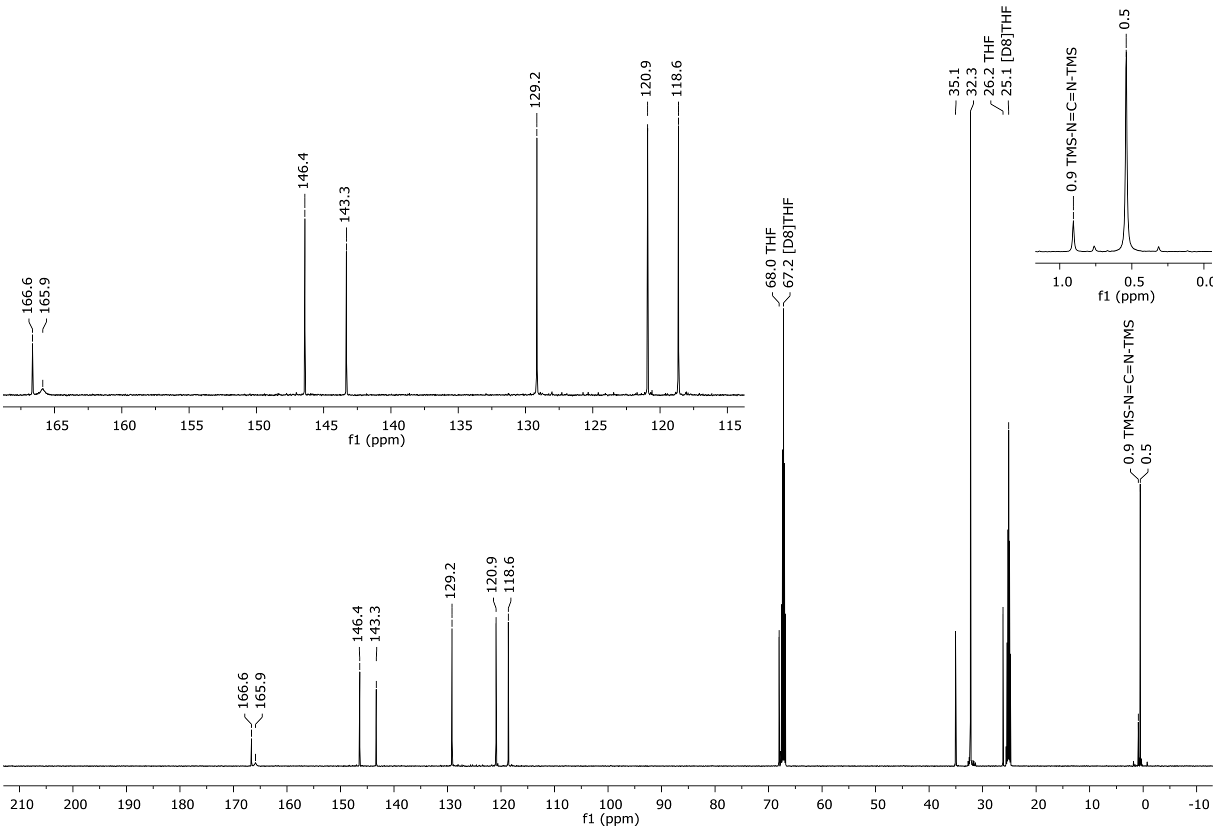

Figure S41. ^{13}C{^{1}H} NMR spectrum of Na[**8**] (125.8 MHz, [D$_8$]THF).

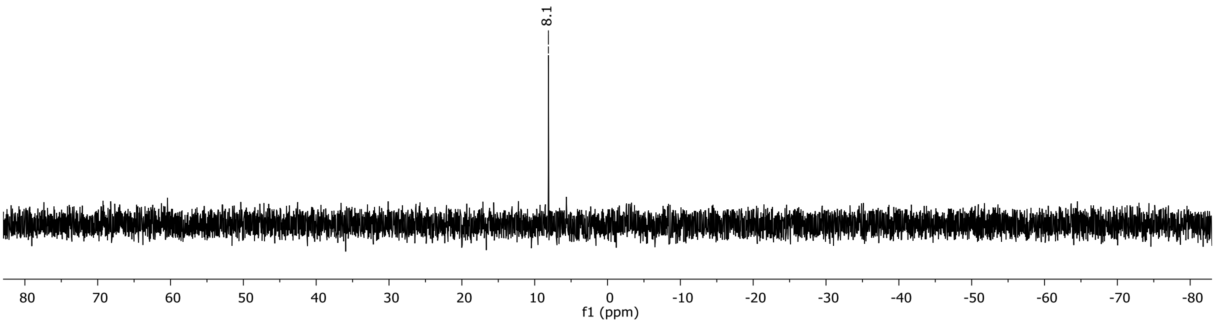

Figure S42. ^{29}Si INEPT NMR spectrum of Na[**8**] (99.4 MHz, [D$_8$]THF).

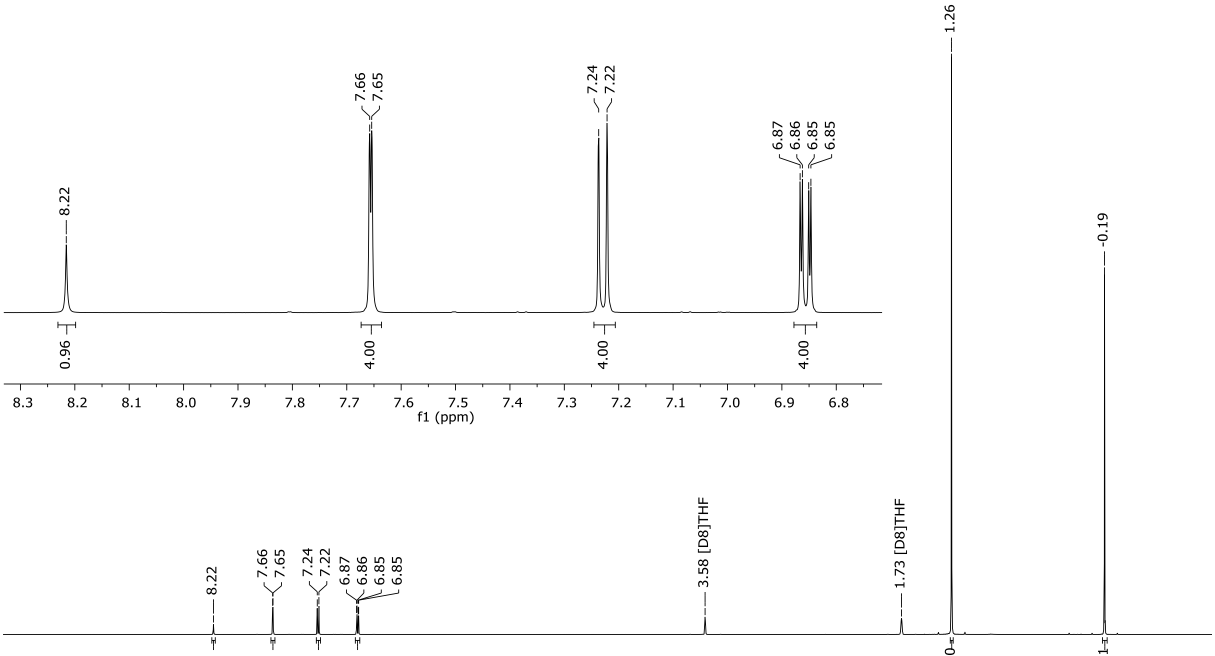

Figure S43. ^{1}H NMR spectrum of K[**8**] (500.2 MHz, [D$_8$]THF).

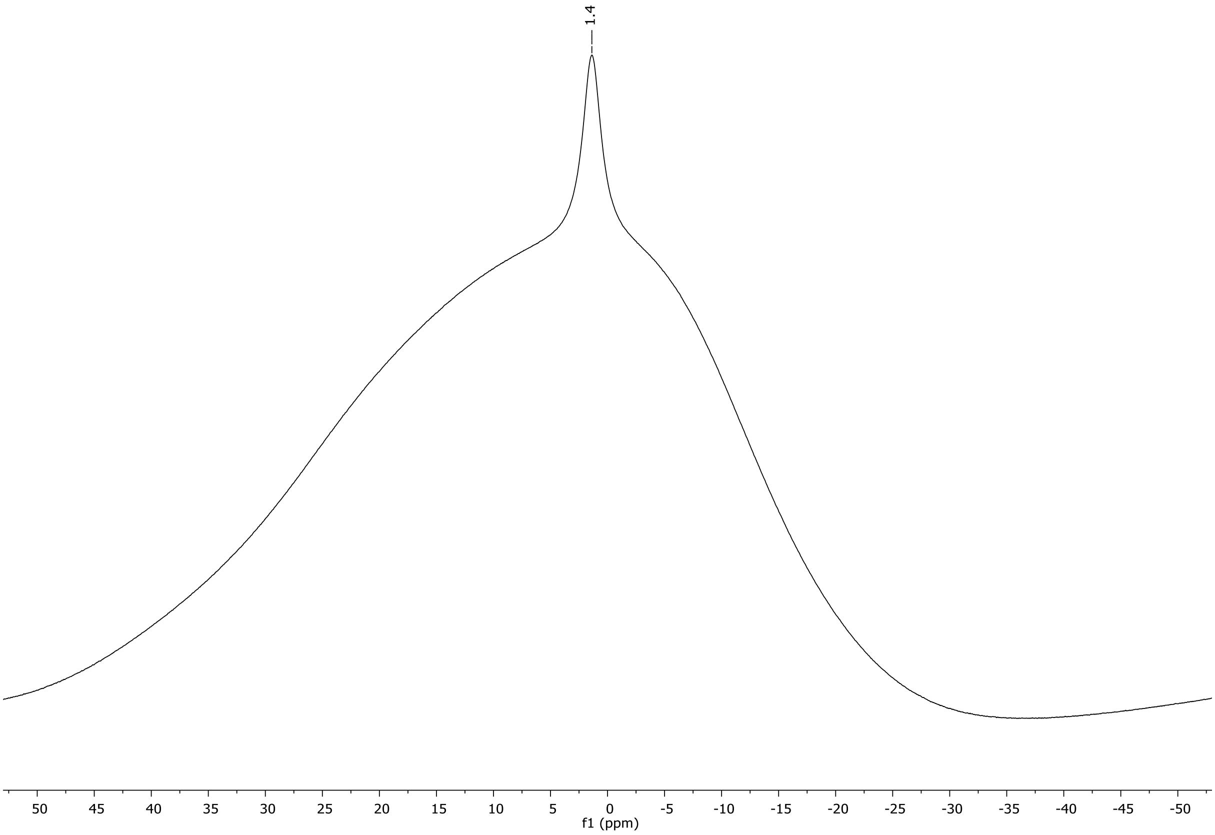

Figure S44. ^{11}B NMR spectrum of K[**8**] (160.5 MHz, [D_8]THF).

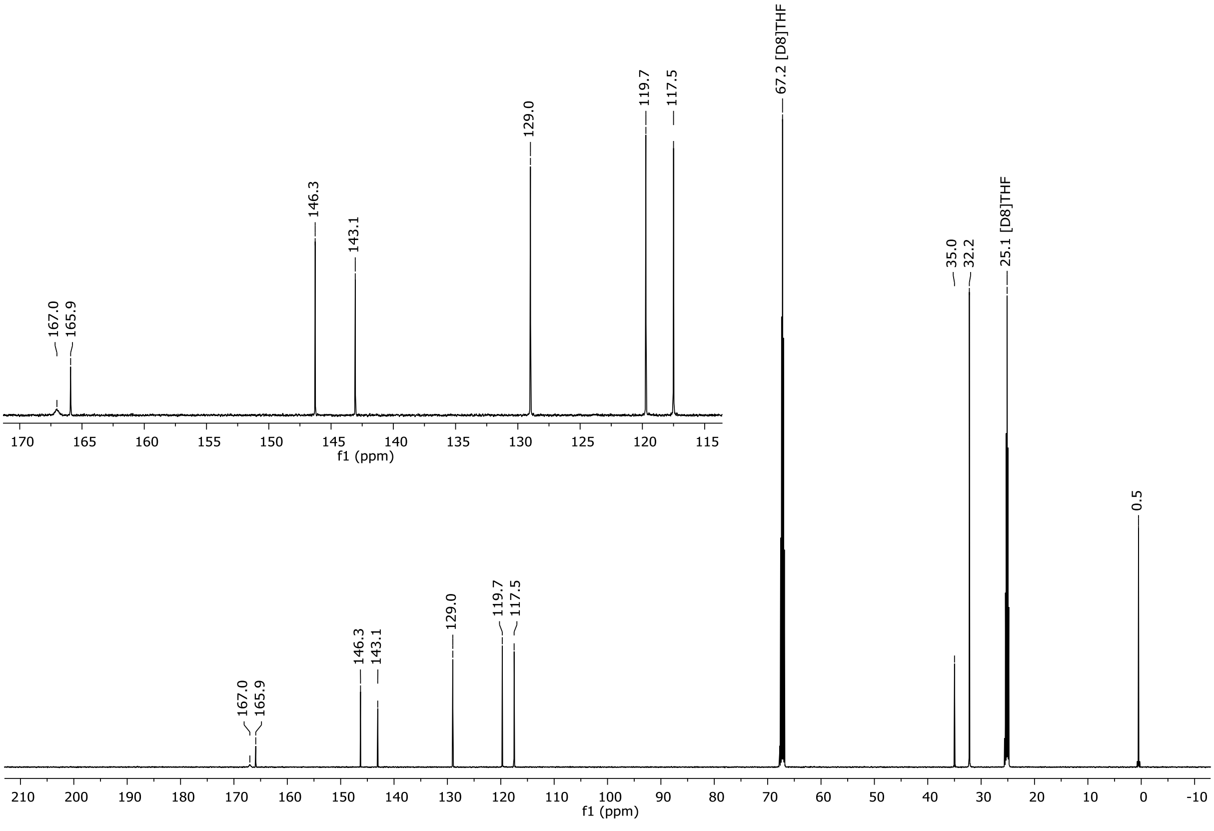

Figure S45. $^{13}C\{^1H\}$ NMR spectrum of K[**8**] (125.8 MHz, [D_8]THF).

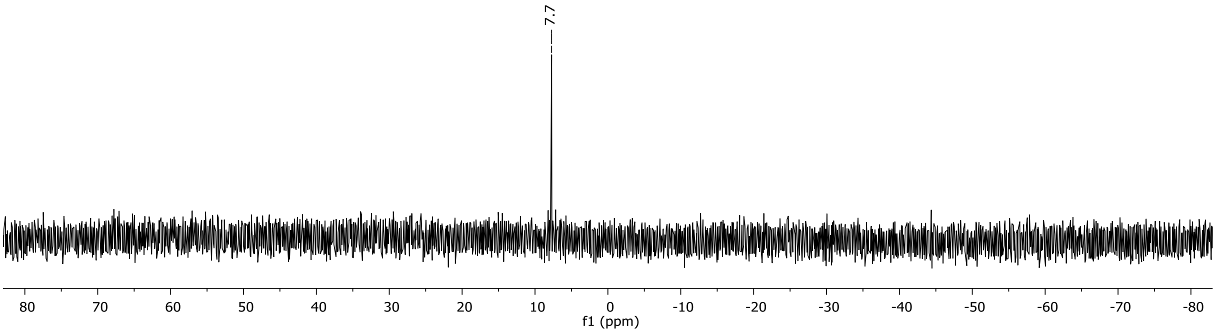

Figure S46. ^{29}Si{^{1}H} NMR spectrum of K[**8**] (99.4 MHz, [D$_8$]THF).

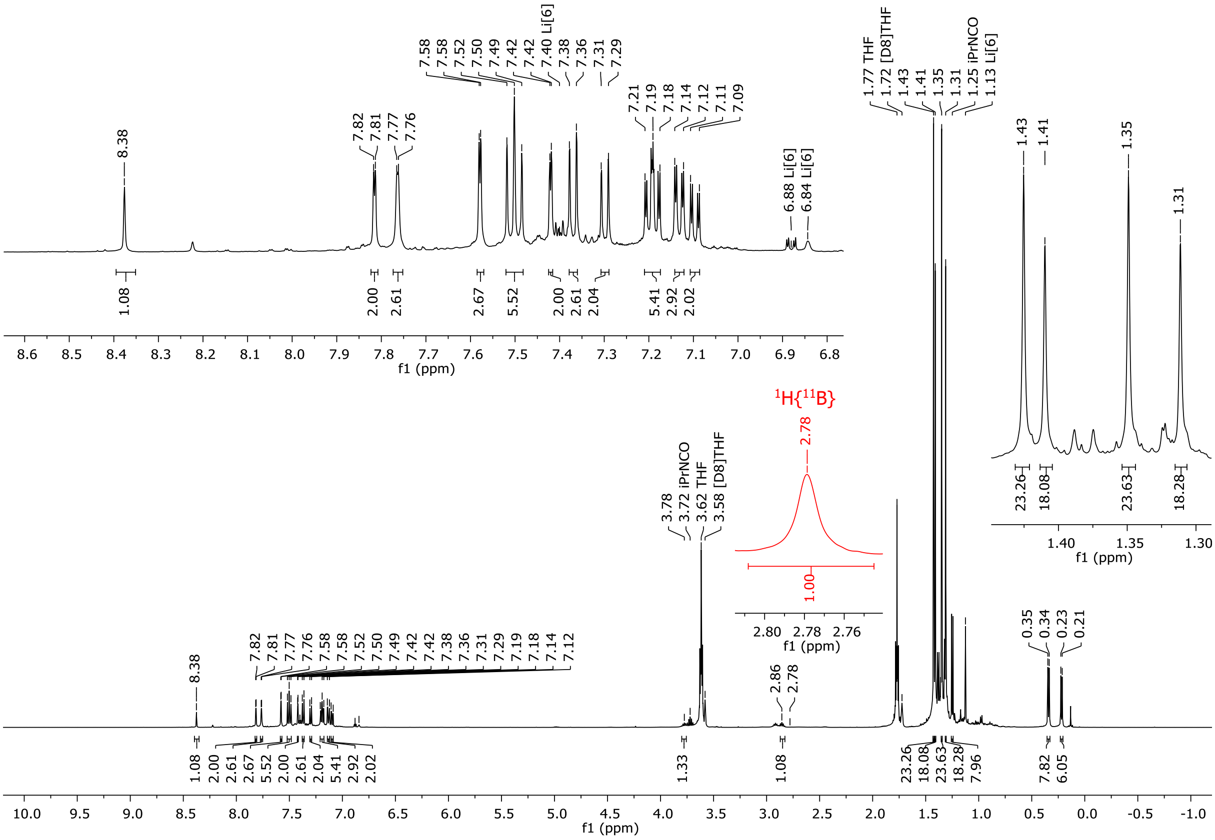

Figure S47. ^{1}H NMR spectrum of the reaction mixture of Li[**1**H] with exc. isopropyl isocyanate (500.2 MHz, [D$_8$]THF). The signals of the two main products Li[**4**H] and Li[**5**] are picked and integrated; signals of one known minor component Li[**6**] are picked and labelled accordingly but are not integrated.

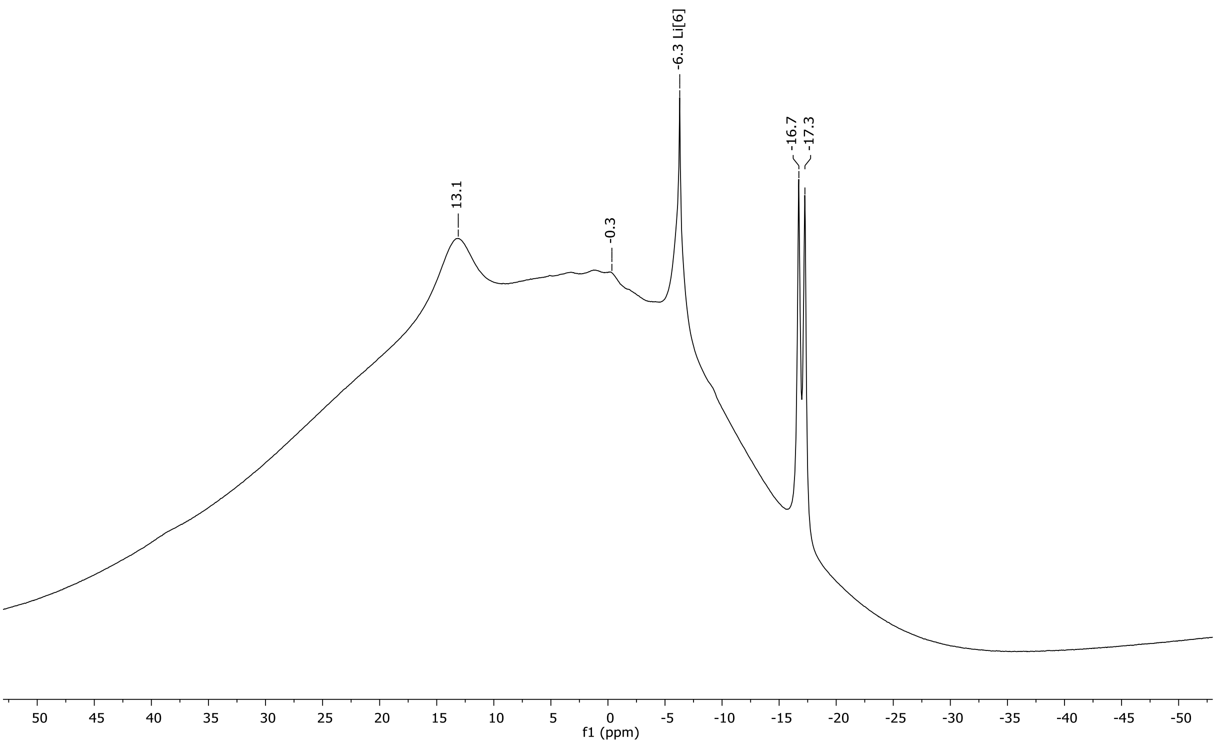

Figure S48. ^{11}B NMR spectrum of the reaction mixture of Li[**1**H] with exc. isopropyl isocyanate (160.5 MHz, [D$_8$]THF). The signals of the two main products Li[**4**H] and Li[**5**] are picked; signals of one known minor component Li[**6**] are picked as well and labelled accordingly.

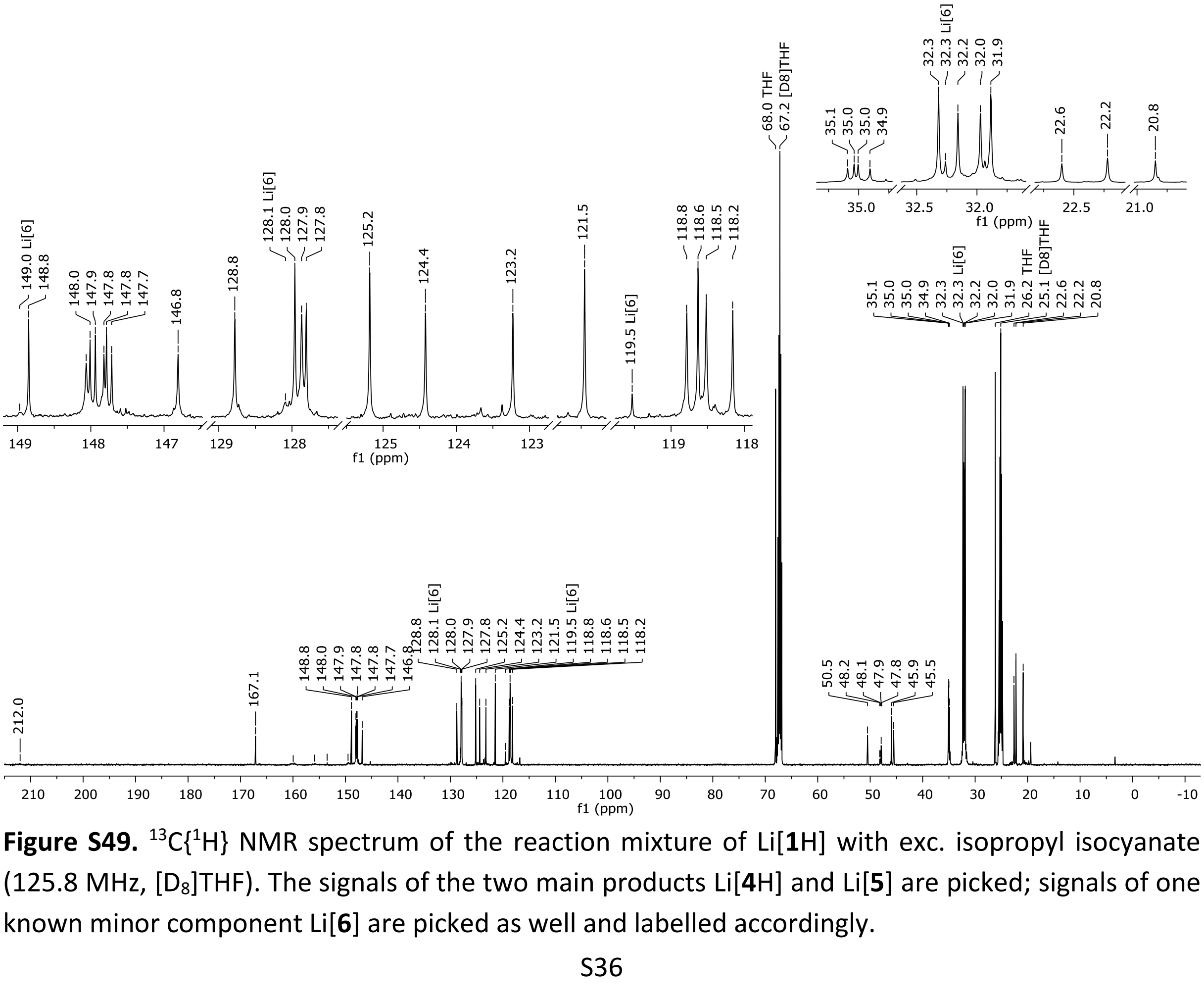

Figure S49. ^{13}C{^{1}H} NMR spectrum of the reaction mixture of Li[**1**H] with exc. isopropyl isocyanate (125.8 MHz, [D$_8$]THF). The signals of the two main products Li[**4**H] and Li[**5**] are picked; signals of one known minor component Li[**6**] are picked as well and labelled accordingly.

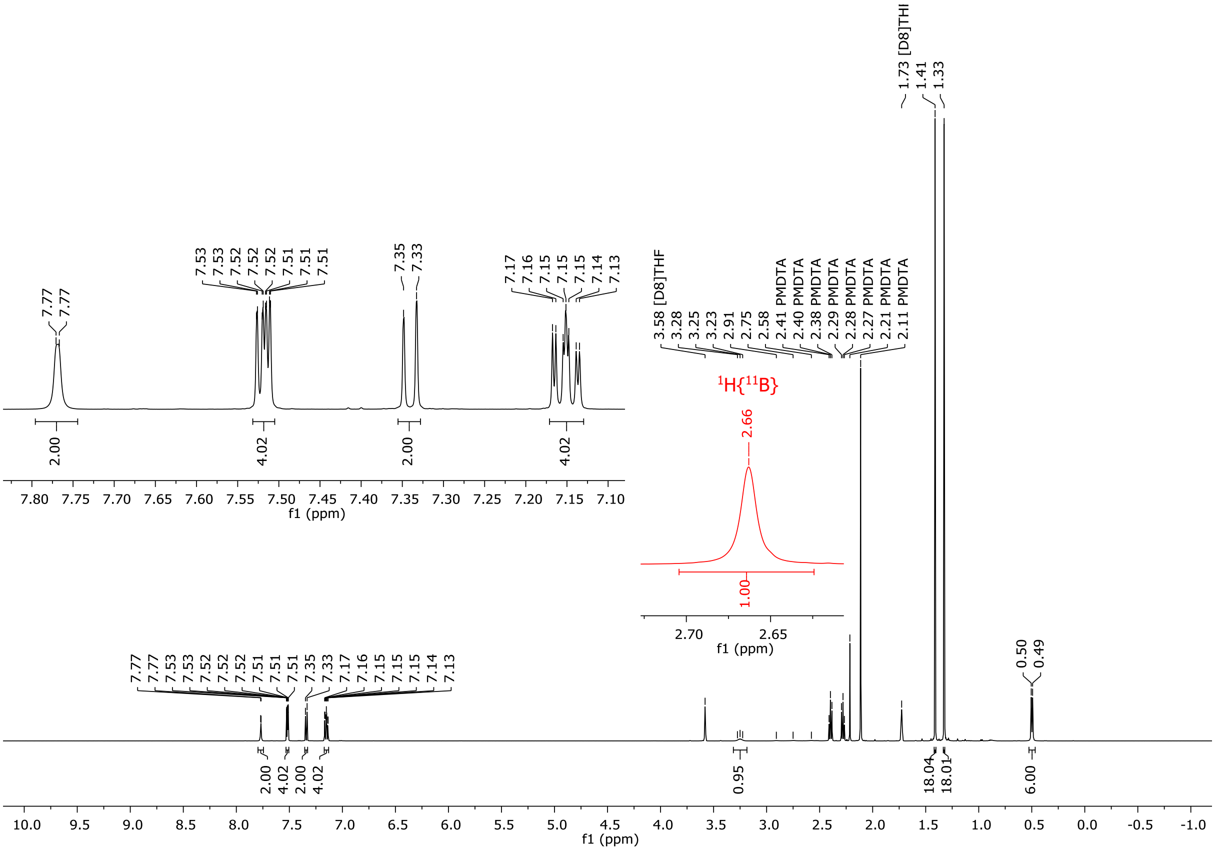

Figure S50. ^1H NMR spectrum of Na[**4**H] (500.2 MHz, [D$_8$]THF).

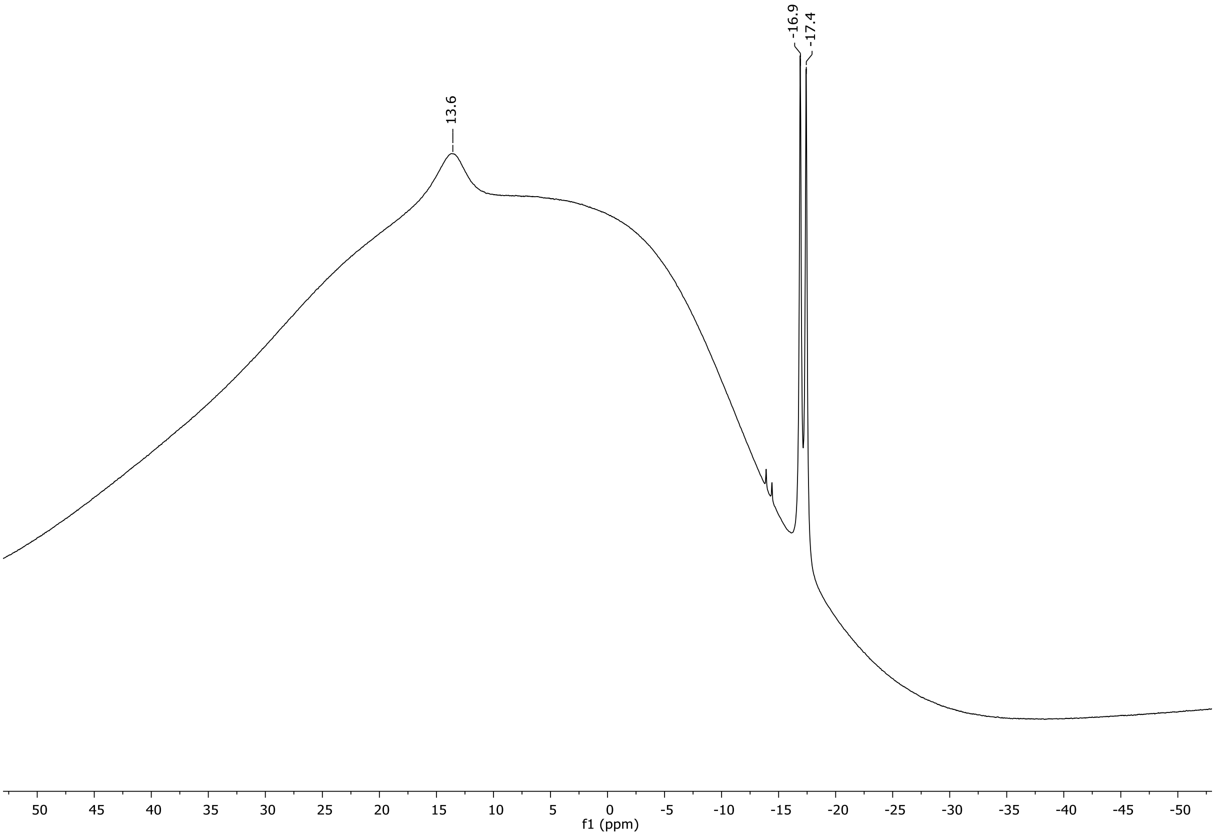

Figure S51. ^{11}B NMR spectrum of Na[**4**H] (160.5 MHz, [D$_8$]THF).

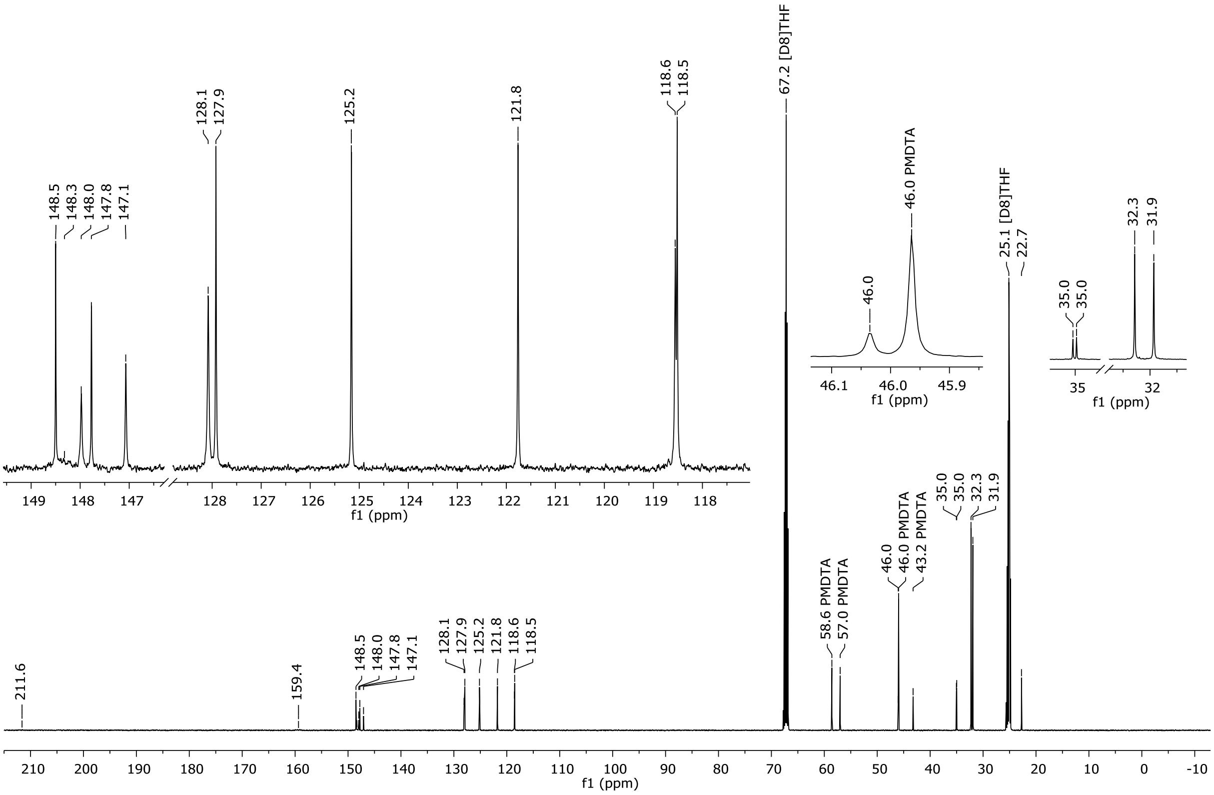

Figure S52. $^{13}C\{^1H\}$ NMR spectrum of Na[**4**H] (125.8 MHz, [D$_8$]THF).

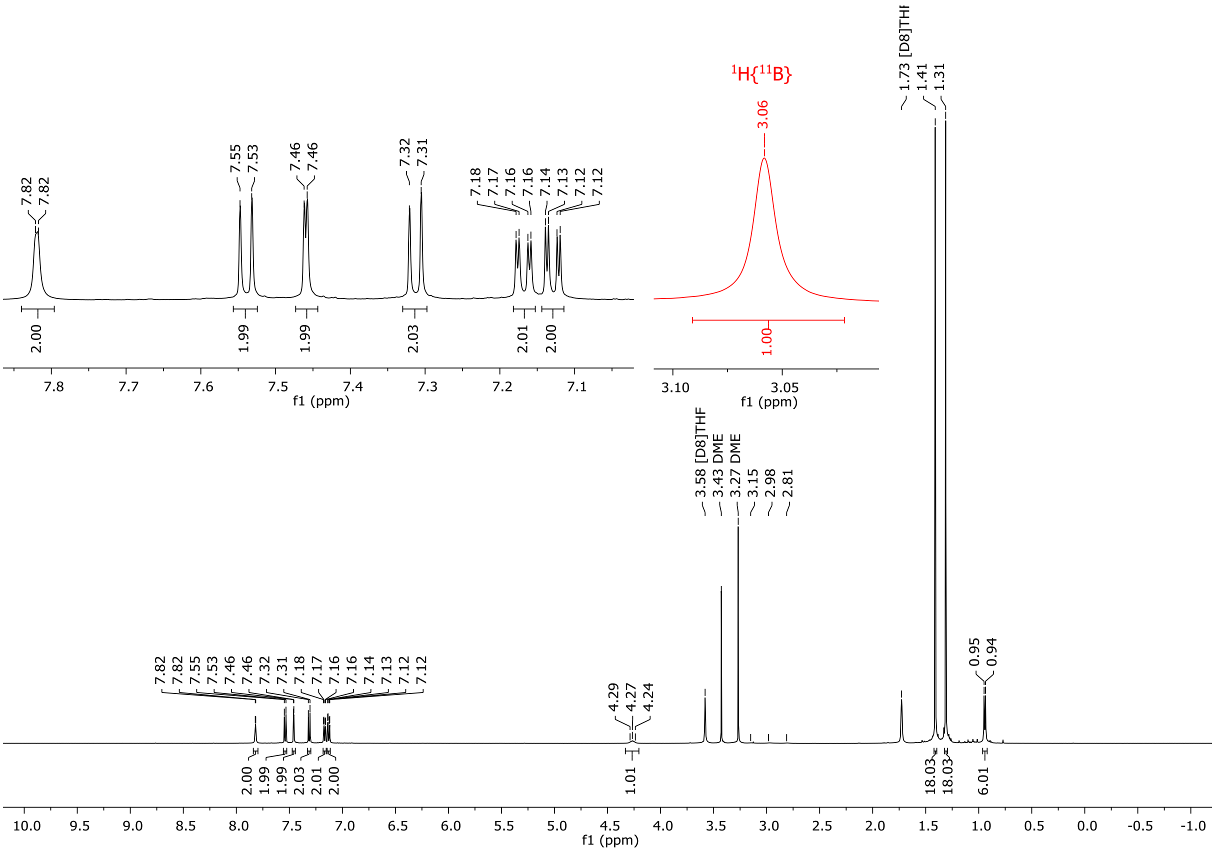

Figure S53. ^1H NMR spectrum of K[**4**H] (500.2 MHz, [D$_8$]THF).

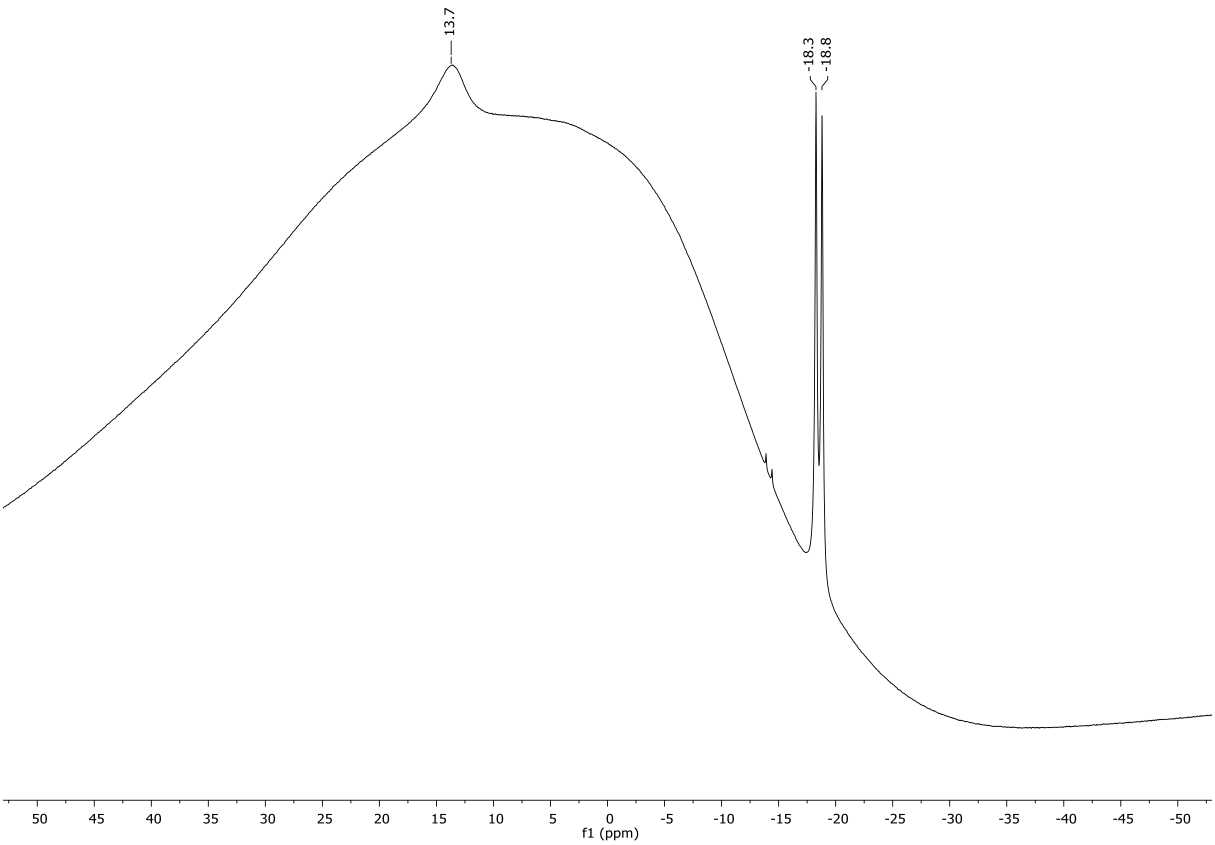

Figure S54. ^{11}B NMR spectrum of K[**4**H] (160.5 MHz, [D$_8$]THF).

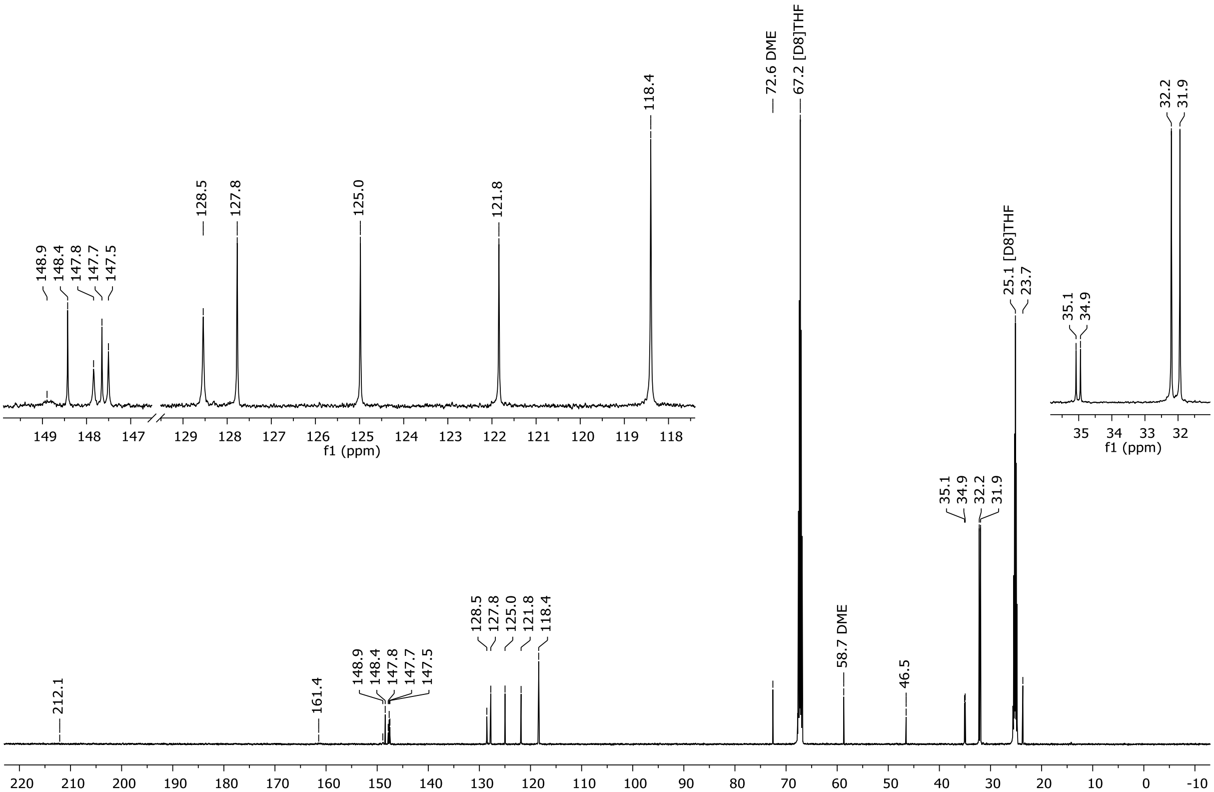

Figure S55. ^{13}C{^{1}H} NMR spectrum of K[**4**H] (125.8 MHz, [D$_8$]THF).

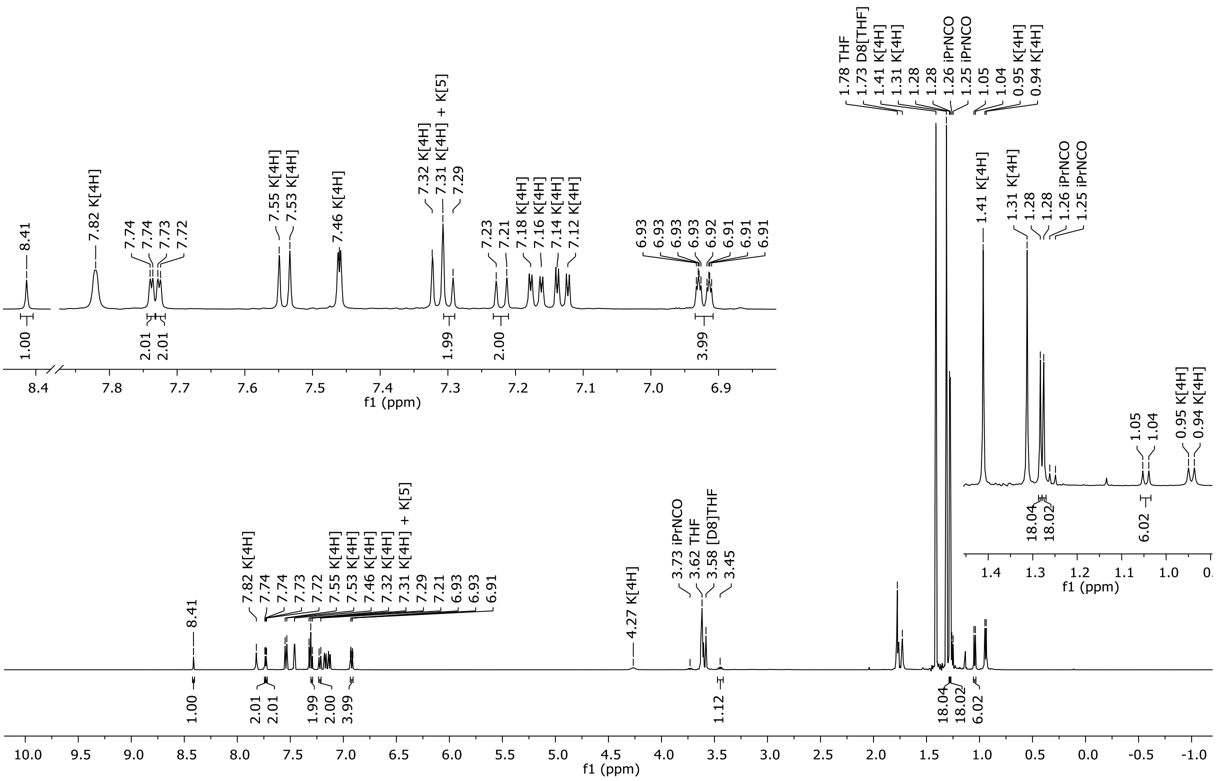

Figure S56. ^{1}H NMR spectrum of a mixture of K[**4**H] and K[**5**] (500.2 MHz, [D$_8$]THF). Signals of K[**4**H] are picked and labelled accordingly but are not integrated.

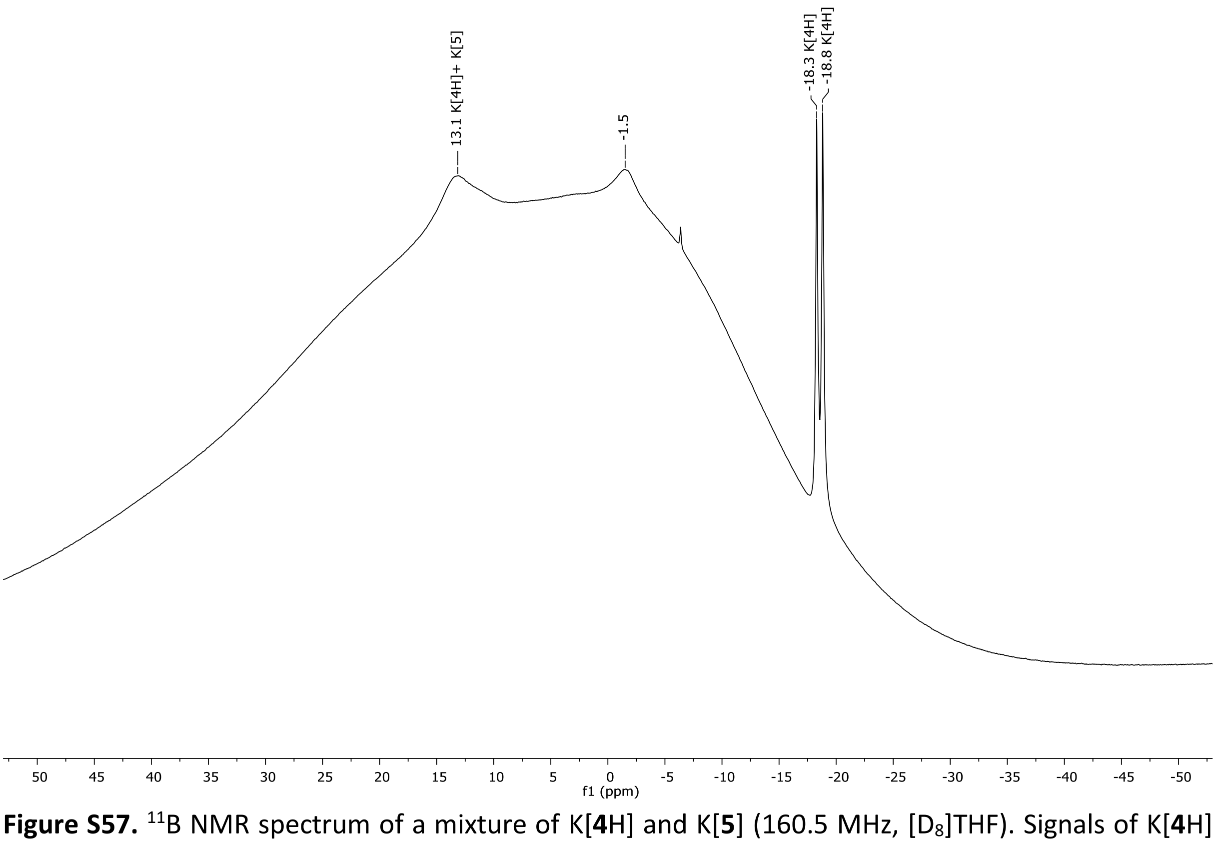

Figure S57. ^{11}B NMR spectrum of a mixture of K[**4**H] and K[**5**] (160.5 MHz, [D$_8$]THF). Signals of K[**4**H] are picked and labelled accordingly.

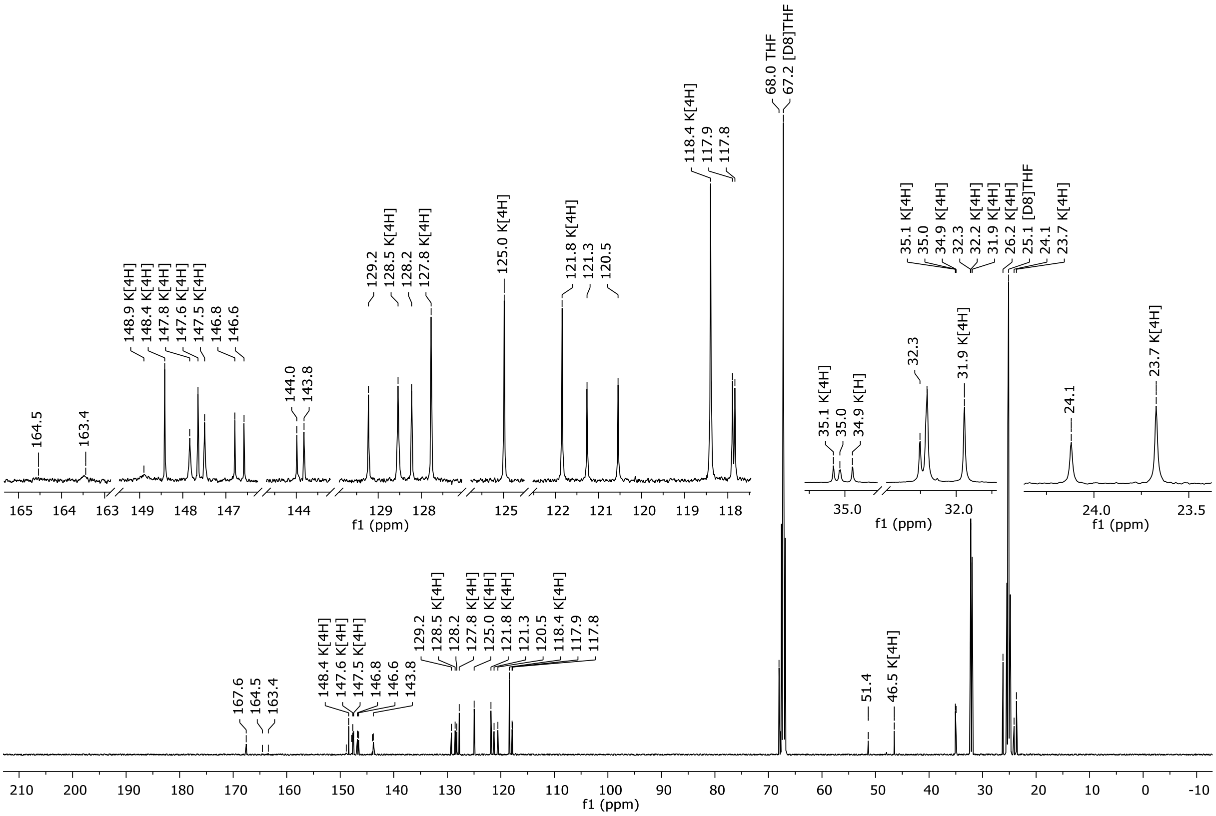

Figure S58. $^{13}C\{^{1}H\}$ NMR spectrum of a mixture of K[**4**H] and K[**5**] (125.8 MHz, [D$_8$]THF). Signals of K[**4**H] are picked and labelled accordingly.

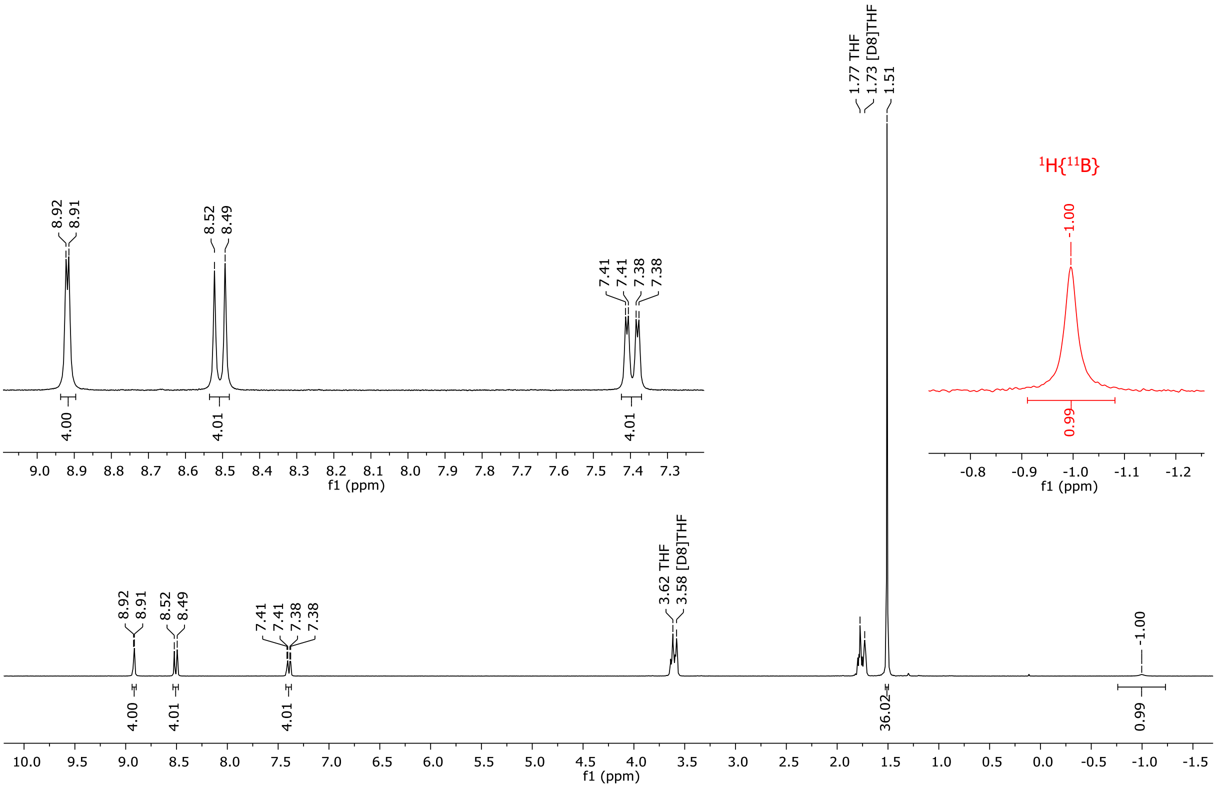

Figure S59. ^{1}H NMR spectrum of Na[**1**H] (300.0 MHz, [D$_8$]THF).

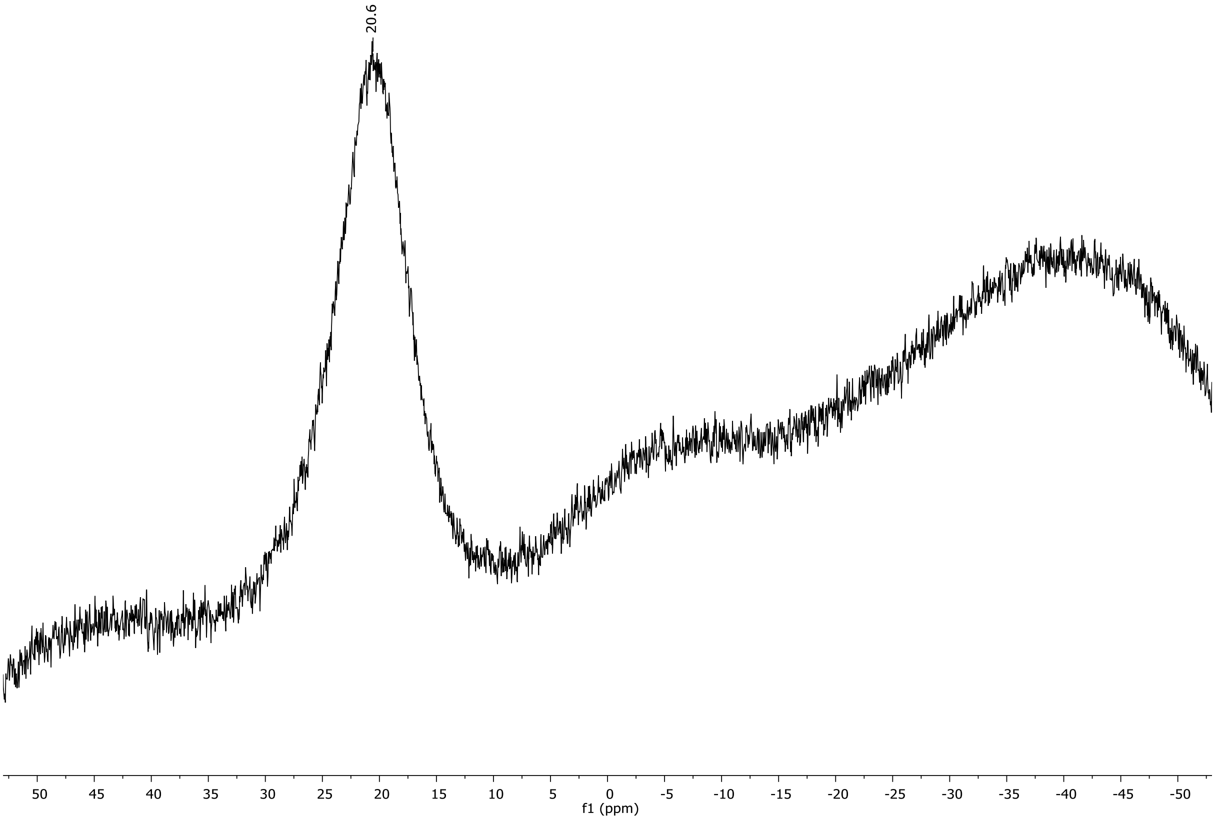

Figure S60. ^{11}B NMR spectrum of Na[**1**H] (96.3 MHz, [D$_8$]THF).

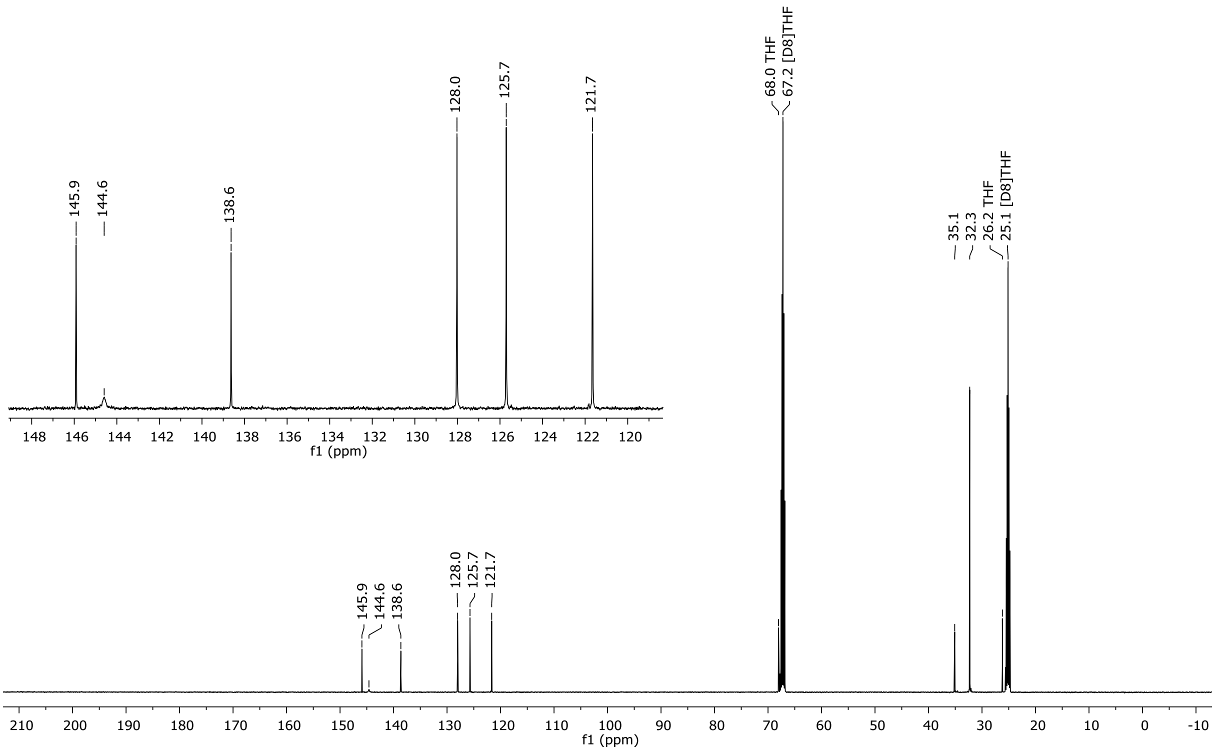

Figure S61. ^{13}C{^{1}H} NMR spectrum of Na[**1**H] (125.8 MHz, [D$_8$]THF).

4. X-ray crystal structure determinations

Data for all structures were collected on a STOE IPDS II two-circle diffractometer with a Genix Microfocus tube with mirror optics using MoK$_\alpha$ radiation (λ = 0.71073 Å). The data were scaled using the frame-scaling procedure in the *X-AREA* program system.[S5] The structures were solved by direct methods using the program *SHELXS* and refined against F^2 with full-matrix least-squares techniques using the program *SHELXL*.[S6]

Structure	**Internal code**	**CCDC reference number**
[Li(pmdta)][**2**H]	wa2996	2067773
{[K(pmdta)][**2**H]}$_2$·THF	wa2985	2067774
[Li(12-c-4)$_2$][**3**]	wa2692	2067775
[Na(thf)$_2$][**3**]·*n*-hexane	wa2904	2067776
[K(thf)$_2$][**3**]	wa2933	2067777
[Li(dme)$_3$][**7**]	wa2939	2067778
[K(dme)][**8**]	wa2993	2067779
[Li(thf)$_3$][**5**]	wa2908	2067780
[Na(pmdta)][**4**H]	wa3013	2067781
[K(dme)$_3$][K][**4**H]$_2$	wa3016	2067782
[Li(pmdta)Li(thf)][**9**]	wa3011	2067783
[Na(thf)$_3$][**1**H]	wa2586	2067784

[Li(pmdta)][2H]

Colorless single crystals of [Li(pmdta)][**2**H] were grown through gas-phase diffusion of *n*-hexane into a concentrated THF solution of Li[**2**H] containing PMDTA (0.1 mL), followed by slow evaporation of the solvents under ambient pressure and temperature while maintaining inert conditions.

In [Li(pmdta)][**2**H], one *t*Bu group is disordered over two sets of sites with a site occupation factor of 0.631(18) for the major occupied sites. The displacement parameters of the disordered atoms were restrained to an isotropic behavior. The geometric parameters of the two disordered sites were restrained to be equal to those of a non-disordered *t*Bu group. The B···B-bridging H(1) atom was isotropically refined. The contribution of additional solvent molecules that could not be further characterized was suppressed by using the *SQUEEZE* routine in *PLATON*.[S7]

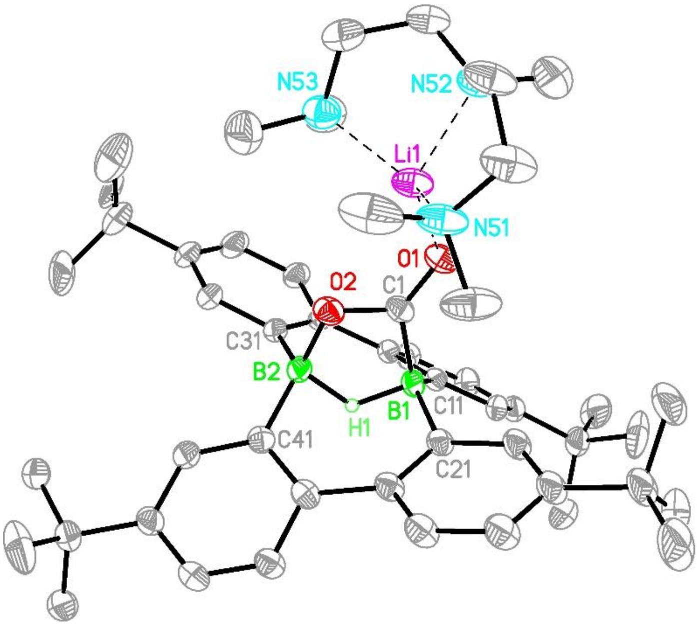

Figure S62. Molecular structure [Li(pmdta)][**2**H] in the solid state. Carbon-bonded hydrogen atoms are omitted for clarity. Displacement ellipsoids are drawn at the 30% probability level. Selected short contacts and bond lengths [Å]: B(1)···B(2) = 2.128(4), Li(1)···O(1) = 1.882(5); B(1)–H(1) = 1.23(2), B(2)–H(1) = 1.27(2), B(1)–C(1) = 1.601(4), C(1)–O(1) = 1.225(3), C(1)–O(2) = 1.346(3), B(2)–O(2) = 1.519(3), B(1)–C(11) = 1.584(4), B(1)–C(21) = 1.601(4), B(2)–C(31) = 1.604(4), B(2)–C(41) = 1.593(4).

{[K(pmdta)][2H]}$_2$·THF

Colorless single crystals of {[K(pmdta)][**2**H]}$_2$·THF were grown through gas-phase diffusion of *n*-hexane into a concentrated THF solution of K[**2**H] containing PMDTA (0.1 mL).

The solid-state structure of {[K(pmdta)][**2**H]}$_2$·THF features centrosymmetric dimers with all atoms located on general positions. Each K$^+$ cation is coordinated by two O atoms of one [**2**]$^-$ anion and three N atoms of one pmdta ligand. The sixth coordination site is occupied by one O atom of a symmetry-equivalent [**2**]$^-$ anion. The space between the {[K(pmdta)][**2**H]}$_2$ dimers is filled by one disordered THF molecule per dimer.

In {[K(pmdta)][**2**H]}$_2$·THF, one *t*Bu group is disordered over two sets of sites with a site occupation factor of 0.635(5) for the major occupied sites. In the non-coordinating THF molecule, three methylene groups are disordered over two sets of sites with a site occupation factor of 0.523(9) for the major occupied sites. This molecule and the B···B-bridging H(1) atom were both isotropically refined.

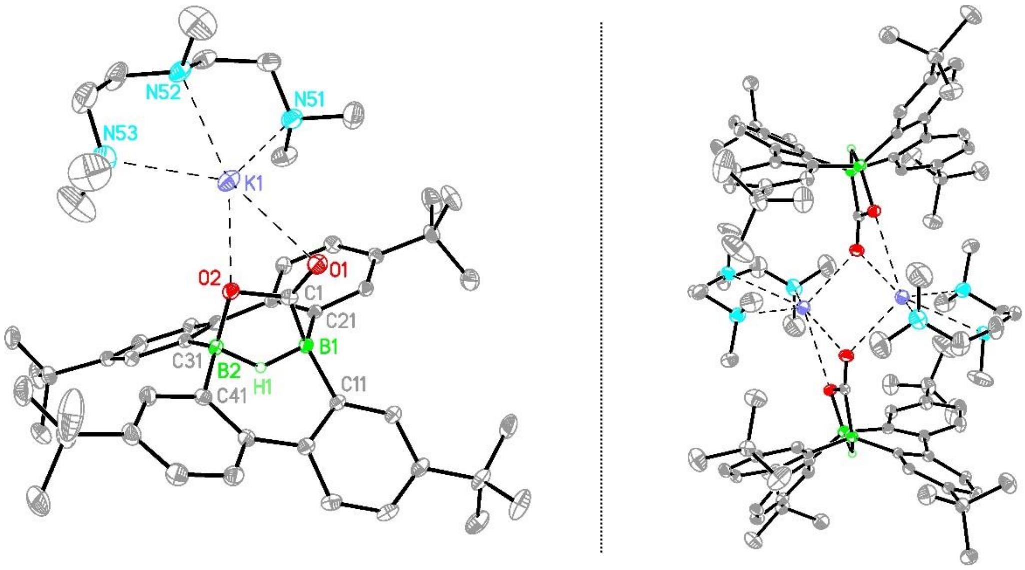

Figure S63. Left: Monomeric unit [K(pmdta)][**2**H] in the solid state. Carbon-bonded hydrogen atoms are omitted for clarity. Displacement ellipsoids are drawn at the 50% probability level. Selected short contacts and bond lengths [Å]: B(1)···B(2) = 2.141(3), K(1)···O(1) = 2.7927(16), K(1)···O(2) = 2.8568(14); B(1)–H(1) = 1.23(2), B(2)–H(1) = 1.27(2), B(1)–C(1) = 1.601(3), C(1)–O(1) = 1.224(2), C(1)–O(2) = 1.354(2), B(2)–O(2) = 1.524(3), B(1)–C(11) = 1.593(3), B(1)–C(21) = 1.607(3), B(2)–C(31) = 1.589(3), B(2)–C(41) = 1.599(3).
Right: Molecular structure of {[K(pmdta)][**2**H]}$_2$·THF in the solid state. Carbon-bonded hydrogen atoms as well the non-coordinating THF molecule are omitted for clarity. Displacement ellipsoids are drawn at the 50% probability level.

[Li(12-c-4)$_2$][3]

Yellow single crystals of [Li(12-c-4)$_2$][**3**] were grown by layering a concentrated THF solution of Li[**3**] with a solution of 12-crown-4 in *n*-hexane.

In [Li(12-c-4)$_2$][**3**], one *t*Bu group is disordered over two sets of sites with a site occupation factor of 0.63(3) for the major occupied sites. The displacement parameters of the disordered atoms were restrained to an isotropic behavior.

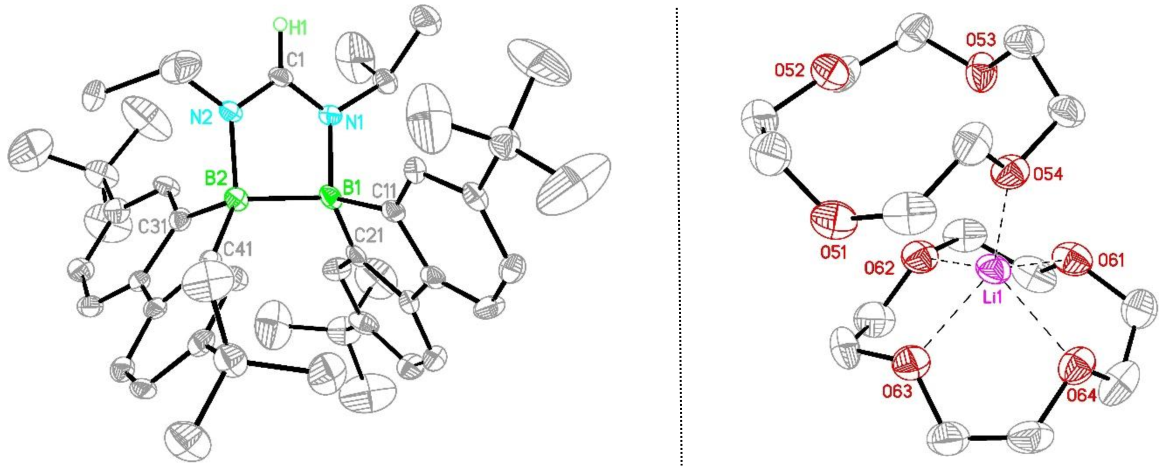

Figure S64. Molecular structures of the anion [**3**]$^-$ (left) and the solvent-separated [Li(12-c-4)$_2$]$^+$ cation (right) of [Li(12-c-4)$_2$][**3**] in the solid state. Carbon-bonded hydrogen atoms, except for H(1), are omitted for clarity. Displacement ellipsoids are drawn at the 50% probability level. Selected bond lengths [Å]: B(1)–B(2) = 1.809(6), B(1)–N(1) = 1.585(5), C(1)–N(1) = 1.312(5), C(1)–N(2) = 1.300(5), B(2)–N(2) = 1.604(5), B(1)–C(11) = 1.632(5), B(1)–C(21) = 1.600(6), B(2)–C(31) = 1.616(5), B(2)–C(41) = 1.605(6). Dihedral angle between the best planes through the two 9-borafluorene moieties: 72.60(8)°.

[Na(thf)$_2$][3]·n-hexane

Yellow single crystals of [Na(thf)$_2$][**3**]·*n*-hexane were grown through gas-phase diffusion of *n*-hexane into a concentrated THF solution of Na[**3**], followed by slow evaporation of the solvents under ambient pressure and temperature while maintaining inert conditions.

In one thf ligand of [Na(thf)$_2$][**3**]·*n*-hexane, two methylene groups are disordered over two sets of sites with a site occupation factor of 0.63(3) for the major occupied sites. The displacement parameters of the disordered atoms were restrained to an isotropic behavior. The *n*-hexane molecule is located on a center of inversion.

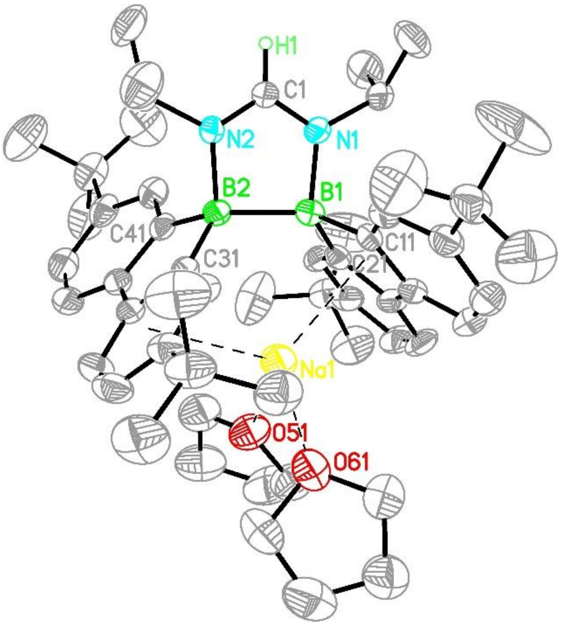

Figure S65. Molecular structure [Na(thf)$_2$][**3**]·*n*-hexane in the solid state. Carbon-bonded hydrogen atoms, except for H(1), as well as the *n*-hexane molecule are omitted for clarity. Displacement ellipsoids are drawn at the 50% probability level. Selected short contacts and bond lengths [Å]: Na(1)···COG(C(21)) = 3.493(2), Na(1)···COG(C(31)) = 2.948(2); B(1)–B(2) = 1.823(6), B(1)–N(1) = 1.587(4), C(1)–N(1) = 1.314(4), C(1)–N(2) = 1.299(4), B(2)–N(2) = 1.589(4), B(1)–C(11) = 1.626(5), B(1)–C(21) = 1.619(5), B(2)–C(31) = 1.622(5), B(2)–C(41) = 1.628(5). Dihedral angle between the best planes through the two 9-borafluorene moieties: 87.26(5)°. COG(C(X)): centroid of the phenylene ring containing C(X).

[K(thf)$_2$][3]

Yellow single crystals of [K(thf)$_2$][**3**] were grown through gas-phase diffusion of *n*-hexane into a concentrated THF solution of K[**3**], followed by slow evaporation of the solvents under ambient pressure and temperature while maintaining inert conditions.

In [K(thf)$_2$][**3**], one *t*Bu group is disordered over two sets of sites with a site occupation factor of 0.687(10) for the major occupied sites. In one thf ligand, two methylene groups are disordered over two sets of sites with a site occupation factor of 0.560(15) for the major occupied sites. One methyl moiety of an *i*Pr group is disordered over two sets of sites with a site occupation factor of 0.615(13) for the major occupied sites. The displacement parameters of the disordered atoms were restrained to an isotropic behavior.

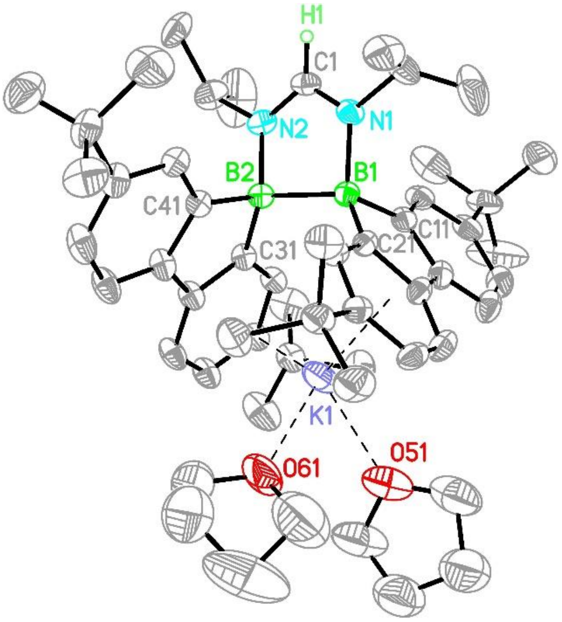

Figure S66. Molecular structure [K(thf)$_2$][**3**] in the solid state. Carbon-bonded hydrogen atoms except for H(1) are omitted for clarity. Displacement ellipsoids are drawn at the 30% probability level. Selected short contacts and bond lengths [Å]: K(1)···COG(C(21)) = 3.355(2), K(1)···COG(C(31)) = 2.860(2); B(1)–B(2) = 1.821(6), B(1)–N(1) = 1.593(5), C(1)–N(1) = 1.319(5), C(1)–N(2) = 1.308(5), B(2)–N(2) = 1.581(5), B(1)–C(11) = 1.611(5), B(1)–C(21) = 1.618(5), B(2)–C(31) = 1.616(5), B(2)–C(41) = 1.604(5). Dihedral angle between the best planes through the two 9-borafluorene moieties: 70.55(7)°. COG(C(X)): centroid of the phenylene ring containing C(X).

[Li(dme)$_3$][7]

Yellow single crystals of [Li(dme)$_3$][**7**] were grown through gas-phase diffusion of *n*-hexane into a concentrated THF/DME (1:1) solution of Li[**7**].

In [Li(dme)$_3$][**7**], two *t*Bu groups are disordered over two sets of sites with site occupation factors of 0.817(9) and 0.784(9) for the respective major occupied sites. The displacement parameters of the disordered atoms were restrained to an isotropic behavior. The contribution of additional solvent molecules that could not be further characterized was suppressed by using the *SQUEEZE* routine in *PLATON*.[S7]

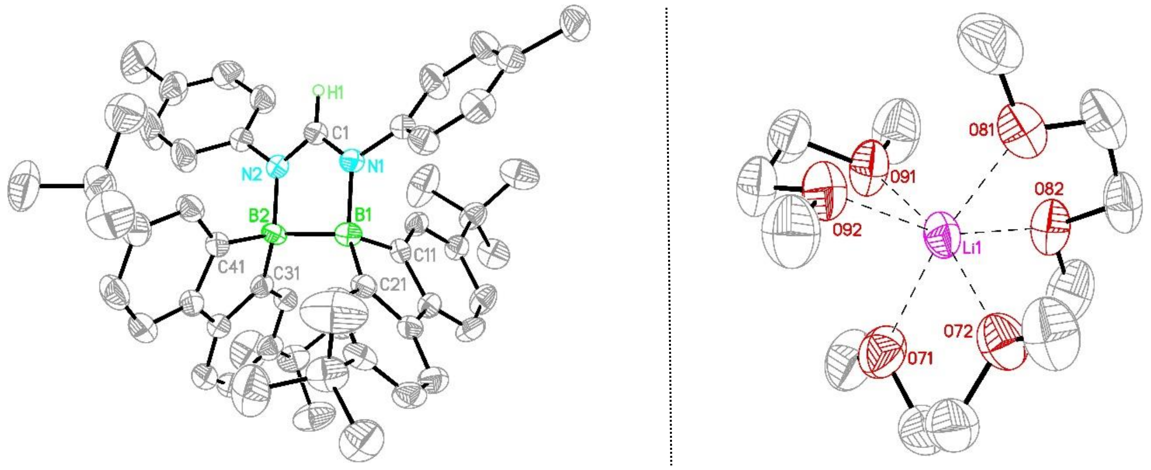

Figure S67. Molecular structures of the anion [**7**]$^-$ (left) and the solvent-separated [Li(dme)$_3$]$^+$ cation (right) of [Li(dme)$_3$][**7**] in the solid state. Carbon-bonded hydrogen atoms, except for H(1), are omitted for clarity. Displacement ellipsoids are drawn at the 30% probability level. Selected bond lengths [Å]: B(1)–B(2) = 1.796(7), B(1)–N(1) = 1.614(6), C(1)–N(1) = 1.323(5), C(1)–N(2) = 1.320(5), B(2)–N(2) = 1.590(6), B(1)–C(11) = 1.612(6), B(1)–C(21) = 1.619(6), B(2)–C(31) = 1.597(6), B(2)–C(41) = 1.618(6). Dihedral angle between the best planes through the two 9-borafluorene moieties: 63.33(7)°.

[K(dme)][8]

Yellow single crystals of [K(dme)][**8**] were grown in the following way: First, *n*-hexane was slowly added to a concentrated DME solution of K[**8**] through gas-phase diffusion. After 4 d, the volume of the DME/*n*-hexane solution was slowly reduced by evaporation under ambient pressure and temperature while maintaining inert conditions.

The solid-state structure of [K(dme)][**8**] does not exhibit any peculiarities worth discussing.

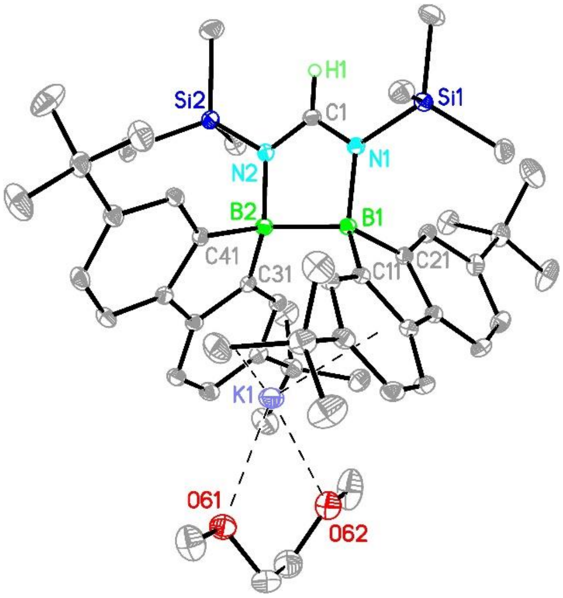

Figure S68. Molecular structure [K(dme)][**8**] in the solid state. Carbon-bonded hydrogen atoms, except for H(1), are omitted for clarity. Displacement ellipsoids are drawn at the 30% probability level. Selected short contacts and bond lengths [Å]: K(1)···COG(C(11)) = 2.8120(11), K(1)···COG(C(31)) = 3.5155(11); B(1)–B(2) = 1.830(3), B(1)–N(1) = 1.602(3), C(1)–N(1) = 1.320(3), C(1)–N(2) = 1.320(3), B(2)–N(2) = 1.607(3), B(1)–C(11) = 1.618(3), B(1)–C(21) = 1.614(3), B(2)–C(31) = 1.617(3), B(2)–C(41) = 1.619(3). Dihedral angle between the best planes through the two 9-borafluorene moieties: 68.73(4)°. COG(C(X)): centroid of the phenylene ring containing C(X).

[Li(thf)$_3$][5]

Colorless single crystals of [Li(thf)$_3$][**5**] were grown in the following way: First, *n*-hexane was slowly added to a concentrated THF solution of a mixture of Li[**4**H] and Li[**5**] through gas-phase diffusion. After 3 d, the volume of the solution was slowly reduced by evaporation under ambient pressure and temperature while maintaining inert conditions.

In [Li(thf)$_3$][**5**], one *t*Bu group is disordered over two sets of sites with a site occupation factor of 0.64(2) for the major occupied sites. In two thf ligands, one methylene group is disordered over two sets of sites with site occupation factors of 0.57(3) and 0.51(3) for the respective major occupied sites. The displacement parameters of all atoms were restrained to an isotropic behavior.

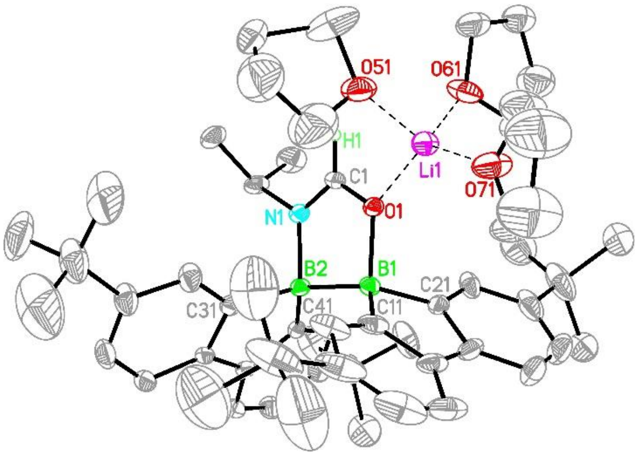

Figure S69. Molecular structure [Li(thf)$_3$][**5**] in the solid state. Carbon-bonded hydrogen atoms, except for H(1), are omitted for clarity. Displacement ellipsoids are drawn at the 30% probability level. Selected short contact and bond lengths [Å]: Li(1)···O(1) = 1.957(9); B(1)–B(2) = 1.801(7), B(1)–O(1) = 1.652(6), C(1)–O(1) = 1.295(6), C(1)–N(1) = 1.281(6), B(2)–N(1) = 1.605(6), B(1)–C(11) = 1.619(8), B(1)–C(21) = 1.613(7), B(2)–C(31) = 1.628(7), B(2)–C(41) = 1.619(6). Dihedral angle between the best planes through the two 9-borafluorene moieties: 85.37(11)°.

[Na(pmdta)][4H]

Colorless single crystals of [Na(pmdta)][**4**H] were grown in the following way: First, *n*-hexane was slowly added to a concentrated THF solution of Na[**4**H] containing PMDTA (0.1 mL) through gas-phase diffusion. After 2 d, the volume of the solution was slowly reduced by evaporation under ambient pressure and temperature while maintaining inert conditions.

In [Na(pmdta)][**4**H], one *t*Bu group is disordered over two sets of sites with a site occupation factor of 0.731(13) for the major occupied sites. The displacement parameters of the disordered atoms were restrained to an isotropic behavior. The boron-bonded H(1) atom was isotropically refined.

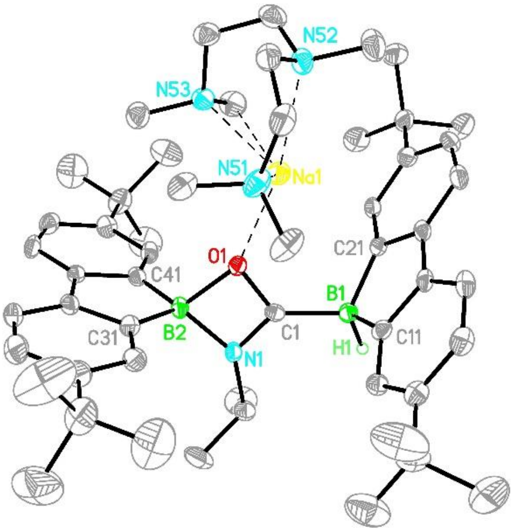

Figure S70. Molecular structure [Na(pmdta)][**4**H] in the solid state. Carbon-bonded hydrogen atoms are omitted for clarity. Displacement ellipsoids are drawn at the 30% probability level. Selected short contact, bond lengths [Å], and bond angles [°]: Na(1)···O(1) = 2.290(4); B(1)–H(1) = 1.15(5), B(1)–C(1) = 1.588(8), C(1)–O(1) = 1.352(6), C(1)–N(1) = 1.309(6), B(2)–N(1) = 1.559(7), B(2)–O(1) = 1.598(7), B(1)–C(11) = 1.618(8), B(1)–C(21) = 1.612(8), B(2)–C(31) = 1.587(8), B(2)–C(41) = 1.602(8); N(1)–B(2)–O(1) = 80.9(3), C(1)–N(1)–B(2) = 90.8(4), C(1)–O(1)–B(2) = 87.6(4), N(1)–C(1)–O(1) = 100.7(4). Dihedral angle between the best planes through the two 9-borafluorene moieties: 61.24(9)°.

[K(dme)$_3$][K][4H]$_2$

Colorless single crystals of [K(dme)$_3$][K][**4**H]$_2$ were grown in the following way: First, *n*-hexane was slowly added to a concentrated THF/DME (1:1) solution of K[**4**H] through gas-phase diffusion. After 3 d, the volume of the solution was slowly reduced by evaporation under ambient pressure and temperature while maintaining inert conditions.

The solid-state structure of [K(dme)$_3$][K][**4**H]$_2$ features two molecules of [**4**H]$^–$, which are symmetry related through the symmetry operator (–x, –y+1, –z+1). The two [**4**H]$^–$ molecules are connected through one K$^+$ cation, which is located on a center of inversion. This cation is coordinated by two O atoms (O(1), O(1B)) and two phenyl rings (Ph(C11), Ph(C11B)) of two 9-borafluorene moieties. The second K$^+$ cation is coordinated by three dme ligands and is separated from the {[K][**4**H]$_2$}$^–$ subunit.
In [K(dme)$_3$][K][**4**H]$_2$, one *t*Bu group is disordered over two sets of sites with a site occupation factor of 0.51(2) for the major occupied sites. In one dme ligand, two methylene groups are disordered over two sets of sites with a site occupation factor of 0.61(2) for the major occupied sites. The displacement parameters of the disordered atoms were restrained to an isotropic behavior. The boron-bonded H(1) and H(1B) atoms were isotropically refined. The contribution of additional solvent molecules that could not be further characterized was suppressed by using the *SQUEEZE* routine in *PLATON*.[S7]

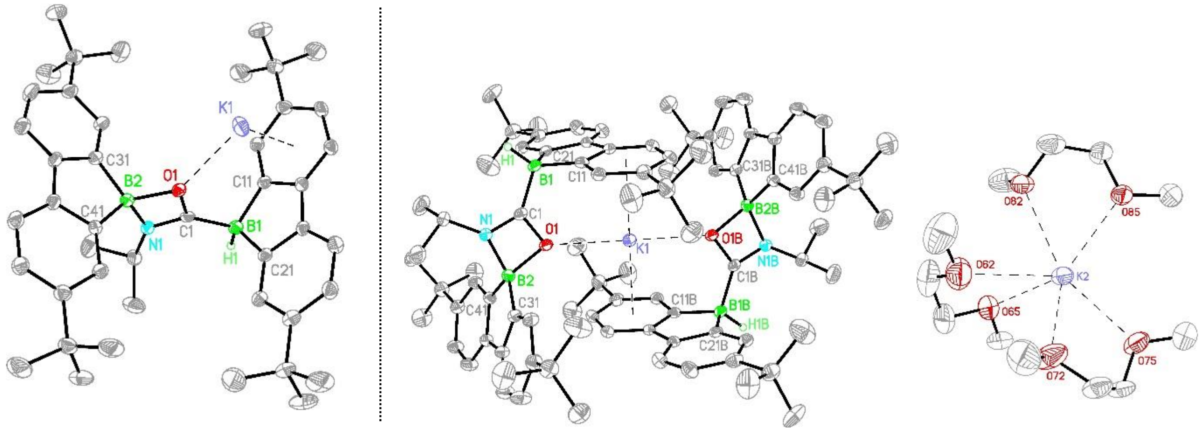

Figure S71. Left: Monomeric unit K[**4**H] in the solid state. Carbon-bonded hydrogen atoms are omitted for clarity. Displacement ellipsoids are drawn at the 50% probability level. Selected short contacts, bond lengths [Å], and bond angles [°]: K(1)···COG(C(11)) = 2.9967(19), K(1)···O(1) = 2.714(3); B(1)–H(1) = 1.12(5), B(1)–C(1) = 1.601(7), C(1)–O(1) = 1.353(5), C(1)–N(1) = 1.306(6), B(2)–N(1) = 1.586(6), B(2)–O(1) = 1.570(6), B(1)–C(11) = 1.617(7), B(1)–C(21) = 1.625(7), B(2)–C(31) = 1.611(7), B(2)–C(41) = 1.613(7); N(1)–B(2)–O(1) = 81.9(3), C(1)–N(1)–B(2) = 89.3(4), C(1)–O(1)–B(2) = 87.5(3), N(1)–C(1)–O(1) = 101.3(4). Dihedral angle between the best planes through the two 9-borafluorene moieties: 65.35(8)°. COG(C(X)): centroid of the phenylene ring containing C(X).
Right: Molecular structures of {[K][**4**H]$_2$}$^–$ and the solvent-separated second counter-cation [K(dme)$_3$]$^+$ in the solid state. Carbon-bonded hydrogen atoms are omitted for clarity. Displacement ellipsoids are drawn at the 50% probability level. Equivalent atoms labelled with suffix B were generated by the symmetry operator (–x, –y+1, –z+1).

[Li(pmdta)Li(thf)][9]

Li[**2**H] in [D_8]THF was heated to *T* = 55 °C under an atmosphere of CO_2 (sealed NMR tube). NMR monitoring after 4 h showed that the signals of Li[**2**H] had completely vanished and new, broad (proton) signals of still unknown thermolysis products had appeared. Colorless single crystals of [Li(pmdta)Li(thf)][**9**] were grown after the addition of PMDTA (0.1 mL) through gas-phase diffusion of *n*-hexane into the thermolysis mixture, followed by slow evaporation of the solvents under ambient pressure and temperature while maintaining inert conditions.

In the pmdta ligand of [Li(pmdta)Li(thf)][**9**], one methylene group is disordered over two sets of sites with a site occupation factor of 0.603(11) for the major occupied sites. In the thf ligand, one methylene group is disordered over two sets of sites with a site occupation factor of 0.73(1) for the major occupied sites. The displacement parameters of the disordered atoms and of two *t*-butyl groups were restrained to an isotropic behavior. The contribution of additional solvent molecules that could not be further characterized was suppressed by using the *SQUEEZE* routine in *PLATON*.[S7]

Discussion of the solid-state structure: One formula unit of [Li(pmdta)Li(thf)][**9**] contains four B atoms, two Li^+ cations, and four biphenyl units, which corresponds to the incorporation of 2 equiv of Li[**2**H]. B-bonded H^- ions could no longer be detected. On the other hand, if we assume that the O atoms O(3) and O(5) originate from the CO_2 bridges of thermolyzed Li[**2**H] (2 equiv of CO being released), the dianion [**9**]$^{2-}$ features one excess O atom (O(4)) and two excess CO_2 fragments. The dimer can be divided into two equal halves by cutting it along a line through Li(1) and O(4). Each half contains one biphenyl unit that still bridges two B atoms (B(1)/B(2) or B(3)/B(4); same structural motif as in Li[**2**H]). The other biphenyl group is connected to only one B atom (B(1) or B(4)) and has been transformed into an aryl carboxylate. A conceivable mechanism for the underlying C–C-coupling reaction could involve the insertion of a C=O bond of CO_2 into one B–C bond of a 9-borafluorene moiety (for comparable reactions, see: Ref.[S8]). The presumed existence of an intermediate 9-borafluorene, in turn, would suggest that part of the molecule was on the way to a 9,9'-difluorene-type structure.

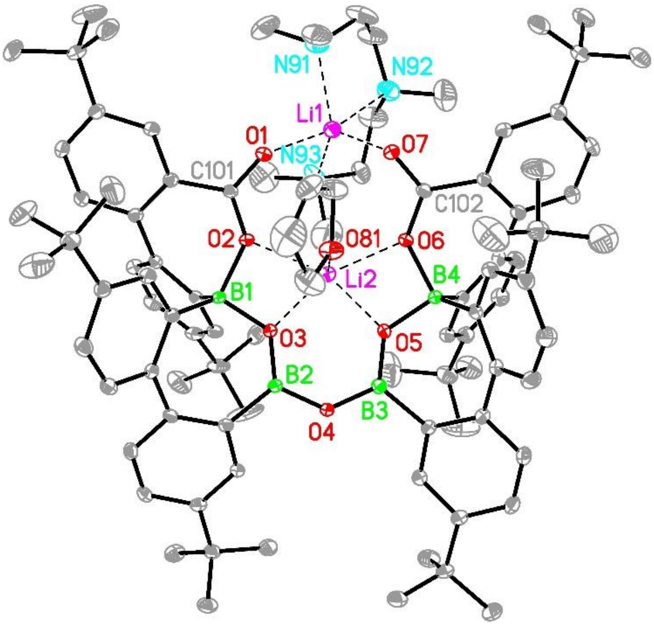

Figure S72. Molecular structure of [Li(pmdta)Li(thf)][**9**] in the solid state. Carbon-bonded hydrogen atoms are omitted for clarity. Displacement ellipsoids are drawn at the 30% probability level. Selected short contacts and bond lengths [Å]: Li(1)···O(1) = 2.072(6), Li(1)···O(7) = 1.937(6), Li(2)···O(2) = 2.152(5), Li(2)···O(3) = 1.993(5), Li(2)···O(5) = 2.005(5), Li(2)···O(6) = 2.112(5); C(101)–O(1) = 1.226(3), C(101)–O(2) = 1.307(3), B(1)–O(2) = 1.569(3), B(1)–O(3) = 1.493(4), B(2)–O(3) = 1.347(4), B(2)–O(4) = 1.384(4), B(3)–O(4) = 1.386(4), B(3)–O(5) = 1.341(4), B(4)–O(5) = 1.491(4), B(4)–O(6) = 1.562(4), C(102)–O(6) = 1.308(3), C(102)–O(7) = 1.229(3).

[Na(thf)$_3$][1H]

Yellow single crystals of [Na(thf)$_3$][**1**H] were grown through gas-phase diffusion of *n*-hexane into a concentrated THF solution of Na[**1**H].

In [Na(thf)$_3$][**1**H], three *t*Bu groups are disordered over two sets of sites with site occupation factors of 0.681(5), 0.753(5), and 0.58(2) for the respective major occupied sites. In two thf ligands, one methylene group is disordered over two sets of sites with site occupation factors of 0.69(3) and 0.74(3) for the respective major occupied sites. The displacement parameters of the disordered atoms were restrained to an isotropic behavior. The H(1) atom bridging the B–B bond was isotropically refined.

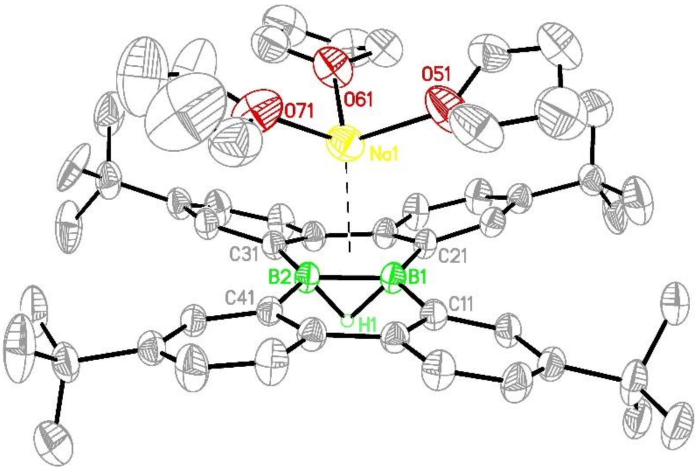

Figure S73. Molecular structure of [Na(thf)$_3$][**1**H] in the solid state. Carbon-bonded hydrogen atoms are omitted for clarity. Displacement ellipsoids are drawn at the 50% probability level. Selected short contacts and bond lengths [Å]: B(1)···Na(1) = 2.785(3), B(2)···Na(1) = 2.712(3); B(1)–B(2) = 1.658(3), B(1)–H(1) = 1.29(2), B(2)–H(1) = 1.23(2), B(1)–C(11) = 1.581(3), B(1)–C(21) = 1.568(3), B(2)–C(31) = 1.573(3), B(2)–C(41) = 1.581(3).

Table S1. Selected crystallographic data for [Li(pmdta)][**2**H], {[K(pmdta)][**2**H]}$_2$·THF, and [Li(12-c-4)$_2$][**3**].

	[Li(pmdta)][**2**H]	{[K(pmdta)][**2**H]}$_2$·THF	[Li(12-c-4)$_2$][**3**]
formula	$C_{50}H_{72}B_2LiN_3O_2$	$C_{108}H_{156}B_4K_2N_6O_6$	$C_{63}H_{95}B_2LiN_2O_8$
M [g mol^{-1}]	775.66	1755.82	1036.96
color, shape	colorless, block	colorless, block	yellow, block
T [K]	173(2)	173(2)	173(2)
radiation, λ [Å]	MoK_α, 0.71073	MoK_α, 0.71073	MoK_α, 0.71073
crystal system	monoclinic	monoclinic	triclinic
space group	$P2_1/n$	$P2_1/c$	$P\bar{1}$
a [Å]	17.9787(6)	15.5339(6)	11.4323(10)
b [Å]	17.1205(8)	20.0316(5)	12.1113(13)
c [Å]	18.8527(7)	18.0591(7)	22.6192(19)
α [°]	90	90	85.878(8)
β [°]	110.042(3)	108.566(3)	76.690(7)
γ [°]	90	90	85.863(8)
V [Å^3]	5451.5(4)	5327.0(3)	3034.9(5)
Z	4	2	2
D_{calcd} [g cm^{-3}]	0.945	1.095	1.135
μ [mm^{-1}]	0.056	0.142	0.072
F(000)	1688	1904	1128
crystal size [mm^3]	0.29 x 0.24 x 0.24	0.29 x 0.29 x 0.27	0.19 x 0.12 x 0.12
rflns collected	63430	57418	25274
independent rflns (R_{int})	10225 (0.0642)	9969 (0.0334)	11346 (0.0962)
data/restraints/parameters	10225 / 72 / 555	9969 / 24 / 588	11346 / 36 / 713
GOF on F^2	1.066	1.060	1.211
R_1, wR_2 [$I > 2\sigma(I)$]	0.0770, 0.1974	0.0600, 0.1565	0.1015, 0.1674
R_1, wR_2 (all data)	0.1175, 0.2320	0.0730, 0.1686	0.1775, 0.1887
largest diff peak and hole [e Å^{-3}]	0.356, –0.275	1.220, –0.508	0.541, –0.258

Table S2. Selected crystallographic data for [Na(thf)$_2$][**3**]·*n*-hexane, [K(thf)$_2$][**3**], and Li(dme)$_3$][**7**].

	[Na(thf)$_2$][**3**]·*n*-hexane	[K(thf)$_2$][**3**]	Li(dme)$_3$][**7**]
formula	$C_{58}H_{86}B_2N_2NaO_2$	$C_{55}H_{79}B_2KN_2O_2$	$C_{67}H_{93}B_2LiN_2O_6$
M [g mol^{-1}]	887.89	860.92	1050.99
color, shape	yellow, plate	yellow, block	yellow, needle
T [K]	173(2)	173(2)	173(2)
radiation, λ [Å]	MoK_α, 0.71073	MoK_α, 0.71073	MoK_α, 0.71073
crystal system	triclinic	monoclinic	monoclinic
space group	$P\bar{1}$	$C2/c$	$C2/c$
a [Å]	12.2187(10)	35.9563(11)	35.3153(12)
b [Å]	16.2604(18)	15.1061(2)	16.6312(6)
c [Å]	16.2958(17)	23.4218(8)	23.2536(8)
α [°]	61.770(7)	90	90
β [°]	79.087(7)	121.286(2)	105.586(3)
γ [°]	82.091(8)	90	90
V [Å^3]	2796.7(5)	10871.8(6)	13155.5(8)
Z	2	8	8
D_{calcd} [g cm^{-3}]	1.054	1.052	1.061
μ [mm^{-1}]	0.068	0.136	0.066
F(000)	970	3744	4560
crystal size [mm^3]	0.21 x 0.14 x 0.09	0.51 x 0.49 x 0.32	0.29 x 0.11 x 0.03
rflns collected	23804	93616	42035
independent rflns (R_{int})	9836 (0.0753)	9582 (0.0590)	11783 (0.0795)
data/restraints/parameters	9836 / 24 / 605	9582 / 60 / 616	11783 / 144 / 761
GOF on F^2	1.005	1.102	1.261
R_1, wR_2 [$I > 2\sigma(I)$]	0.0843, 0.1571	0.1090, 0.2650	0.1143, 0.1861
R_1, wR_2 (all data)	0.1694, 0.1890	0.1317, 0.2877	0.1812, 0.2192
largest diff peak and hole [e Å^{-3}]	0.267, –0.209	0.832, –0.578	0.313, –0.268

Table S3. Selected crystallographic data for [K(dme)][**8**], [Li(thf)$_3$][**5**], and Na(pmdta)][**4**H].

	[K(dme)][**8**]	[Li(thf)$_3$][**5**]	Na(pmdta)][**4**H]
formula	$C_{51}H_{77}B_2KN_2O_2Si_2$	$C_{56}H_{80}B_2LiNO_4$	$C_{53}H_{79}B_2N_4NaO$
M [g mol^{-1}]	867.04	859.77	832.81
color, shape	yellow, plate	colorless, rod	colorless, block
T [K]	173(2)	173(2)	173(2)
radiation, λ [Å]	MoK_α, 0.71073	MoK_α, 0.71073	MoK_α, 0.71073
crystal system	monoclinic	triclinic	monoclinic
space group	$P2_1/c$	$P\bar{1}$	$P2_1/n$
a [Å]	18.5445(8)	9.6243(7)	13.0931(6)
b [Å]	16.8811(5)	14.9307(10)	26.6170(10)
c [Å]	19.3634(9)	20.6743(16)	15.9341(8)
α [°]	90	69.874(6)	90
β [°]	118.010(3)	82.002(6)	103.292(4)
γ [°]	90	73.617(6)	90
V [Å^3]	5351.7(4)	2673.3(4)	5404.3(4)
Z	4	2	4
D_{calcd} [g cm^{-3}]	1.076	1.068	1.024
μ [mm^{-1}]	0.181	0.064	0.067
F(000)	1880	936	1816
crystal size [mm^3]	0.24 x 0.21 x 0.09	0.26 x 0.12 x 0.08	0.26 x 0.21 x 0.19
rflns collected	48741	30499	34100
independent rflns (R_{int})	10053 (0.0495)	10022 (0.0600)	9542 (0.0932)
data/restraints/parameters	10053 / 0 / 541	10022 / 484 / 625	9542 / 48 / 582
GOF on F^2	1.091	1.344	1.246
R_1, wR_2 [$I > 2\sigma(I)$]	0.0600, 0.1259	0.1512, 0.3770	0.1348, 0.2464
R_1, wR_2 (all data)	0.0831, 0.1355	0.2182, 0.4192	0.2020, 0.2857
largest diff peak and hole [e Å^{-3}]	0.844, –0.433	1.289, –0.516	0.823, –0.344

Table S4. Selected crystallographic data for [K(dme)$_3$][K][**4**H]$_2$, [Li(pmdta)Li(thf)][**9**], and [Na(thf)$_3$][**1**H].

	[K(dme)$_3$][K][**4**H]$_2$	[Li(pmdta)Li(thf)][**9**]	[Na(thf)$_3$][**1**H]
formula	$C_{100}H_{142}B_4K_2N_2O_8$	$C_{95}H_{127}B_4Li_2N_3O_8$	$C_{52}H_{73}B_2NaO_3$
M [g mol^{-1}]	1621.59	1496.11	790.71
color, shape	colorless, block	colorless, block	yellow, block
T [K]	173(2)	173(2)	173(2)
radiation, λ [Å]	MoK_α, 0.71073	MoK_α, 0.71073	MoK_α, 0.71073
crystal system	triclinic	triclinic	monoclinic
space group	$P\bar{1}$	$P\bar{1}$	$P2_1/c$
a [Å]	12.6458(5)	12.0344(4)	14.8315(7)
b [Å]	18.8110(8)	15.7136(5)	21.4829(7)
c [Å]	22.3127(9)	27.0349(9)	15.5290(7)
α [°]	87.687(3)	86.859(3)	90
β [°]	82.704(3)	88.314(3)	106.774(4)
γ [°]	77.661(3)	70.701(3)	90
V [Å^3]	5142.7(4)	4817.5(3)	4737.4(4)
Z	2	2	4
D_{calcd} [g cm^{-3}]	1.047	1.031	1.109
μ [mm^{-1}]	0.143	0.063	0.073
F(000)	1756	1616	1720
crystal size [mm^3]	0.32 x 0.28 x 0.17	0.44 x 0.30 x 0.27	0.26 x 0.21 x 0.18
rflns collected	43791	45892	46623
independent rflns (R_{int})	19157 (0.0588)	17955 (0.0458)	8363 (0.0520)
data/restraints/parameters	19157 / 78 / 1103	17955 / 48 / 1029	8363 / 270 / 631
GOF on F^2	1.190	1.198	1.048
R_1, wR_2 [$I > 2\sigma(I)$]	0.1158, 0.2348	0.0830, 0.1759	0.0651, 0.1634
R_1, wR_2 (all data)	0.1814, 0.2736	0.1193, 0.1982	0.0904, 0.1770
largest diff peak and hole [e Å^{-3}]	0.940, –0.454	0.488, –0.447	0.349, –0.335

5. Computational details

DFT calculations were carried out with the Gaussian program package.[S9] The PBE0[S10–S13] hybrid functional was used and combined with the D3BJ atom-pairwise dispersion correction with Becke-Johnson damping as devised by Grimme.[S14,S15] Geometry optimizations and harmonic frequency calculations were generally computed with the SMD solvation model[S16] (to account for effects of the THF solvent) using the TZVP basis set.[S17] All Gibbs free energies reported correspond to the total energies of the system calculated with the SMD solvation model[S16], corrected by thermal contributions from the frequency analyses. All stationary points reported were characterized as minima or first order saddle points by eigenvalue analysis of the diagonalized Hessians.

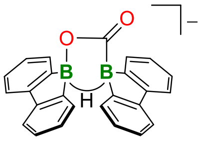

[**2a**H]$^-$

G = –1162.34611014 Ha

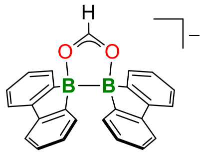

[**2b**]$^-$

G = –1162.32917494 Ha

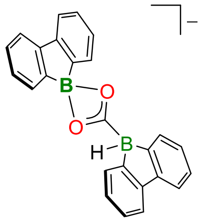

[**2c**H]$^-$

G = –1162.34689452 Ha

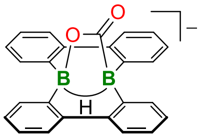

[**2**H]$^-$

G = –1162.32052499 Ha

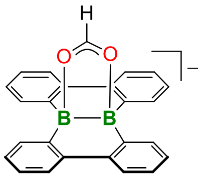

[**2d**]$^-$

G = –1162.321667763 Ha

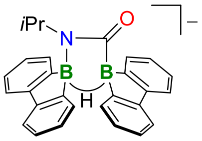

[**4b**H]$^-$

G = –1260.30990980 Ha

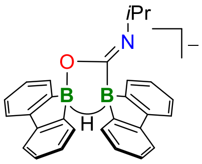

[**4a**H]$^-$

G = –1260.29075843 Ha

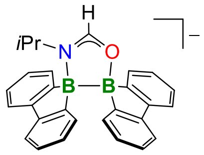

[**5**]$^-$

G = –1260.30713407 Ha

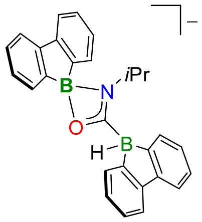

[**4**H]$^-$

G = –1260.31428575 Ha

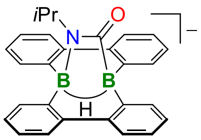

[**4c**H]$^-$

G = –1260.28189804 Ha
(one imaginary frequency)

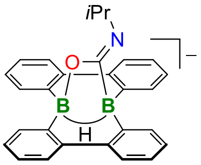

[**4d**H]$^-$

G = –1260.26791585 Ha

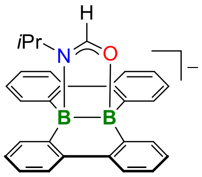

[**5a**]$^-$

G = –1260.29324263 Ha

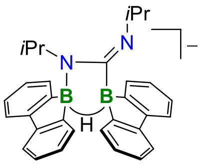

[**3a**H]$^-$

G = –1358.2404761 Ha

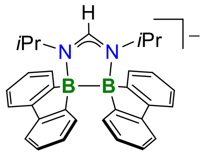

[**3**]$^-$

G = –1358.27858830 Ha

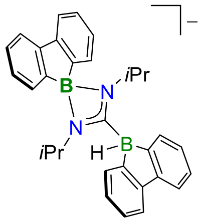

[**3b**H]$^-$

G = –1358.27047566 Ha

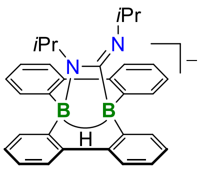

[**3c**H]$^-$

G = –1358.22897208 Ha

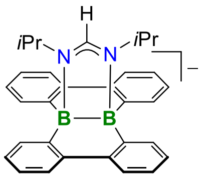

[**3d**]$^-$

G = –1358.25305935 Ha

Figure S74. Computed anion structures with respective Gibbs free energies (*G*) in Hartree (Ha). All structures except for [**4c**H]$^-$ were found to be minima. [**4c**H]$^-$ was found to be a first order saddle point.

6. References

[S1] A. Hübner, M. Diefenbach, M. Bolte, H. W. Lerner, M. C. Holthausen, M. Wagner, *Angew. Chem. Int. Ed.* **2012**, *51*, 12514–12518; *Angew. Chem.* **2012**, *124*, 12682–12686.

[S2] T. Kaese, H. Budy, M. Bolte, H. Lerner, M. Wagner, *Angew. Chem. Int. Ed.* **2017**, *56*, 7546–7550; *Angew. Chem.* **2017**, *129*, 7654–7658.

[S3] G. R. Fulmer, A. J. M. Miller, N. H. Sherden, H. E. Gottlieb, A. Nudelman, B. M. Stoltz, J. E. Bercaw, K. I. Goldberg, *Organometallics* **2010**, *29*, 2176–2179.

[S4] M. Hesse, H. Meier, B. Zeeh, *Spektroskopische Methoden in der organischen Chemie*, *8th edition*, G. Thieme Verlag, Stuttgart, New York, **2012**.

[S5] Stoe & Cie, *X-AREA*. *Diffractometer control program system*. Stoe & Cie, Darmstadt, Germany, **2002**.

[S6] G. M. Sheldrick, *Acta Crystallogr., Sect. A: Found. Crystallogr.* **2008**, *64*, 112–122.

[S7] A. L. Spek, *Acta Crystallogr., Sect. D: Biol. Crystallogr.* **2009**, *65*, 148–155.

[S8] a) J. F. Araneda, W. E. Piers, M. J. Sgro, M. Parvez, *Organometallics* **2015**, *34*, 3408–3413; b) K. R. Bluer, L. E. Laperriere, A. Pujol, S. Yruegas, V. A. K. Adiraju, C. D. Martin, *Organometallics* **2018**, *37*, 2917–2927; c) X. Su, T. A. Bartholome, J. R. Tidwell, A. Pujol, S. Yruegas, J. J. Martinez, C. D. Martin, *Chem. Rev.* **2021**, acs.chemrev.0c01068.

[S9] M. J. Frisch, G. W. Trucks, H. B. Schlegel, G. E. Scuseria, M. A. Robb, J. R. Cheeseman, G. Scalmani, V. Barone, B. Mennucci, G. A. Petersson, H. Nakatsuji, M. Caricato, X. Li, H. P. Hratchian, A. F. Izmaylov, J. Bloino, G. Zheng, J. L. Sonnenberg, M. Hada, M. Ehara, K. Toyota, R. Fukuda, J. Hasegawa, M. Ishida, T. Nakajima, Y. Honda, O. Kitao, H. Nakai, T. Vreven, J. A. Montgomery, Jr., J. E. Peralta, F. Ogliaro, M. Bearpark, J. J. Heyd, E. Brothers, K. N. Kudin, V. N. Staroverov, T. Keith, R. Kobayashi, J. Normand, K. Raghavachari, A. Rendell, J. C. Burant, S. S. Iyengar, J. Tomasi, M. Cossi, N. Rega, J. M. Millam, M. Klene, J. E. Knox, J. B. Cross, V. Bakken, C. Adamo, J. Jaramillo, R. Gomperts, R. E. Stratmann, O. Yazyev, A. J. Austin, R. Cammi, C. Pomelli, J. W. Ochterski, R. L. Martin, K. Morokuma, V. G. Zakrzewski, G. A. Voth, P. Salvador, J. J. Dannenberg, S. Dapprich, A. D. Daniels, O. Farkas, J. B. Foresman, J. V. Ortiz, J. Cioslowski, D. J. Fox, *Gaussian 09, Revision D.01*, Gaussian, Inc., Wallingford, CT, USA, **2013**.

[S10] J. P. Perdew, K. Burke, M. Ernzerhof, *Phys. Rev. Lett.* **1996**, *77*, 3865–3868.

[S11] J. P. Perdew, K. Burke, M. Ernzerhof, *Phys. Rev. Lett.* **1997**, *78*, 1396–1396.

[S12] J. P. Perdew, M. Ernzerhof, K. Burke, *J. Chem. Phys.* **1996**, *105*, 9982–9985.

[S13] C. Adamo, V. Barone, *J. Chem. Phys.* **1999**, *110*, 6158–6170.

[S14] L. Goerigk, S. Grimme, *J. Chem. Theory Comput.* **2011**, *7*, 291–309.

[S15] S. Grimme, S. Ehrlich, L. Goerigk, *J. Comput. Chem.* **2011**, *32*, 1456–1465.

[S16] A. V Marenich, C. J. Cramer, D. G. Truhlar, *J. Phys. Chem. B* **2009**, *113*, 6378–6396.

[S17] A. Schäfer, C. Huber, R. Ahlrichs, *J. Chem. Phys.* **1994**, *100*, 5829–5835.